

SPATIAL NAVIGATION IN GEOMETRIC MAZES: A COMPUTATIONAL MODEL OF RODENT BEHAVIOR

THÈSE N° 3922 (2007)

PRÉSENTÉE LE 20 NOVEMBRE 2007

À LA FACULTÉ INFORMATIQUE ET COMMUNICATIONS

Laboratoire de calcul neuromimétique (IC/SV)

SECTION D'INFORMATIQUE

ÉCOLE POLYTECHNIQUE FÉDÉRALE DE LAUSANNE

POUR L'OBTENTION DU GRADE DE DOCTEUR ÈS SCIENCES

PAR

Denis SHEYNIKHOVICH

Master's Degree in Mathematics, Saint-Petersburg State College of Fine Mechanics and Optics (Technical University), Russie
et de nationalité russe

acceptée sur proposition du jury:

Prof. P. Fua, président du jury
Prof. W. Gerstner, directeur de thèse
Prof. A. Ijspeert, rapporteur
Prof. B. Poucet, rapporteur
Prof. W. Senn, rapporteur



ÉCOLE POLYTECHNIQUE
FÉDÉRALE DE LAUSANNE

Lausanne, EPFL

2007

SPATIAL NAVIGATION IN GEOMETRIC
MAZES: A COMPUTATIONAL MODEL OF
RODENT BEHAVIOR

Сергею де Рокамболо
Анне Николаевой

Abstract

Navigation is defined as the capability of planning and performing a path from the current position towards a desired location. Different types, or strategies, of navigation are used by animals depending on the task they are trying to solve. Visible goals can be approached directly, while navigation to a hidden goal usually requires a memorized representation of relative positions of the goal and surrounding landmarks.

Neurophysiological and behavioral experiments on rodents suggest that different brain areas are responsible for the expression of different navigation strategies. Specifically, dorsal striatum has been related to storage and recall of stimulus-response associations underlying simple goal-approaching behaviors, whereas hippocampus is thought to store the spatial representation of the environment. Such a representation is built during an unrewarded spatial exploration and appears to be employed in cases when simple stimulus-response strategies fail. Discovery of neurons with spatially correlated activity, i.e. place cells and grid cells, in the hippocampal formation complements behavioral and lesion data suggesting its role for spatial orientation.

The overall objective of this work is to study the neurophysiological mechanisms underlying rodent spatial behavior, in particular those that are responsible for the implementation of different navigational strategies. Special attention is devoted to the question of how various types of sensory cues influence goal-oriented behavior.

The model of a navigating rat described in this work is based on functional and anatomical properties of brain regions involved in encoding and storage of space representation and action generation. In particular, place and grid cells are modeled by two interconnected populations of artificial neurons. Together, they form a network for spatial learning, capable of combining different types of sensory inputs to produce a distributed representation of location. Goal-directed actions can be generated in the model via two different neural pathways: the first one drives stimulus-response behavior and associates visual input directly to motor responses; the second one associates motor actions with *places* and hence depends on the representation of location. The visual input is represented by responses of a large number of orientation-sensitive filters to visual images generated according to the position and orientation of the simulated rat in a virtual three-dimensional world.

The model was tested in a large array of tasks designed by analogy to experimental studies on animal behavior. Results of several experimental studies, behavioral as well as neurophysiological, were reproduced. Based on these results we formulated a hypothesis about the influence that the rat's perception of surrounding environment exerts on goal-oriented behavior. This hypothesis may provide an insight into several issues in animal behavior research that were not addressed by theoretical models until now.

Keywords: rat, model, navigation, place cells, grid cells, geometry of space, neural network, reinforcement learning.

Résumé

La navigation est la capacité de prévoir et de parcourir le trajet liant une position actuelle à une position cible. Différents types de navigation, ou stratégies, peuvent être utilisées par l'animal selon la tâche qu'il essaie de résoudre. Une cible visible pourra être approchée directement alors que la navigation vers une cible cachée nécessitera une représentation interne des positions relatives de la cible et de l'environnement.

Les expérimentations comportementales et neurophysiologiques sur les rongeurs suggèrent que différentes aires du cerveau sont responsables de la réalisation des stratégies de navigation. En particulier, le striatum dorsal est lié aux stratégies d'approche directe d'une cible visible alors que l'hippocampe est susceptible de contenir une représentation spatiale de l'environnement. Une telle représentation s'établit lors d'une phase d'exploration spatiale et semble être employée quand les simples stratégies à base de stimulus-réponse échouent. La découverte de neurones de l'hippocampe dont l'activité est corrélée à la localisation spatiale de l'animal comme les cellules de lieu ou les grid cells s'ajoute aux données comportementales et issues de lésions expérimentales et ne fait que confirmer son rôle dans l'orientation spatiale.

L'objectif principal de ce travail est l'étude des mécanismes neurophysiologiques qui sous-tendent les comportements de navigation spatiale chez les rongeurs, notamment ceux qui génèrent les différentes stratégies de navigation. Une attention particulière sera portée sur la question de savoir comment les différents types d'indices sensoriels influencent le comportement de navigation vers une cible.

Le modèle de navigation du rat décrit dans ce travail est basé sur les propriétés fonctionnelles et anatomiques des régions du cerveau qui participent à l'encodage et à l'enregistrement de la représentation spatiale et la génération des actions. Par exemple, les cellules de lieu et les grid cells sont modélisées par deux populations interconnectées de neurones artificiels. Ensemble, elles forment un réseau d'apprentissage spatiale, capable de combiner différents types de stimulus sensoriels pour produire une représentation distribuée de l'espace. Les actions visant à atteindre une cible peuvent être produites par le modèle via deux voies neuronales différentes: la première gère les comportements à base de stimulus-réponse et associe directement les stimulus visuels aux réponses motrices; la seconde associe les actions motrices au lieu où se trouve l'animal et dépend donc de la représentation de l'espace. Le stimulus visuel est représenté par l'ensemble des réponses d'un grand nombre de filtres sensibles à l'orientation appliqués à l'image visuelle perçue par le rat simulés dans un environnement à trois dimensions.

Le modèle est testé dans un ensemble de tâches conçues par analogie avec des expériences comportementales réelles. Les résultats de quelques études expérimentales, aussi bien comportementales que neurophysiologiques, sont reproduits. Enfin, une hypothèse concernant l'influence qu'à la perception de l'environnement sur le comportement du rat est formulée sur la base des résultats des simulations. Cette hypothèse pourra fournir un éclairage théorique nouveau sur différents problèmes rencontrés par la recherche comportementale sur l'animal.

Mots clés: rat, modèle, navigation, cellules de lieu, grid cells, géométrie de l'espace, réseau de neurones, apprentissage par renforcement.

Acknowledgements

I would like to thank the people who contributed to the achievement of this thesis. First of all, I would like to express my deep gratitude to my Ph.D. supervisor, Prof. Wolfram Gerstner, for his great advice and for showing me how the science works. I would also like to thank the members of the thesis committee: Prof. Pascal Fua, Prof. Bruno Poucet, Prof. Walter Senn and Prof. Auke Ijspeert.

I am particularly grateful to Dr. Ricardo Chavarriaga and Dr. Thomas Strösslin for introducing me into the field and with whom I had a pleasure to work during the first two years of my Ph.D.

I want to thank my coworkers at the Laboratory of Computational Neuroscience who made my stay at the EPFL a pleasant one. I am especially indebted to Laurent Badel, Eleni Vasilaki, Gedi Luksys, Brice Bathellier, Magnus Richardson, Nicolas Marcille, Claudia Clopath and Taro Toyozumi. I also want to thank our secretaries Brigitte Ramuz and Chantal Mellier for their excellent work.

I thank the doctoral school band for all the fun we had together: Šarunas, Maciej, Michal, Kasia, Dan, Ivana², Maxim, Valka, Irinka, Gleb, Yurka

Above all I thank Natashka and Timour.

Contents

Acknowledgements	vii
1 Introduction	1
1.1 Motivation	1
1.2 Road-map of the thesis	2
2 Background	5
2.1 Neural networks	5
2.2 Reinforcement learning	6
2.3 Environment model	10
3 Rat navigation	13
3.1 Memory systems underlying navigation	15
3.1.1 Locale and taxon strategies in the watermaze	15
3.1.2 Radial mazes	16
3.2 Basal ganglia	17
3.2.1 Reward-based learning	20
3.3 Role of sensory cues during goal-oriented behavior	21
3.3.1 Geometric module hypothesis	21
3.4 Models of rodent navigation: state of the art	22
3.4.1 Models of Hippocampus-dependent navigation	23
3.4.2 Models of Basal ganglia and S-R learning	28
4 Spatial representation in the rat	33
4.1 Anatomy of the hippocampal formation	33
4.2 Grid cells in the dorsomedial entorhinal cortex	38
4.3 Hippocampal place cells	39
4.3.1 Firing determinants of place cells	40
4.4 Modeling space representation: state of the art	43
4.4.1 Models of place cells	43
4.4.2 Models of grid cells	51

5	A new model of rat behavior	53
5.1	Model of visual input	55
5.2	Action selection model	56
5.3	Space representation model	60
5.3.1	Path integration in the network of grid cells	60
5.3.2	Place cells	64
5.3.3	Head direction and visual input	65
5.4	Latent <i>vs</i> motivational learning	70
6	Spatial representation in the model	71
6.1	Experimental setup for latent learning	72
6.2	Experiment 1: learning spatial representation	73
6.2.1	Grid cells	73
6.2.2	Place cells	75
6.3	Dynamics of place fields	76
6.3.1	Experiment 2: Shrinking linear track	76
6.3.2	Experiments 3 and 4: Stretching rectangular rooms	80
6.4	Discussion	83
7	Simulation of rat goal-oriented behavior	87
7.1	Watermaze navigation	88
7.1.1	Experimental procedures	89
7.1.2	Results	91
7.1.3	Discussion	96
7.2	Is there a geometric module in the rat brain?	97
7.2.1	Experimental procedures	99
7.2.2	Results	100
7.2.3	Discussion	103
7.3	Transfer of goal information between environments	107
7.3.1	Discussion	111
7.4	General discussion	112
8	Conclusions	115
8.1	Contributions	115
8.2	Limitations and perspectives	116
	References	119
	Curriculum vitae	137

Chapter 1

Introduction

1.1 Motivation

Probably the oldest question in neuroscience is how actions are generated by living organisms. Early theories suggest that any action is a response to an appropriate stimulus, and hence any behavior may be described as a complex chain of associations between stimuli and responses (Pavlov, 1927). An alternative theory, relatively recent, is that organisms constantly build and update a model of the external world. Actions, in this case, are chosen by the organism so as to bring the highest possible outcome, according to the world model (Glimcher, 2003), and not in response to any sensory stimuli. The first theory suggests that any action is a response, while the second one that there is no such thing as a response.

Consider a rat swimming in a tank filled with some opaque liquid, e.g. milky water. If the water is cold enough, the rat wants to get out of it as fast as possible. A small circular platform can be introduced in the water-tank, such that the rat can climb on it in order to avoid staying in the water. If the platform protrudes slightly above the water, so that the rat can see it, it will learn very quickly to swim directly to the platform from any location in the water-tank (Morris, 1981).

In agreement with the first theory, this behavior can be explained by a learned stimulus-response chain. Whenever the rat sees the platform, it centers its image in the view field and swims straight until the platform is reached.

However, when the platform is submerged below the water level, so that it becomes invisible for the rat, the rat can still learn to swim straight to the platform from any location in the pool (although the learning is slower, Morris (1981)). The most intuitive explanation for this behavior is that once placed in the water-tank, the rat

estimates its position relative to the goal and calculates the path. This explanation suggest that rat has some sort of a map in the head with respect to which the positions can be estimated. The map in this case represents a model of the environment.

Note that invoking a concept of a map in the first case would be an unnecessary complication, while it is hard to explain the second case by a stimulus-response chain.

Hence we can examine both theories in a simple experimental setting. The next step is to understand what is exactly happening in the rat's brain during these experiments in order to reject either one or the other theory, or come up with a new one. In the limit of infinite time the answer to the question posed in the beginning of this introduction may be answered.

In the meantime, an interesting question is whether we can understand currently available experimental data. By understanding we mean the ability to build a computer model that can reproduce, at least to some extent, these data. We believe that such a model can provide an insight into the processes underlying decision making in the rat, thereby decreasing the amount of time needed to get the final answer.

Hence in this work we propose a model of rat navigation that can reproduce several experimental results, both behavioral and neurophysiological. Our main attention is devoted to the following questions: *(i)* how different strategies might be implemented in the rat brain and *(ii)* what is the role of sensory stimuli (both internal and external) during goal-oriented navigation.

1.2 Road-map of the thesis

This thesis consists of three main parts. The first part (Chapters 3 and 4) reviews neurophysiological and behavioral data concerning the biological networks underlying navigation and spatial representation in the rat. In the second part (Chapter 5) we propose a bio-inspired model of goal-oriented behavior. Finally, in the last part (Chapters 6 and 7) results of computer simulations in various experimental paradigms are presented and discussed. Topics treated in each chapter are:

Chapter 3 reviews spatial navigation in rats. In particular, it presents evidence for the existence of at least two different navigational strategies: taxon and locale; next, it reviews behavioral and lesion data that suggests dissociation of these navigational strategies in terms of underlying memory systems and action-generating pathways; finally, several existing theoretical models of navigations are described and their main advantages and drawbacks are discussed.

Chapter 4 reviews anatomical and neurophysiological data concerning the hippocampal formation, brain structure thought to be involved in encoding and storage of a spatial representation of the environment. In addition, firing properties of place cells and grid cells – neurons with spatially correlated activity residing in the hippocampal formation – are reviewed. Finally, short descriptions of several theoretical

models of place- and grid-cell activity are given.

Chapter 5 presents a new model of rat goal-oriented behavior, with detailed description of its components and learning algorithms.

Chapter 6 analyzes properties of modeled grid- and place cells. First, cell activities are analyzed during exploration of a novel environment; second, dynamics of place-cell firing fields are examined in geometrically manipulated environments. Discussion of the simulation results concludes the chapter.

Chapter 7 examines results of computer simulations that tested model performance in several behavioral tasks. Each simulation is followed by a discussion, and a general discussion concludes the chapter.

Chapter 8 summarizes the contributions and possible future developments of this thesis.

Chapter 2

Background

2.1 Neural networks

The model presented here relies on the artificial neural network paradigm (Hertz et al., 1991; Haykin, 1994). A neural network is a massively parallel distributed system suitable for storage and processing of complex information.

The elementary constituents of a biological neural network are simple computing units referred to as neurons. Each neuron i receives a large number of input connections termed dendrites, and transmits its response through the axon output connection. The computational power of a neural network derives from the massive interconnections between its neurons. Synapses are the elementary components that mediate the interaction between neurons.

An artificial neural network is a machinery designed to model the adaptive way in which the brain processes information to perform a given task. In particular, a neural network resembles the brain in two aspects (Haykin, 1994): *(i)* It acquires the necessary knowledge to solve a problem through a non-symbolic learning process; *(ii)* Storing this knowledge occurs through the modification of the weights of the inter-connections between neurons (i.e., synaptic plasticity).

Therefore, artificial neural networks offer a suitable tool for designing a model of navigation with learning capabilities, and allow us to model the functional properties as well as anatomical interconnections between the brain regions involved in spatial learning.

We employ a highly simplified neuronal model in which the firing activity, or *rate*, of a neuron is measured by temporally averaging the number of spikes emitted by the neuron during a particular time window (Hertz et al., 1991). The concept of rate

coding has been largely employed in artificial neural systems for its simplicity and power.

2.2 Reinforcement learning

Learning of navigation strategies in the model is performed using *reinforcement learning* (RL). Here we present a brief overview of the main concepts of RL (for a comprehensive introduction to the RL theory see Sutton and Barto (1998)).

In reinforcement learning an *agent* can be in certain *states* and perform *actions*. By performing an action, the agent changes its state, in which it can choose a new action. At certain states, the environment, in which the agent operates, can present a reward to the agent. RL is a class of methods which aims at optimizing the agent's behavior in order to maximize the reward.

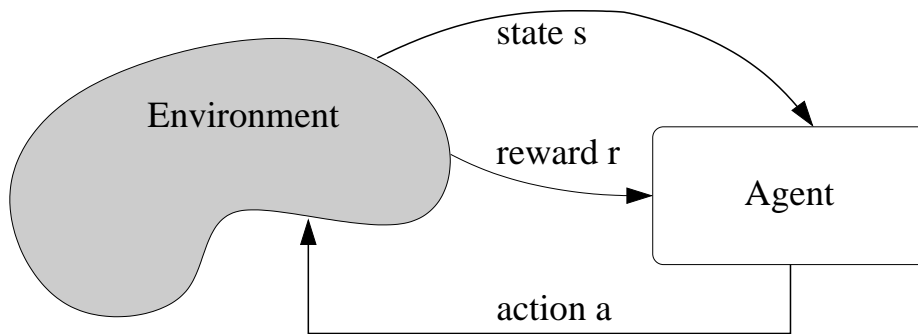


Figure 2.1: Agent-environment interaction in reinforcement learning (adapted from Sutton and Barto (1998)).

States, actions and policies

At each discrete¹ time step t , the agent is in some state $s_t \in \mathcal{S}$ where \mathcal{S} is the set of all possible states. In this state it can select an action $a_t \in \mathcal{A}(s_t)$ where $\mathcal{A}(s_t)$ denotes all possible actions available in state s_t . At the beginning of the next time step, it receives a scalar reward $r_{t+1} \in \mathcal{R}$ and ends up in state s_{t+1} . Note that states and actions are vectors. The agent has to decide which action to execute at each time step, given the perceived state (Fig. 2.1). This can be described as a mapping of the states to actions. This mapping is called a *policy* $\pi(s, a \mid \omega)$ where ω is a vector of tunable parameters:

¹We only consider the time-discrete case here, but generalizations to continuous time have been proposed (Doya, 1996, 2000)

$$\pi(s, a \mid \omega) = \Pr\{a_t = a \mid s_t = s, \omega_t = \omega\} \quad (2.1)$$

It specifies the probability of selecting action a when in state s , given the parameters ω . A policy which always selects the action which seems best according to the current information is called a *greedy policy*. It tries to maximize rewards according to the current knowledge even if this would prevent access to more abundant rewards in the future. An ϵ -*greedy policy* selects the greedy action most of the time, but with small probability ϵ randomly chooses between other available actions.

Rewards and returns

We mentioned earlier that the objective of learning was to maximize the reward. Here we focus on tasks that have a terminal state, which means that at some time step t_T the *trial* or *episode* terminates. The *expected return* $R(s_t)$ is then defined as the total discounted reward from time t up to the end of the trial:

$$R(s_t) = r_{t+1} + \gamma r_{t+2} + \gamma^2 r_{t+3} + \dots + \gamma^{(T-t-1)} r_T = \sum_{k=0}^{T-t-1} \gamma^k r_{t+1+k} \quad (2.2)$$

where $\gamma \in [0, 1]$ is the *reward discount rate*. It determines how important a future return is if it were received at the present time. The higher γ the more far-sighted is the agent. If $\gamma = 0$, future rewards are worth nothing. For the remainder of this thesis, we always refer to the discounted version when speaking of return. The RL task now consists in tuning the parameters ω of policy $\pi(s, a \mid \omega)$ such as to maximize the discounted expected return.

Value functions and Bellman equation

In order to plan an appropriate action, the agent has to estimate how good it is to be in some state, and how much an action is worth in that state. These expected returns are called *value functions*. They depend on what actions the agent will take in the future, i.e. on the agent's policy π . The *state-action value function* $Q^\pi(s, a)$ is defined for taking action a at state s , following policy π thereafter:

$$Q^\pi(s, a) = E^\pi\{R_t \mid s_t = s, a_t = a\} \quad (2.3)$$

The state-action value function follows a recursive relationship to their previous or successor value, i.e. for policy π , state s and action a , state-action values satisfy the following equation:

$$Q^\pi(s, a) = \sum_{s'} \mathcal{P}_{s \rightarrow s'}^a \left[\mathcal{R}_{s \rightarrow s'}^a + \gamma \cdot \underbrace{\sum_{a'} \pi(s', a') Q^\pi(s', a')}_{V^\pi(s')} \right] \quad (2.4)$$

where $\mathcal{P}_{s \rightarrow s'}^a$ denotes the probability that state s' is reached when taking action a in state s . $\mathcal{R}_{s \rightarrow s'}^a$ is the expected value for the reward received when action a leads from state s to s' . Equation (2.4) is called the Bellman equation for Q^π . Due to such recursive relationships the state-action value can be propagated to a previous state-action pair. The Bellman equation forms the basis of many approaches for approximating value functions, in particular for the temporal-difference (TD) learning.

Temporal difference learning

One of the most important methods to estimate the value functions is *temporal difference* (TD) learning. It allows the agent to learn directly from experience by iteratively updating state-action value estimates. Several variants of TD-learning have been proposed.

According to the *Sarsa* algorithm, state-action value $Q(s_t, a_t)$ is updated at each time step by amount $\Delta Q(s_t, a_t)$:

$$\Delta Q(s_t, a_t) = \eta \cdot \delta_t \quad (2.5)$$

$$\delta_t = [r_{t+1} + \gamma Q(s_{t+1}, a_{t+1}) - Q(s_t, a_t)] \quad (2.6)$$

where η is the learning rate and δ_t is the *reward prediction error*, that corresponds to the difference between the actual reward r_{t+1} and the predicted reward $Q(s_t, a_t) - \gamma Q(s_{t+1}, a_{t+1}^\pi)$.

Sarsa is an *on-policy* method because it updates Q by actually performing action a_{t+1} . For small learning rates η , *Sarsa* converges to an optimal state-action value function Q^* if all state-action pairs are visited an infinite number of times and if the policy converges to the greedy policy (Singh et al., 2000).

Q-learning algorithm, in contrast to *Sarsa* is an *off-policy* algorithm. The update of the state-action value function is performed according to Eq. (2.5), but the reward prediction error is calculated based on the *best*, rather than the *selected* action:

$$\delta_t = \left[r_{t+1} + \gamma \max_a Q(s_{t+1}, a) - Q(s_t, a_t) \right] \quad (2.7)$$

Q-learning directly estimates Q^* while following an arbitrary policy. Like *Sarsa*, it also converges if all state-action pairs are tried indefinitely (Watkins, 1989; Watkins and Dayan, 1992; Jaakkola et al., 1994).

Eligibility traces

So far the value functions have been calculated on the basis of a neighboring state or state-action pair only. *Eligibility traces* (ETs) extend this idea to benefit from estimates that lie further away in time. ETs can be combined with almost any TD learning variant. An ET is a memory of previously occurred states or state-action pairs. The update of the value function estimates can then be done for all states and actions *eligible* for learning. For Q-learning, an eligibility trace $e_t(s, a)$ at time t can be defined as follows:

$$e_t(s, a) = \begin{cases} \gamma\lambda e_{t-1}(s, a) + 1 & \text{if } (s, a) = (s_t, a_t) \\ \gamma\lambda e_{t-1}(s, a) & \text{else} \end{cases} \quad (2.8)$$

For undiscounted returns ($\gamma = 1.0$), this trace decays exponentially with a *trace decay factor* of λ . When the future rewards are discounted, however, the ET decays at least with the discount rate ($\lambda \leq 1$). With eligibility traces, the update $\Delta Q(s_t, a_t)$ of Eq. 2.5 extends to:

$$\Delta Q(s_t, a_t) = \eta \cdot \delta_t \cdot e_t(s, a) \quad (2.9)$$

Equations 2.8 and 2.9 make all previously visited state-action pairs eligible for learning. Most recent actions get more “credit” for the current estimate of expected return and their values are modified to a greater extent than for decisions taken far in the past. For Q-learning, eligibility traces are valid only until a non-greedy action is taken (Watkins, 1989). This considerably reduces the benefit of ETs for Q-learning. Other variants of off-policy TD methods seem to work well in practice but their convergence is still an open question (Peng and Williams, 1996), but see also (Precup et al., 2000).

Continuous spaces and generalization

One of the problems in reinforcement learning is that the learning speed highly depends on the dimensionality of the state and action spaces. A related issue is the case of continuous spaces. Both problems can be solved by using function approximation for the state and action values.

The key idea is that updating an estimate for a specific state also affects the estimates of similar states.

This idea thus applies to the problem of continuous states/actions as well as to generalization. In special cases, convergence has been proved, whereas other cases are known to diverge (Gordon, 1995; Baird III, 1995; Tsitsiklis and Roy, 1996; Sutton et al., 1999; Precup et al., 2000, 2001). In our model (Chapter 5), we implicitly use function approximation to generalize in continuous state and action spaces.

2.3 Environment model

This thesis follows the animat approach, in which the modeling of cognitive functions takes explicit interest in the interactions between the modeled individual and its environment (Guillot and Meyer, 2001).

The performance of the model is assessed through experimental tests using a computer program, referred to as ‘simulated rat’, which is able to gather external sensory information from the environment and use it, along with a self-motion input, to select among future possible actions.

The experimental environment is modeled as a three-dimensional virtual room, the size and visual features of which are set depending on the experiment (see below). The position of the simulated rat in the room is changed in discreet time steps of 0.125 s according to its speed (constant and equal to 16 cm/s) and direction. At each time step an input visual image is generated by calculating a snapshot of the virtual environment according to the position and gaze direction of the model animal using a standard computer graphics algorithm (ray casting, Foley et al. (1995)). The horizontal view field of the model rat is 300°.

Testing environments

Two types of experiments were conducted, similar to ‘behavioral’ and ‘neurophysiological’ experiments with rats.

For behavioral experiments simulating watermaze tasks were performed in a square room of 2m×2m with high walls. Photographs of a typical laboratory environment were attached to the walls of the room with the aim of simulating multiple visual cues. The experimental arena, located in the center of the room, was surrounded by a grey circular wall 1.2m in diameter and 0.2m high so as to simulate the wall of the watermaze (environment B-I, Fig. 2.2). An invisible target area 6 cm in diameter located in the southwest quadrant of the simulated watermaze served as a hidden goal. Environment B-II was designed analogous to the experiment of Cheng (1986) and consisted of a rectangular room with grey walls and distinct landmarks in the four corners. The room size was 1m×0.5m with walls of 0.6m high.

For ‘neurophysiological’ experiments on the model, i.e. when activities of single cells were analyzed, we re-used environment B-I, except that the circular watermaze was replaced by a square area of 1m×1m with transparent walls at the center of the room (environment N-I, Fig. 2.2). In the experiments with shrinking and stretching environments two series of rectangular rooms were used (N-II and N-III). In each series the first room (N-IIa and N-IIIa) is referred to as ‘original’ environment and the other rooms as shrunk (N-II) or stretched (N-III) versions of the original room. All rooms had the same width (1.2m) and their lengths were 1.8m, 1.5m, 1.2m, 0.9m and 0.6m for the N-II series and 0.6m, 0.75m, 0.9m and 1.2m for the N-III series.

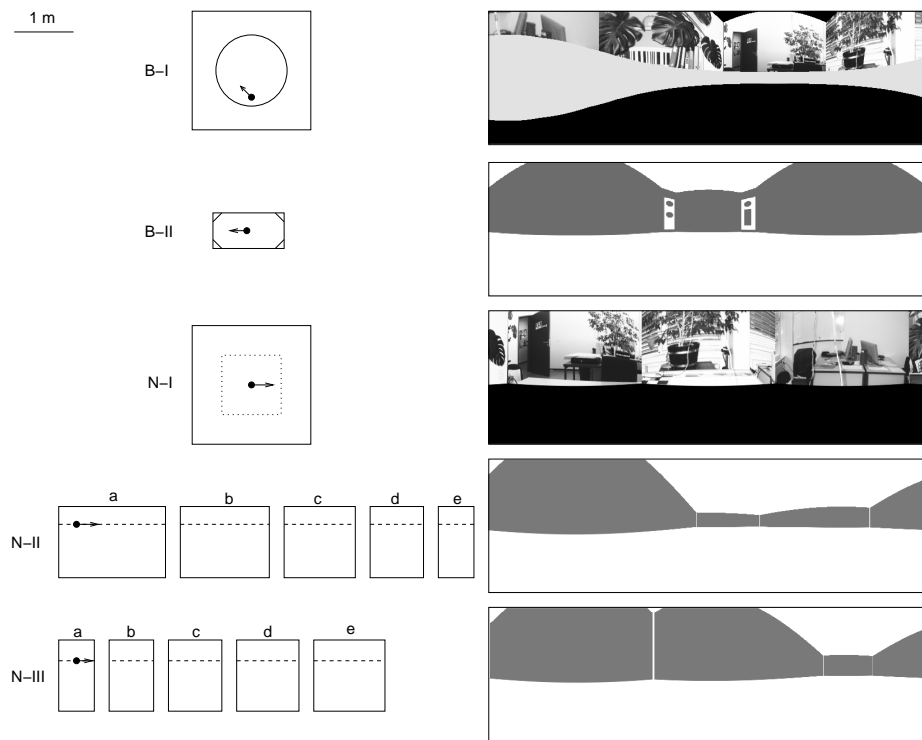


Figure 2.2: Testing environments used in computer simulations. In each row the left part of the figure shows the top view of the virtual room and the right part shows an example snapshot of the room (the black dot and the arrow show the position and direction at which the snapshot was taken). The circle in the top view of room B-I marks the border of the simulated watermaze. The dotted line in the top view of the room N-I marks the area accessible to the model rat in this environment. The dashed line in rooms N-IIa-e and N-IIIa-e marks a linear trajectory of the model rat.

The lengths were chosen to approximate the real experimental conditions (Gothard et al., 1996; O’Keefe and Burgess, 1996). Each room had grey walls 0.6m high.

Chapter 3

Rat navigation

Navigation is defined as the capability of planning and performing a path from the current position towards a desired location (Gallistel, 1990). Two fundamentally different types, or strategies, of navigation can be distinguished (O’Keefe and Nadel, 1978). *Taxon navigation* is the one in which goal-oriented movements are defined by a reference to a specific sensory cue (or a set of cues) external to the organism, e.g. movement in the direction of a particular landmark or away from it, movement along a wall, movement in the direction of a specific odor, etc. In contrast, *locale navigation* defines movement as happening from one place to another, where ‘place’ is an abstract notion defined as a position on the map of the environment (experimental evidence for the existence of such a map in the mammalian brain is reviewed in Chapter 4). An important difference between these two types, or strategies, of navigation¹ is in the flexibility with which different goal-directed paths can be generated. Whereas the taxon navigation suggests a particular path and is easily disrupted by the alteration of relevant cues, the locale navigation is flexible in the choice of the path from one place to another and is relatively resistant to the effects of environmental changes.

Several dichotomies related to the one of locale/taxon are used in the experimental literature (see Table 3.1) and reflect different aspects of the two strategies

Egocentric vs Allocentric. The egocentric frame of reference is defined relative the animal. The current position of the animal defines the origin of such a reference frame and its the current heading defines the reference direction (i.e. 0°, Fig. 3.1a). In contrast, the allocentric frame of reference is defined with respect to static sensory cues external to the animal, i.e. independent of the animal’s current position and

¹A number of different taxonomies of navigation exist that propose further subclasses of either the taxon or locale navigation (see Gallistel (1990); Trullier et al. (1997); Redish (1999))

Navigation type	taxon	locale
Frame of reference	egocentric	allocentric
Learning mode	stimulus-response	place
Dimensionality of trajectory space	1D (route)	2D (map)

Table 3.1: Distinctions between stimulus-response and cognitive navigation strategies

heading. For example, the center of a recording chamber can serve as the origin of an allocentric reference frame, and direction towards the eastern wall can serve as a reference direction. An important distinction between the goal-oriented behaviors organized in the two reference frames is that knowing the goal position in the egocentric reference frame is sufficient to approach the goal, whereas knowledge of the goal's allocentric coordinates can be used only if the current allocentric position of the animal is known as well.

Response vs Place learning. Behavioral experiments dealing with dissociation between different navigation strategies (see Section 3.1) usually describe behavioral decision in terms of response and place strategies (the terms are equivalent to the taxon and locale strategies, but emphasize the result of learning). The response learning strategy² amounts to remembering a specific motor response to a set of visual or other sensory stimuli (e.g. turning right in the central junction of the cross maze, Fig. 3.1b), whereas the place strategy requires memory for a location of the food with respect to the extra-maze visual cues. The two strategies can be dissociated by observing rat behavior in altered experimental conditions: animals that learned the response strategy will repeat the same motor response, while those who learned the place strategy will go to the same place. Such dissociation experiments together with lesion studies (see Section 3.1) provide an insight into the biological mechanisms that implement those strategies.

Routes vs Maps. Finally, the taxon and locale strategies can be distinguished on the basis of trajectories that these strategies generate. The taxon behavior suggests movement along a one-dimensional route since each stimulus-response association implies a particular motor response or movement in a particular direction. In contrast, the locale strategy does not specify how to get from one place to another, allowing for making shortcuts and detours. In addition, locale strategy can be used to approach the goal from novel starting positions, provided that these starting positions belong to the map, whereas taxon navigation assumes an exact repetition of learned responses and hence unable to generalize to novel starting positions not seen during training. The latter distinction has been used to experimentally dissociate the two strategies.

²Sometimes it is also referred to as *stimulus-response* or *cue-response* strategy, when response to a particular visual cue is learned

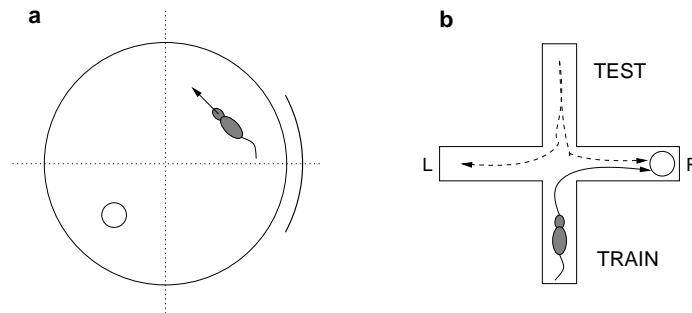


Figure 3.1: (a) Circular environment with a cue card (arc). If the goal (circle) is visible, its egocentric direction (with respect to the rat) can be estimated from visual input as 90° to the left. The goal can be approached solely on the basis of this egocentric information, i.e. without knowing the relative positions of the cue card and the goal. If the goal is hidden, its position has to be remembered with respect to the cue card. In order to approach the goal, an estimation of rat's position in this allocentric reference frame is required. (b) Cross maze with the food source in the right arm. If the starting position is changed from the bottom arm (used during learning) to the top one, the response strategy leads the animal to the left arm (L), whereas the place strategy leads them to the right arm (R).

Large body of experimental evidence, both behavioral and neurophysiological, suggest that the two strategies are implemented by distinct brain areas. In particular, expression of the taxon navigation has been related to the function of the dorsal striatum of the basal ganglia, whereas locale navigation is thought to be mediated by the hippocampus and nearby areas.

This chapter is organized as follows: Section 3.1 describes behavioral and lesion data showing that the two strategies can be acquired independently from each other and hence mediated by different memory systems; Section 3.2 is devoted to the question of how a particular memory system can modulate goal-oriented behavior; Section 3.3 reviews the role of sensory cues during goal-oriented behavior, in particular the influence of geometry of space is discussed; finally, Section 3.4 reviews existing models of navigation.

3.1 Memory systems underlying navigation

3.1.1 Locale and taxon strategies in the watermaze

The difference between locale and taxon navigation strategies has been investigated in the watermaze as well as in radial mazes (including T-mazes).

Locale strategy in the watermaze was first demonstrated by Morris (Morris, 1981). In the standard version of this task, the rat is placed in a circular pool filled with colored water and has to learn the location of a platform hidden somewhere in the pool. The rat is released from different starting locations in the watermaze in different trials so that it has the opportunity to see the extra-maze cues from different perspectives and to encode a representation of the location of the platform based on the relations among them. The kind of memory formed is flexible in the sense that, after the rat has learned the task, it can find the platform even after being released from a starting location that it has never experienced during the training. Lesion or inactivation of the hippocampal formation (including the fimbria fornix) disrupts this kind of place learning (Da Cunha et al., 2003; Morris et al., 1982; Sutherland et al., 1983).

However, Eichenbaum et al. (1990) showed that fimbria fornix-lesioned rats were able to learn a version of this task in which they were trained to always begin from the same location. This kind of training encouraged rats to associate the extra-maze cues with a particular swim trajectory, which was reinforced by successful escape from the water. It also offered the rats the opportunity to see all the cues as a unique set of extra-maze stimuli (i.e. an environment snapshot) that could be associated with a response strategy to find the platform. In other words, this protocol transformed the water maze task from a multiple relational task including multiple distal stimuli into another task that could be solved in a stimulus-response (S-R) way.

As learning of spatial/relational tasks has often been suggested to depend on the hippocampus or fimbria fornix (Morris et al., 1982; O'Keefe and Nadel, 1978; White, 2004), S-R habit learning, in which a stimulus or a set of stimuli is repeatedly associated with a rewarded response, has often been reported to depend on components of the basal ganglia, such as the dorsal striatum (McDonald et al., 2004; Packard et al., 1989; Packard and McGaugh, 1992a; White, 2004) and the substantia nigra pars compacta (Da Cunha et al., 2003; Cunha et al., 2006; Miyoshi et al., 2002).

A double dissociation of the dependency on the hippocampus and the SNc for the watermaze tasks with hidden and visible platforms has been demonstrated by Da Cunha et al. (2003). A double dissociation of the hippocampus and the dorsal striatum for acquisition of these two tasks has been demonstrated by Packard and McGaugh (1992a).

In Chapter 7 we will use our novel model of navigation (described in detail in Chapter 5) to reproduce some of the experimental results described above, in particular those of Morris (1981); Morris et al. (1982); Eichenbaum et al. (1990).

3.1.2 Radial mazes

A similar dissociation of the locale and taxon strategies has been shown in experiments with radial mazes.

Using an 8-arm maze, McDonald and White (1993) showed a triple dissociation of learning and memory functions in the mammalian brain. This dissociation was demonstrated by assessing the behavioral effects of lesions to the amygdala, dorsal striatum, or hippocampus. Groups of rats with lesions to these brain areas were trained on three behavioral tasks including a *(i)* a stimulusresponse habit task, *(ii)* a spatial memory task, and *(iii)* a conditioned cue preference task.

(i) During acquisition of the stimulusresponse (SR) habit task (Packard et al., 1989), rats learned an association between a particular stimulus (light) and a motor response (turn) that is repeatedly reinforced. Rats with lesions of the dorsal striatum were impaired at this SR habit task but rats with lesions of the lateral amygdala or hippocampus showed normal acquisition of this task.

(ii) For the spatial version of the radial maze, rats learned to obtain eight food rewards (one found at the end of each arm) by entering each arm once and avoiding previously visited locations within each day (win-shift task). Evidence suggests that during training, rats form a spatial representation of the environment and use it to distinguish visited from unvisited arms (O'Keefe and Speakman, 1987; S. Suzuki et al., 1980). Rats with lesions of the hippocampus were impaired at this form of spatial learning whereas rats with lesions of the lateral amygdala or dorsal striatum showed normal acquisition of this task.

(iii) For the conditioned cue preference task, rats learned to associate different visual cues with the presence or absence of highly palatable and rewarding food. On the test day, the rats were given a choice between the two arms, neither of which contained food. Normal animals spent more time in the arm and associated cue condition that was associated with food than the other arm that was never associated with food. Rats with lesions of the lateral amygdala were impaired at this form of classical conditioning but rats with lesions of the dorsal striatum or hippocampus showed normal acquisition of this task.

Together, these findings demonstrate a triple dissociation among memory systems (White and McDonald, 2002) and leads to conclusion that learning in each of these situations required some unique information processing that was normally mediated by one of the damaged brain structures. These data also suggest that the different systems may acquire information independent from one another.

3.2 Basal ganglia

The data above suggests that that different memory systems mediate the expression of the two navigation strategies. The next question is how these memory systems are involved in the generation of behavior.

In addition to its role in S-R learning described above, the basal ganglia has been related to the high-level control of movement because of its involvement in such

motor disorders as Parkinson's and Huntington's diseases (Graybiel, 2000; Packard and Knowlton, 2002). The anatomy of basal ganglia connections suggests that, at least in part, these structures operate as part of recurrent circuits (loops) with the cortex (Alexander and Crutcher, 1990; Alexander et al., 1986). Broad subdivisions exist within these cortico-basal ganglia loops, suggesting that different loops operate in relation to different types of cortical function, and potentially to different types of behavior. Before describing these loops we briefly review the anatomy of the basal ganglia.

The main input structures to the BG are the striatum and the sub-thalamic nucleus (STN) (see Fig. 3.2). The striatum is innervated by almost all cortical areas and the hippocampus. It is further subdivided along the dorso-ventral axis into the dorsal striatum, or *caudate putamen* (CP) whose main afferents come from cortical areas and the *nucleus accumbens* (NA), which is innervated by both the hippocampus and cortical areas.

The dorsal striatum is anatomically divided in two regions: patch and matrix. The matrix is structurally segregated in isolated neural compartments and projections from this area to output structures of the BG preserve the compartmental segregation, except for projections to the STN. Such a segregated structure has been proposed to implement independent sensory-motor associations (Mink, 1996). This is in agreement with behavioral studies described above which suggest the role of the dorsal striatum in stimulus-response behaviors.

The NA is one of the major targets of the fornix (Witter et al., 1990) which can carry place information from subiculum and CA1. Lesions of NA produce deficits in the hidden platform version of the watermaze, but not in the visible platform (Annett et al., 1989; Sutherland and Rodriguez, 1990), suggesting that it can mediate hippocampus-dependent navigation.

The main outputs of the BG are the *substantia nigra pars reticulata* (SNr) and the *globus pallidus pars interna* (called entopeduncular nucleus (EP) in rodents). This areas project back to the cortex, in particular to the motor cortex, the brainstem and to the superior colliculus, areas that are involved in motor control (Amaral and Witter, 1995; Heimer et al., 1995; Mink, 1996).

This closed cortico-striatal-cortical circuit is subdivided in parallel independent loops originated in different regions of cortex, passing through specific sub-regions of the BG nuclei (Alexander and Crutcher, 1990; Alexander et al., 1986), and projecting back from there to the same cortical areas. In particular, two such loops can be related to the implementation of the locale and taxon strategies:

1. Motor loop, consisting on the dorsal pathway of the BG, including the CP, the globus pallidus and the lateral part of the SNr. It also involves motor regions of the cortex. It has been suggested to be involved in instrumental memory, and developing of stimulus-response associations (Graybiel, 1998).

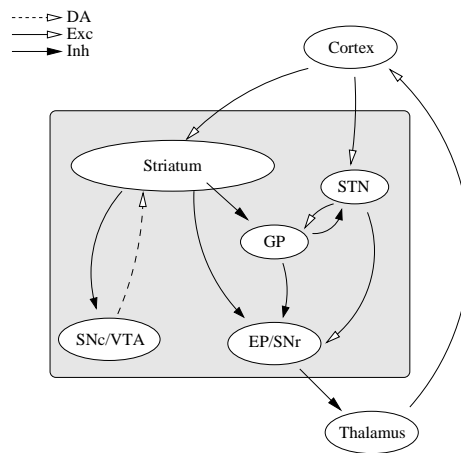


Figure 3.2: Schematic representation of the interconnectivity in the BG. Projections from the hippocampus and amygdala to the ventral part of the striatum are not represented. Dopaminergic projections are represented by dashed arrows. Open arrowhead denotes excitatory connections and filled arrowheads denote inhibitory connections. See the text for further description.

2. Limbic loop, corresponding to the ventral pathway of the BG, including the ventral striatum (particularly the NA) and the hippocampus (Thierry et al., 2000). Several models of hippocampus-dependent navigation have proposed the NA as the putative locus for selecting actions based on place coding projections from the hippocampus (Burgess et al., 1994; Brown and Sharp, 1995; Arleo and Gerstner, 2000b).

Each one of these loops may be further segregated in independent parallel sub-circuits.

The dorsal striatum and nucleus accumbens receive dopaminergic input from *substantia nigra pars compacta* (SNc) and the ventral tegmental area (VTA) of the basal ganglia, respectively. Dopaminergic neurons in these areas tend to synapse on the same spines than cortical and hippocampal afferents (Freund et al., 1984). Dopaminergic activity is believed to regulate the plasticity of cortico-striatal synapses (Schultz, 2002) and hence provides the possibility of reward-based learning in the basal ganglia, in particular reward-based learning of navigational strategies.

Our model of navigation, described in Chapter 5, is based on the anatomical data described above. In particular, the taxon navigation pathway in the model is a simplified implementation of the cortico-striatal motor loop, whereas the locale navigation pathway represents the limbic loop.

3.2.1 Reward-based learning

There is increasing evidence that dopamine is involved in reward-related learning. As mentioned before, dopaminergic neurons (DNs) in the SNc and VTA project to the caudate putamen, nucleus accumbens and most parts of neocortex. DN's show regular or tonic firing patterns, as well as transient or phasic firing activity. DN's phasic activity is related to primary rewards (Hollerman and Schultz, 1998) and predicted reward (Schultz, 1998; Apicella et al., 1992; Schultz et al., 1992).

Several studies suggest that phasic dopamine release could serve as a biological implementation of the TD-error of reinforcement learning (Houk et al., 1995; Schultz et al., 1997; Suri and Schultz, 1998, 1999, 2001; Doya, 2002) and code for the reward prediction error (see Chapter 2).

As mentioned before, dopaminergic neurons in the striatum tend to synapse on the same spines as the afferent axons from cortical areas. It is therefore possible that DN's influence or modulate either synaptic transmission or synaptic plasticity of cortico-striatal connections (Freund et al., 1984; Sesack and Pickel, 1990; Smith et al., 1994). There are at least two possibilities how DN's can influence learning. First, dopamine has been shown to focalize cortico-striatal transmission, which only allows the strongest signals to pass (Otmakhova and Lisman, 1998; Schultz, 1998; Redgrave et al., 1999; Schultz, 2002). This can be seen as a gating signal which only enables the most important inputs to reach the postsynaptic neuron. Alternatively, phasic dopamine release might directly influence plasticity in the target area. In striatum, prefrontal cortex and hippocampus, dopamine agonists enhance synaptic potentiation whereas antagonists impair potentiation (Otmakhova and Lisman, 1996, 1998; Gurden et al., 1999; Kerr and Wickens, 2001). In recent experiments dopaminergic neurons in the SNr were electrically stimulated to simulate a reward prediction error. This resulted in potentiation of cortico-striatal projections (Wickens et al., 1996; Reynolds et al., 2001). Prefrontal and auditory cortex also show potentiation if a phasic dopamine release is simulated (Bao et al., 2001; Blond et al., 2002).

Other neuromodulators have been suspected to correspond to reinforcement learning variables. Serotonin may regulate the discount rate of future rewards (Eq. (2.2)). Indeed, rats with depleted serotonin levels tend to impulsively favor small immediate over larger, but delayed rewards (Doya, 2000; Mobini et al., 2000; Doya, 2002)

Noradrenaline seems to be involved in the control of arousal and relaxation and is suspected to govern the exploration-exploitation tradeoff (Doya, 2000, 2002). Activity of noradrenergic neurons is correlated with the accuracy of action selection, especially in urgent situations (Aston-Jones et al., 1994; Usher et al., 1999)

Acetylcholine may regulate the speed of learning (η in equation 2.5) (Doya, 2000, 2002).

In our model of navigation, reward based learning of navigational strategies is performed in the simplified model of basal ganglia subareas, in particular, caudate

nucleus and nucleus accumbens. In agreement with the data described above our learning algorithm makes use of the reward signal, presumably received by these subareas in the form of phasic dopamine input. More specifically, the dopamine signal is associated with the *reward prediction error* δ (see Chapter 2).

3.3 Role of sensory cues during goal-oriented behavior

During both locale and taxon navigation, animals rely on different types of sensory cues. In the taxon condition external cues that mark the position of or direction to the goal are important. In the Morris watermaze the visible platform itself or another intra-maze object that marks the position of the platform can be used as an beacon (Morris et al., 1982; Packard and McGaugh, 1992a; Devan and White, 1999). In the watermaze task with the constant start (Eichenbaum et al., 1990; Cunha et al., 2006), a configuration of landmarks visible from the starting position can serve as an extra-maze directional cue. In homing tasks where the use of self-motion cues was prevented, the animals could return to the starting position using smell (Maaswinkel and Whishaw, 1999).

The locale navigation was shown to depend on path integration (i.e. integration of self-motion information over time (Etienne, 1998; Maaswinkel and Whishaw, 1999)) in addition to distal visual cues (McNaughton, Leonard, and Chen, 1989; Knierim et al., 1995; Wilson and McNaughton, 1993). Behavioral studies suggest that when several types of cues are available that give conflicting predictions about the goal location, visual cues predominate over other types of cues, e.g. olfactory and self-motion (S. Suzuki et al., 1980; Maaswinkel and Whishaw, 1999). Is there a similar hierarchy within the set of all possible visual cues? Cheng (1986) and later Gallistel (1990) suggested that geometry of environment plays a primary role during navigation.

3.3.1 Geometric module hypothesis

Cheng (1986) proposed that information about the shape of the surrounding environment, presumably extracted from the visual information, predominate over the non-geometric information such as texture, visual pattern, etc. In Cheng's experiments, food-deprived rats were shown food hidden inside a rectangular box. Multimodally distinct features (including olfactory, visual, and tactile characteristics) were attached to the corners of the box. After disorientation the rats were allowed to search for the food. Surprisingly, the rats made systematic rotational errors, i.e. they went to the location that was diagonally opposite to the correct location, as if they were orienting by the rectangular shape of the room and discarded information from the corner landmarks. Similar findings have been reported by other investigators

(Margules and Gallistel, 1988; Cheng and Newcombe, 2005) and have led to the proposal that disoriented rats re-orient themselves in a familiar environment by means of a ‘geometric module,’ impenetrable to non-geometric information (Gallistel, 1990; Wang and Spelke, 2003).

Impenetrability, or encapsulation, of a mind module (Fodor, 1983) means that it deals only with a restricted subset of potentially available sensory data. Such a property increases the efficiency of computation to which the module is dedicated by limiting the number of relevant inputs. In the case of the geometric module this subset is represented by the information about the spatial arrangement of surrounding surfaces, the shape of the environment. The non-geometric information, according to this hypothesis, is not used during reorientation due to the encapsulation property. In a follow-up experiment Cheng (1986) has shown that rats were able to distinguish one corner from the others on the basis of the landmark information, if they started each trial from the same location (the center of the arena). This result was taken as an evidence that rats could see the landmarks but did not use them during reorientation, in agreement with the geometric module hypothesis.

In a study aimed at testing directly the geometric module hypothesis Pearce et al (Pearce et al., 2004) first trained rats to swim to a target platform hidden in the corner of a featureless rectangular water pool, and then examining their corner choices in an environment with a different shape (a kite-shaped pool). In this new environment, one of the corners was identical to the target corner in the training environment. If the rats were orienting themselves using only the shape information, then their corner choices in the new environment would be random, since the shapes are different. In contrast, rats in this experiment choose the similar-to-target corner significantly more often than would be predicted by chance. These results contradict the geometric module hypothesis and suggest that rats might use local-cue matching strategy in this task.

One of the major goals of the present study is to analyze the rat’s behavior in the experiments of Cheng (1986) and (Pearce et al., 2004) from the point of view of neuronal networks that are thought to underly navigational behavior. In particular, in Sections 7.2 and 7.3 our model is used to reproduce these results.

3.4 Models of rodent navigation: state of the art

In this section several models of rodent navigation and action control are reviewed. Two types of models are presented. Section 3.4.1 reviews models of locale navigation. These models rely on a stored representation of space which interacts with neural representation of action (i.e. directions of movement) or goal locations. Section 3.4.2 reviews the second type of models, in which the neural circuit of the BG implements reward-based action selection (Houk et al., 1995; Montague et al., 1996; Doya, 1999).

They propose that the BG, and more specifically its dorsal pathway, encode different sensory-motor programs (corresponding to S-R associations).

3.4.1 Models of Hippocampus-dependent navigation

Burgess *et al.* (1994)

In the navigation model of Burgess *et al.* (1994), place cells in the subiculum project to a population of eight goal cells. A head direction system consisting of eight cells with fixed one-to-one connections to the goal cells attributes a particular direction to each goal cells. These connections are gated by a reward signal, such that goal cells are only activated if a head direction cell is active *and* a reward is delivered.

Every time the agent reaches a rewarding location, it looks in all eight directions. In each of them, a reward is delivered at the late phase of the θ cycle. Hebbian-type learning is then applied to the binary synapses from the subicular place cells to the goal cells. Place cells that fire at the late phase of θ tend to have receptive fields located *ahead* of the present position. A goal cell coding for ‘north’, for instance, is thus contacted by subicular cells located to the north of the goal. As the receptive fields of subicular place cells are very large, the fields of the goal cells are also large. This allows the system to estimate its bearing and distance with respect to the goal location from almost any place of the environment after only one trial.

This model postulates goal cells in the subiculum which are necessary for locale navigation. This is in contradiction to experimental data where fornix lesions impair rats in the hidden water maze (Eichenbaum *et al.*, 1990; Sutherland and Rodriguez, 1990; Packard and McGaugh, 1992a). Furthermore, the goal cells in this model create a *global* basin of attraction towards the goal. Local information such as obstacles are not taken into account. Finally, this learning mechanism also suffers a ‘distal reward’ problem because only those place cells whose fields contain the goal may learn place to action associations.

Brown and Sharp (1995)

In the model by Brown and Sharp (1995) a population of ‘motor’ cells in nucleus accumbens receives spatial information from the hippocampal place cells (Fig. 3.3). Together with a head direction system, the model learns to perform movement commands which lead to a rewarding location. Nucleus accumbens cells are separated in two clusters of 60 motor neurons and the same amount of inhibitory interneurons. Each of the 60 place cells is connected to a unique interneuron of each cluster. Each interneuron in turn projects to a unique subset of 59 motor cells, which form the output of the navigation system. These synapses are fixed.

Every time the agent encounters a rewarding position in the environment, head

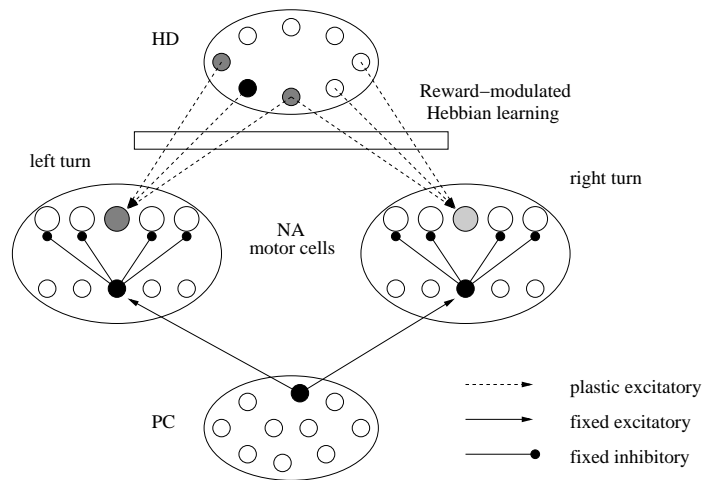


Figure 3.3: Navigation architecture proposed by Brown and Sharp (1995): Nucleus accumbens (NA) consists of two populations; one for right turns, the other for left turns. Each place cell (PC) has a fixed connection to an inhibitory neuron in each NA cluster. Each interneuron is connected to a unique subset of excitatory output cells, containing all but one “motor” cells. Head direction (HD) cells learn to select left or right turn motor cells by reinforcement-modulated Hebbian learning.

direction cells modify their synaptic weights to the active motor unit using a reward-modulated Hebbian-type learning rule. An exponentially decaying memory trace of pre- and postsynaptic coactivation enables the agent to propagate reward information along its trajectory. Most recently active synapses are strengthened most, while the change in synaptic efficacy for previously active synapses is smaller.

In test trials, the two active motor units compete for action selection. A left turn is performed if the ‘left’ motor unit is more active than the right and vice versa. The model is able to solve the hidden water maze task.

This model updates its place-action mapping only when a rewarding location is encountered. Places that are far away from the goal are only associated to actions using a global temporal activity trace. The existence of such long memory traces in animals is still an open question.

Abbott and coworkers (1996, 1997)

The work by Abbott and coworkers (Blum and Abbott, 1996; Gerstner and Abbott, 1997) suggests that hippocampal region CA3 is the neural substrate for navigation maps. Learning on the recurrent CA3 connections using spike timing dependent plasticity results in a shift of receptive fields towards the goal location. Initially, CA3 place cells have perfectly Gaussian receptive fields with high overlap. Training consists

of repeated trials, ending when the agent reaches the goal location. This procedure introduces an inhomogeneity with respect to the experienced trajectories: No path can lead from the target to other places because trials end at the goal location.

Navigation maps to multiple targets can be represented simultaneously: Place cell activity is modulated by the distance to the target location. After learning, navigation maps to multiple targets can be recalled. Routes to novel target location can also be generated by superposition of the learned maps.

The learning rule used in this model produces a shift of the place fields in the direction opposite to the goal location. In order to use this shift for navigation, the original place field centers are accessed explicitly to calculate the agent's next movement, which is a biologically implausible operation. Furthermore, this model of locale navigation is entirely concentrated in the hippocampus. It is not consistent with the impairments reported in the hidden water maze following fornix or nucleus accumbens lesions (Eichenbaum et al., 1990; Sutherland and Rodriguez, 1990; Packard and McGaugh, 1992a).

Gaussier and coworkers (1998, 2000, 2002)

In the navigation model by Gaussier and coworkers (Gaussier et al., 1998, 2000, 2002), a transition prediction network based on place cells 'proposes' candidate future places (see Fig. 3.4). Competition within the transitions recognition layer selects the most active transition (e.g. node BD, leading from place B to place D). This competition is biased by a goal planning layer. Motor actions are associated to transitions using Hebbian-type learning.

The goal-planning layer contains units which code for the same transitions as the recognition layer. Here, however, the transition units are interconnected with constant synaptic weights $w_{ij} < 1$. Whenever a motivation input activates a node (e.g. DG1, the transition from place D to goal G1), this activity $A_0 = 1$ propagates back to all other transitions. Activities $A_i = \max_j(w_{ij}A_j)$ are calculated iteratively until the network settles in a stable state. Once stabilized, node activities are set according to their distance to the goal location. These activities bias the competition in the transition recognition layer, such that transitions which lead to the goal on the shortest path are favored.

According to this model, locale navigation is implemented in the hippocampus, which is in contradiction with experimental data, suggesting that the fornix projection to nucleus accumbens is necessary to solve the hidden water maze task (Eichenbaum et al., 1990; Sutherland and Rodriguez, 1990; Packard and McGaugh, 1992a). The goal planning layer operates on the symbolic place transition nodes. The shortest path to the goal in this layer needn't correspond to the shortest path in the real environment.

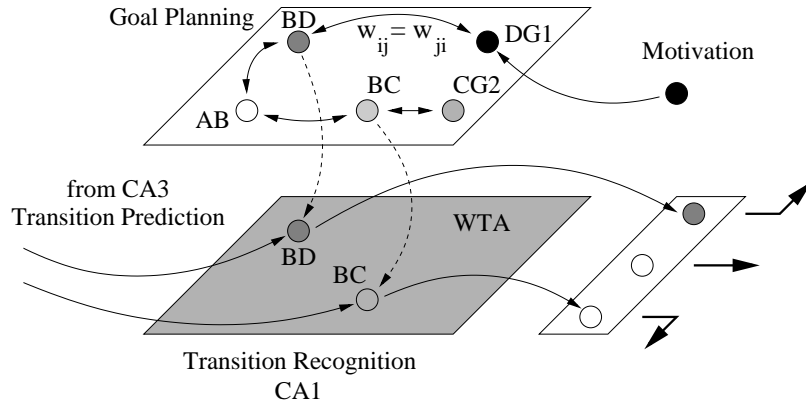


Figure 3.4: Navigation architecture proposed by Gaussier and coworkers: Transition predictions are made in CA3 (not shown) and propagated to the CA1 network. There, winner-take-all (WTA) competition selects the most active transition and executes its attributed motor command. Competition is biased by transition units in the goal planning system which, according to motivation, back-propagates transitions to goal locations (e.g. DG1) through the network.

Foster *et al.* (2000)

The model proposed by Foster *et al.* (2000) (Fig. 3.5) is based on an actor-critic architecture for temporal-difference (TD) reinforcement learning (see section 2.2). A layer of place cells (PCs) with perfectly tuned Gaussian receptive fields provides the navigation system with the agent’s position within its environment.

A ‘critic’ neuron c receives input from each PC i . Its firing rate $r_c = \sum_i w_{ci} r_i$ represents the estimated “value” of the current agent position. The critic also outputs a reinforcement signal δ in the form of a temporal difference of current and previous activities (i.e. position value prediction error). This signal is used to improve value estimation by modifying afferent connection weights w_{ci} towards $\delta \cdot r_i$ and thus reduce the error δ .

An actor network consisting of eight neurons is responsible for selecting actions. Each cell a codes for a direction of movement and receives afferent connections of strengths w_{ai} from each PC i . Actions are selected stochastically, but cells with a high firing rate $r_a = \sum_i w_{ai} r_i$ are favored over cells with low firing rates. The weights w_{ai} are modified using Hebbian-type learning, modulated by the critic’s error signal δ .

Using this mechanism, navigation to a stable hidden goal location can be learned in about ten trials. When a learned target is relocated, however, relearning the new location takes longer due to interference with the previous goal location. To overcome this difficulty, a coordinate system (CS) is added to the model: The CS consists of five neurons: two of them represent the current position of the agent (x, y) , the next

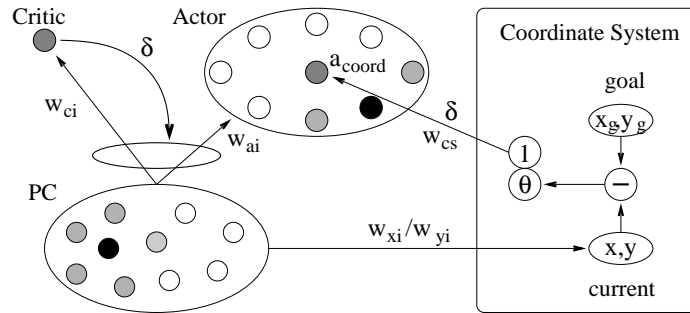


Figure 3.5: Navigation architecture proposed by Foster *et al.*: An actor-critic architecture is employed to learn a navigation map. Places are coded by a place cell population (PCs). The actor selects actions whereas the critic estimates the quality of these actions. The critic also generates a reinforcement signal δ which guides learning of better actions and quality estimations. A task-independent coordinate system (CS) is learned from place cell activity. Once learned, CS can store the goal location and propose goal-oriented actions a_{coord} by vector subtraction.

two code for a goal location (x_g, y_g) to be learned, and the remaining neuron is an action neuron a_{coord} . The mapping of place cell activity to coordinates (x, y) is learned using TD-learning. Each time the reward is found (i.e. at the end of each trial), the current estimated coordinates (x, y) are copied into the goal memory (x_g, y_g) . The ‘abstract’ action a_{coord} neuron competes with all other actor cells for action selection. Its activity, however, doesn’t depend on the agent location, but on how well the coordinate system is tuned. Modification of its weight w_{cs} is similar to other actor neurons, i.e. modulated by δ . Whenever a_{coord} is selected, the direction of movement θ is given by vector subtraction of goal–and current coordinates.

During learning, the agent’s movement is restricted to eight predefined headings. Furthermore, learning does not generalize to neighboring directions. The coordinate-system module, once adapted, creates a global basin of attraction. Local information such as obstacles are then completely ignored. The direction of the next movement is algorithmically calculated by explicitly accessing the coordinates of the goal location, which is not biologically plausible.

Arleo *et al.* (2000, 2001)

Arleo and Gerstner (2000b); Arleo *et al.* (2001) propose a locale navigation system using reinforcement learning (Sutton and Barto, 1998). It is based on the spatial representation outlined in Section 4.4.1. Each place cell projects to four ‘action cells’, coding for north, south, east and west respectively (Fig. 3.6). The synaptic strengths represent a ‘navigation map’ and are modified using a reward-based learning method:

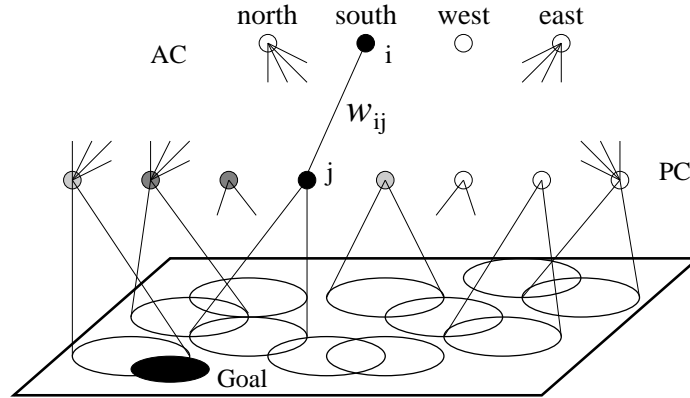


Figure 3.6: Navigation architecture proposed by Arleo *et al.*: Place cells (PCs) drive a set of four action rule (ACs). Connections strengths w_{ij} are modified by a reinforcement learning rule.

Suppose that the agent is at place A . The activity $r_i(s) = \sum_j w_{ij}r_j$ of action cell i depends on place cell activities r_j and synaptic weights w_{ij} . It estimates the ‘value’ of action $a_i(s)$. When taking action a_i , the agent reaches place B and gains access to action value estimates of the new place. The weights w_{ij} are adapted to correct for bad estimates at the previous place A . In particular, Watkins $Q(\lambda)$ (see Section 2.2) is used. This model can learn to navigate from any place in the environment to a hidden goal location. During learning, only one of the four actions can be taken (winner-take-all mechanism). Once the navigation map is learned, however, generalization to continuous actions can be achieved by interpolating between the discrete actions.

A ‘reward expectation cell’ (REC) learns to associate place cell activity with the goal location G_0 using a Hebbian-type learning rule. REC is highly active at G_0 before learning. When the location of the goal has been learned, the reward is expected and the cell is silent at G_0 . If the reward is relocated to place G_1 , however, REC is strongly depressed at G_0 . This depression triggers the relearning of the navigation map. Goal location G_0 will then be forgotten.

During learning, the agent’s movement is restricted to four predefined headings. Because there is no generalization mechanism in action space, the learning time would increase if more headings were allowed.

3.4.2 Models of Basal ganglia and S-R learning

The basal ganglia, and particularly its dorsal pathway, has been largely modeled as implementing the reinforcement paradigm. The interpretation of the dopaminergic activity as encoding the reward prediction error have been the base of such models

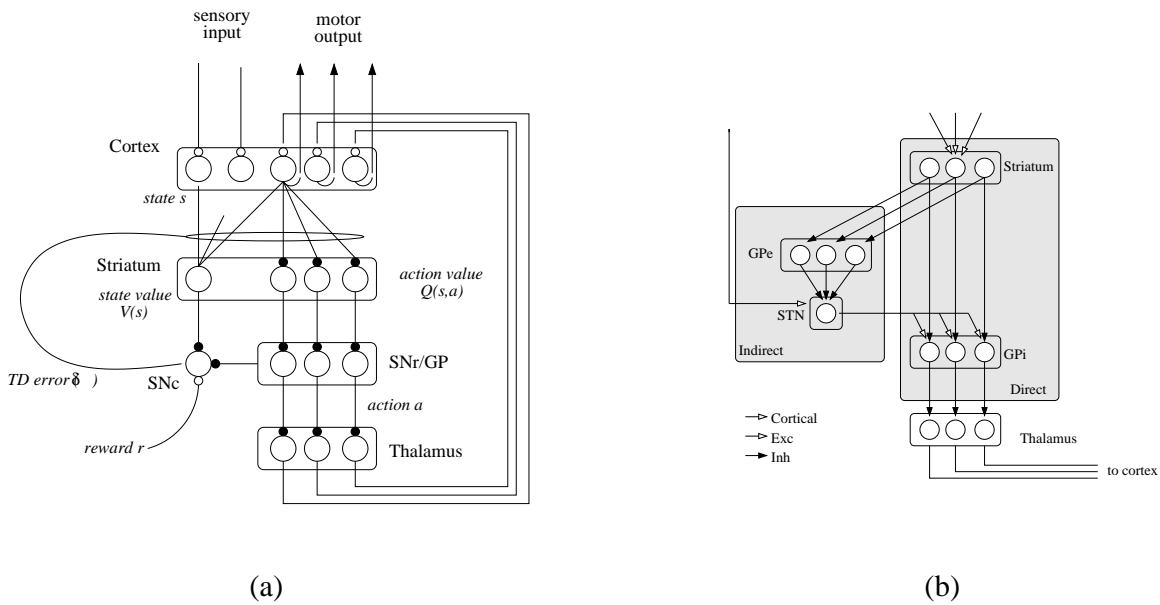


Figure 3.7: (a) Schematic diagram of a model of the basal ganglia implementing the reinforcement learning algorithm. Adapted from (Doya, 2002). (b) Direct and indirect pathways in the output of the BG as modeled by Berns and Sejnowski (1996). Thick arrows: cortical projections to BG. Solid arrowheads: inhibitory connections; open arrowheads: excitatory connections.

(Montague et al., 1996; Doya, 1999; Montes-Gonzalez et al., 2000; Baldassarre, 2002). See (Khamassi et al., 2005; Joel et al., 2002; Houk et al., 1995) for reviews.

In general, those models are designed to select among a repertoire of specific sensory motor programs (or S-R associations), associated to discrete actions in the reinforcement learning paradigm. Cortical projections to the striatum provide information about the state s , and dopaminergic activity represents the TD signal δ . The striatum uses this signal to learn the state value functions $V(s)$, and the action value function $Q(s,a)$ corresponding to the policy $P(a|s)$ (Doya, 2000). The dorsal striatum-patch is proposed as the neural locus for learning the state value function $V(s)$; whereas the action values $Q(s,a)$ would be encoded in the matrix area. Each independent compartment (i.e. channel) in the latter area is proposed to encode the Q-values of independent actions.

A competition mechanism dependent on the Q-values is implemented in the output structures of the BG. Such a competition is believed to take place through a process of selected des-inhibition in the so-called direct/indirect pathways to the output nuclei of the BG (Mink, 1996; Berns and Sejnowski, 1996).

In general, these models have been applied to bio-mimetic agents to implement

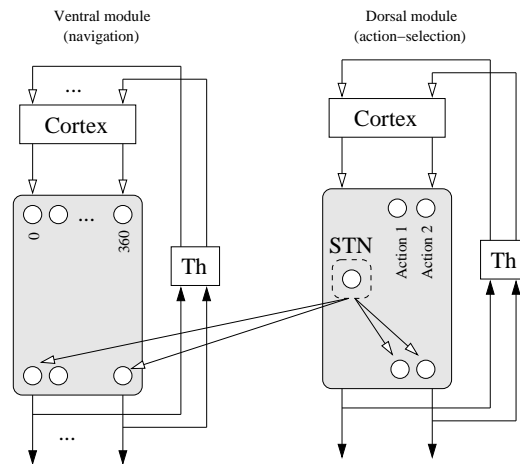


Figure 3.8: Model proposed by Girard. Shaded regions correspond to the competition processes taking place in both the ventral and dorsal modules, these processes are proposed to take place in the corresponding dorsal and ventral pathways of the BG. Selected des-inhibition in the projections from the STN to the ventral module can prevent navigation commands to be performed. Adapted from (Girard, 2003).

selection among independent stereotypic actions like landmark approaching, wall following, mating (i.e. look for other agents) or battery recharge (Khamassi et al., 2005; Doya and Uchibe, 2005; Montes-Gonzalez et al., 2000). Each action is encoded in separate striatal channels.

Recently, Girard *et al.* (Girard et al., 2005; Girard, 2003) proposed a model which integrates the action-selection mechanism with navigation skills. The model is composed of two modules, one selecting directions of movement and the other selecting different stereotypic actions. These modules are assimilated to the ventral and dorsal pathways in the BG, respectively (Fig. 3.8).

Both modules are based in the model proposed by Gurney et al. (2001a, 2001b). The dorsal module selects among non-locomotor stereotypic actions. The ventral module performs a competition between two types of navigation (i) A landmark approaching strategy and (ii) A trajectory planning system based on a topological representation of the environment and goals (Filliat, 2001). The output of this module encodes directions of movement in allocentric coordinates.

An asymmetric interaction between the modules is proposed. Non-locomotor actions in the dorsal module can inhibit the navigation signals generated in the ventral module (i.e. they can stop the navigation). This interaction is proposed to reside in a difference in the relative influence of sub-thalamic projections to the dorsal and ventral pathways.

Navigation in this model relies on a topological representation of space. This rep-

resentation consists in a graph whose nodes encode for explored locations. Each node stores allothetic information of those locations, and the connections between nodes encodes distance and orientation of the represented places. The process of navigation is implemented algorithmically and is not biologically plausible. In addition, the selection depends on predefined parameters and no learning mechanism is proposed to adapt this process.

Chapter 4

Spatial representation in the rat

As the complexity of the task and the perceptual capabilities of biological organisms increase, an explicit spatial representation of the environment appears to be employed to support navigation (Tolman, 1948). Since the discovery of *place cells* (O’Keefe and Dostrovsky, 1971), i.e. neurons whose activity is primarily correlated with animal’s spatial location, the hippocampus is thought to provide a neural basis for such a representation (O’Keefe and Nadel, 1978).

A recent discovery of *grid cells* in the dorsal entorhinal cortex opened up a possibility that place cells inherit some of their properties from the entorhinal neurons, which constitute a principal source of feed-forward input into the dorsal hippocampus where the place cells were first observed (Fyhn et al., 2004; Hafting et al., 2005). The entorhinal-hippocampal network is thus a primary candidate for the biological locus of the cognitive map of the environment, a necessary prerequisite for the locale navigation strategy (McNaughton et al., 2006).

In this chapter we first review the anatomy of the hippocampal formation, an area of mammalian brain where place cells and grid cells are found (Section 4.1). Then in Sections 4.2 and 4.3 we describe basic neurophysiological properties of these neurons and finally review existing computational models of their activity in Section 4.4.

4.1 Anatomy of the hippocampal formation

The hippocampal formation (HF) is a limbic brain area which occupies a considerable percentage of the rat’s brain (Fig. 4.1a). It includes the hippocampus (HPC), the entorhinal cortex (EC) and the subicular complex (SbC) (Amaral and Witter, 1989,

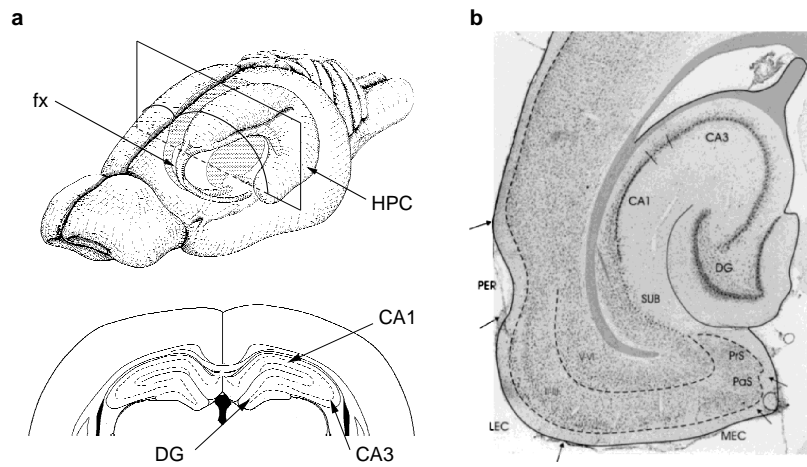


Figure 4.1: Anatomy of the hippocampal formation. (a) Schematic rat brain with the hippocampal formation highlighted (Amaral and Witter, 1995) and coronal section of the hippocampus (Praxinos and Watson, 1998). (b) Subregions of the hippocampal formation (Witter et al., 2000). HPC, hippocampal formation; fx - fimbria fornix; DG - dentate gyrus; CA1/CA3 - Cornu Ammonis subregions; SUB - subiculum; PrS - pre-subiculum; PaS - para-subiculum; MEC - medial entorhinal cortex; LEC - lateral entorhinal cortex; PER - perirhinal cortex.

1995).

Inputs to HF: EC is a target of most higher cortical associative areas. HF can therefore operate on highly processed sensory information from all sensory modalities (Burwell and Amaral, 1998). Through the fornix bundle, the hippocampal formation receives afferent connections from subcortical areas, in particular cholinergic and GABAergic projections from the medial septum. Cholinergic input targets mainly the excitatory pyramidal and granule cells, as well as inhibitory GABAergic interneurons. GABAergic septal neurons, on the other hand, selectively synapse on GABAergic interneurons only (Freund and Antal, 1988).

Outputs of HF: There are two main outputs of the HF: One pathway leaves the HF through the subiculum and projects to subcortical areas. It innervates thalamic nuclei, amygdala and—via the fornix fiber bundle—nucleus accumbens (NA) (Witter, 1993; Legault et al., 2000). A second pathway projects back to the higher cortical areas through EC (Insausti et al., 1997).

Internal connectivity in HF: EC is the primary sensory input area of the HPC. It consists of a medial (mEC) and a lateral (lEC) regions. HPC can be further divided into the dentate gyrus (DG) and the Cornu Ammonis (CA). CA has four subregions, but CA1 and CA3 are the most prominent (Amaral and Witter, 1989; Witter, 1993; Amaral and Witter, 1995). SbC is composed of the subiculum (Sb),

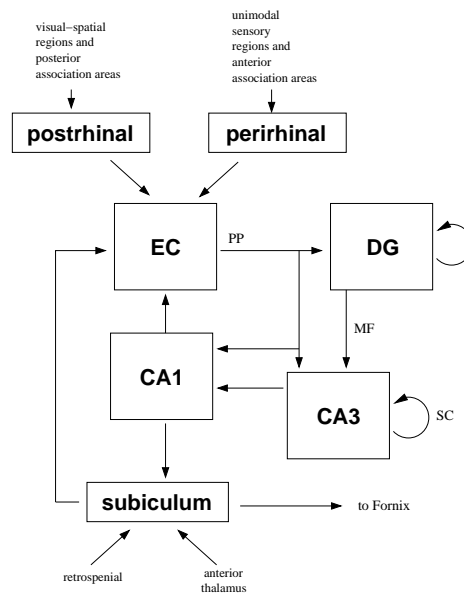


Figure 4.2: Schematic illustration of the HF internal interconnections. See figure 4.1 for a description of the labels.

the pre-subiculum (prSb) and para-subiculum (paSb) (Amaral and Witter, 1989). The simplified scheme of internal connectivity between HF subregions is shown in Figure 4.2. Sensory information can be processed in two parallel pathways: the first pathway goes from the EC directly to the DG, CA3 and CA1 via the perforant path (Yeckel and Berger, 1990; Witter et al., 2000). The second pathway includes EC to DG projections as well but then mossy cells in the DG project to the CA3 pyramidal cells via different set of axons called mossy fibers. Pyramidal cells in the CA3 are recurrently connected and also project to the CA1 via Shaffer collaterals (sc). CA1 projects to the subiculum, and both CA and subiculum project via fornix-fimbria system to subcortical areas, in particular nucleus accumbens, and to the deep layers of the EC. (O'Keefe and Nadel, 1978; Witter, 1993).

Entorhinal cortex

Entorhinal cortex is the cortical gateway to the hippocampus. A distinction can be made between the medial (MEC) and the lateral (LEC) areas. EC follows the general neo-cortical architecture of a six-layered structure that has been extensively studied (Kosel et al., 1981; Witter, 1993; Insausti et al., 1997).

Inputs to EC: Both MEC and LEC receive projections from sensory associative areas (visual, auditory and somatosensory) as well as from the parietal, temporal and

frontal areas via perirhinal and postrhinal cortices (Witter, 1993; W. A. Suzuki and Amaral, 1994; Insausti et al., 1997; Liu and Bilkey, 1997). Olfactory information from the olfactory bulb and piriform cortex is conveyed directly and via perirhinal cortex (Kosel et al., 1981; Witter et al., 1989, 2000). The subiculum as well as CA1 send their output mainly to MEC, but also to LEC. DG and CA3 do not innervate EC (Amaral and Witter, 1989; Witter, 1993).

Outputs of EC: EC cortical efferents target primarily perirhinal, orbitofrontal and piriform cortices, but parietal, temporal, frontal and occipital areas are also innervated (Silva et al., 1990; Witter, 1993; Insausti et al., 1997). Via the perforant path, EC conveys multisensory information from its cortical afferents to DG, CA3, CA1 and Sb (Amaral and Witter, 1989; Witter, 1993). Cells with periodic spatial firing fields (grid cells, see Section 4.2) have been observed in the dorsal part of the MEC. The most dorsolateral band of the MEC provides strongest input to the dorsal part of the hippocampus where place cells with sharpest and most information-rich firing fields were observed (Fyhn et al., 2004).

Internal connections in EC: Neurons in the deep regions connect to cells in the superficial layer of EC (Amaral and Witter, 1989; Witter, 1993; Amaral and Witter, 1995). There is also evidence for strong synaptic innervation from the lateral to the medial region (Quirk et al., 1992).

Dentate gyrus

DG granule cells receive processed sensory input from EC. Granule cells then project to mossy cells. Mossy cells laterally contact other mossy cells as well as strongly project to CA3 (Claiborne et al., 1986; Amaral and Witter, 1995; Hastings et al., 2002). Throughout the entire life, neurogenesis occurs in the rat DG. Stem cells migrate into the granule layer and differentiate into fully functional and networked granule neurons (Bayer, 1982; Kuhn et al., 1996; Ciaroni et al., 1999; Hastings et al., 2002).

Cornu Ammonis or hippocampus proper

The hippocampus proper consists of four subregions CA1-CA4, with CA1 and CA3 being the most distinguishable. Place cells, i.e. cells with spatially correlated activity (see Section 4.3), have originally been found in CA1 (O'Keefe and Dostrovsky, 1971), but later were also observed in CA3 and DG as well (Jung and McNaughton, 1993).

Inputs to CA: The CA3 region receives strong projection from DG via the mossy fibers. Both CA1 and CA3 are also innervated by EC via the perforant path (Amaral and Witter, 1989; Amaral, 1993; Witter, 1993; Amaral and Witter, 1995; Hastings et al., 2002).

Outputs from CA: CA1 and CA3 pyramidal cells connect to subiculum via the Shaffer fiber bundle. The angular bundle connects CA1 to EC (perforant path) (Amaral et al., 1991). CA1 projects directly to septum and the nucleus accumbens via fimbria-fornix (O’Keefe and Nadel, 1978) as well as to the subiculum and the EC (Witter et al., 2000).

Internal connections in CA: CA3 neurons laterally send outputs to other CA3 neurons via the Shaffer collaterals. Also via the Shaffer fibers, CA3 connects to CA1 (Amaral and Witter, 1989; Amaral, 1993; Amaral and Witter, 1995).

Subiculum

The subicular complex (SC) consists of the subiculum (Sb), the pre-subiculum (prSb), whose dorsal part forms the post-subiculum (poSb) and the para-subiculum (paSb).

Inputs to SC: The main input to Sb originates in CA1 and EC (Amaral et al., 1991). The paSb is innervated by the retrosplenial cortex whereas prSb is reached from areas in the temporal and parietal lobes, as well as from thalamic nuclei, which project onto poSb (Burgess et al., 1999).

Outputs from SC: Via the fornix fiber bundle, Sb projects on the nucleus accumbens (NA) and the septal complex. Sb also innervates entorhinal and prefrontal cortex, amygdala and the thalamus. prSb and paSb also synapse on EC (Amaral and Witter, 1989; Witter, 1993).

Internal connections in SC: Within SC, Sb projects to prSb and paSb and prSb also synapses on paSb (Amaral and Witter, 1989; Witter, 1993).

Theta rhythm

The hippocampal EEG shows distinct patterns depending on the rat’s behavior. During motion (active or passive (Gavrilov et al., 1996)), the EEG shows a 6–12Hz oscillation called *theta rhythm* (O’Keefe and Recce, 1993; Burgess et al., 1994; Skaggs et al., 1996). Theta is also observable during sensory scanning (e.g. sniffing) and REM-sleep (Buzsáki, 2002). On top of that, firing is synchronized to a *gamma oscillation* of 40–100Hz throughout the whole hippocampal formation (Chrobak et al., 2000; Csicsvari et al., 2003). Subcortical cholinergic and GABA-ergic inputs from the septal region seem to be responsible for generating the hippocampal theta rhythm (Winson, 1978; Buzsáki, 1984; Miller, 1991; Hasselmo and Bower, 1993). When septal input is inactivated, the CA3 place fields are disrupted whereas the CA1 fields are unaffected. Simultaneously, acquisition of place learning tasks is impaired (Brandner and Schenk, 1998) and errors in working memory increase significantly (S. J. Mizumori et al., 1989).

While eating, drinking or awake-immobility as well as in slow-wave sleep, however, the EEG shows large field high irregular amplitude signature, termed *sharp*

waves. During each sharp wave event, a high frequency ripple volley of 140–200Hz occurs (Chrobak et al., 2000; Chrobak and Buzsáki, 1996). It is speculated that theta/gamma waves synchronize input from cortex to hippocampus, whereas sharp waves/ripples modulate output from hippocampus back to cortex (Chrobak et al., 2000).

4.2 Grid cells in the dorsomedial entorhinal cortex

Individual neurons in the layer II of the dorsal part of the MEC (dMEC) have spatial firing fields that resemble hexagonal grids extending over the whole space (Fyhn et al., 2004; Hafting et al., 2005). These firing grids can be characterized by the grid spacing, grid orientation and the relative spatial location of the grid (i.e. its spatial phase) as illustrated in Fig. 4.3a. For each cell, grid spacing is defined as the distance between two neighboring vertices of the grid, which is constant for any one cell. Grid orientation is defined as the angle between an arbitrary reference direction (e.g. 0° in the figure) and the direction to the first counter-clockwise vertex of the hexagon. The spatial phase of the grid is defined as a spatial position of the grid relative of other grids, i.e. it characterizes the mapping of the firing grid on the actual space (e.g. the floor of the recording room). Each vertex of the grid is characterized by its size, described in the experiments by the area covered by the central peak of the spatial autocorrelogram using a threshold of 0.2 (Hafting et al., 2005).

The grid cells are topographically organized (Hafting et al., 2005), Fig. 4.3b. Nearby cells share the same spacing and orientation but have different spatial phases, i.e. the firing fields of these cells have identical size and orientation, but are offset relative to each other. Hence in the following they are said to belong to a grid-cell population (by analogy to the e.g. population of orientation-sensitive cells with identical tuning curves and different preferred orientations). The cells that are far apart (along the dorsoventral axis of the dMEC) differ by grid spacing, grid orientation and field size (i.e. belong to different grid-cell populations). The more ventral is the location of the population the larger is the grid spacing and field size. Grid orientations differ without any systematic relationship.

Firing grids of individual cells have the following properties (Hafting et al., 2005): (i) The grid pattern is expressed immediately upon exposure to a novel environment, i.e. the grid cells fire the first time the animal passes through the field, both in light and in the dark. (ii) The firing grids are anchored to the external cues in the environment. If a single controlling cue card is rotated 90° the firing grid rotate similarly. (iii) The grids persist after cue removal. After initial period of 10 min with the lights on, the grids were maintained for 30 min in total darkness. However, for the majority of cells the darkness period caused a weak dispersal of the vertices.

Our model, presented in the next chapter, describes a neural network in which

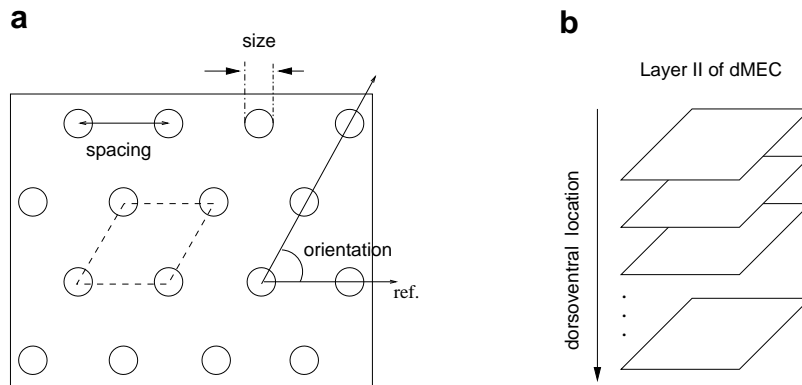


Figure 4.3: (a) Schematic drawing of a firing field of a single grid cell. Large rectangle represents the recording chamber, circles represent the locations of elevated firing. (b) The grid cells are organized in different populations along the dorsoventral axis of the dMEC. Cells in each population share the same spacing and orientation (defined as in a). The more ventral is the location of a population, the larger is spacing and field size.

neurons have periodic firing fields with hexagonal spatial pattern, similarly to the dMEC grid cells (see Chapter 6). The role of this network is assumed to be the integration of self-motion input over time, i.e. path integration.

4.3 Hippocampal place cells

A place cell is a neuron whose firing activity is primarily correlated with the animal's spatial location. A place cell emits action potentials only when the animal is in a specific region of the environment, which defines the place field of the cell.

Place cells recorded in CA3-CA1 areas of the hippocampus have spatially-localized place fields that together tend to cover uniformly the environment, and at any moment only a small proportion of these cells is active. The set of overlapping place fields is thought to encode a distributed representation of the environment (Wilson and McNaughton, 1993). The shape of place fields varies: The firing rate can be distributed approximately like a circular two-dimensional Gaussian (Samsonovich and McNaughton, 1997), but it may also be elongated in one dimension (especially along walls). Rarely a place cell may have a place field in several different environments (Kubie and Ranck, 1983) and a single place cell can have multiple peaks of activity in a single environment (Muller et al., 1987; O'Keefe and Burgess, 1996; McNaughton et al., 1983). There is no topographic relationship between anatomical structure of

the CA3-CA1 populations and environment (O'Keefe and Conway, 1978; Muller and Kubie, 1987; Thompson and Best, 1989)

When the animal follows repeatedly the same route, CA1 place fields, which are initially symmetrical, expand backward with respect to the animal's direction of movement. Such a change only take place during the same block of trials, and its effect disappear the next day (Mehta et al., 1997).

Spatially localized firing of CA1 cells was observed even after selective lesions of the DG, (McNaughton, Barnes, et al., 1989) and partial and complete lesions of the CA3 (S. J. Mizumori et al., 1989; Brun et al., 2002, respectively). Furthermore, directional selectivity in linear tracks is also observed in rats with complete disruption of CA3 inputs to this area. Place fields remain stable across sessions and the firing activity was theta-modulated. These studies suggest that an intact CA3 is not required to maintain the place and directional properties of CA1 neurons which might be supported by the direct feedforward projection from the EC.

Cells with location sensitive firing were also observed in subiculum and the entorhinal cortex. Subicular place fields are broader than those in the hippocampus proper. Furthermore, subiculum exhibits a similar place field topology across different environments (Sharp and Green, 1994; Sharp, 1997, 1999), and seems to be largely influenced by self-motion information (McNaughton et al., 1996). Earlier reports in place-sensitive cells in the EC reported broad single peaked firing fields (Quirk et al., 1992). Recent data (Section 4.2) have shown a gradual change from multi-peaked to single-peaked firing fields along the dorsolateral to ventromedial axis of the dMEC (Fyhn et al., 2004).

4.3.1 Firing determinants of place cells

The discharge of place cells is highly correlated with the location of the animal. However, place cells are also sensitive to visual cues, self motion information (e.g. speed and orientation), sound, odor and reward (McNaughton et al., 1983; Markus et al., 1994, 1995).

Sensory information

Place cell activity is influenced by both idiothetic and allothetic inputs, and there exists a wealth of experimental data focused on the main determinants of place cell firing, as well as the interactions between different sources of information.

Distal vs local visual cues. Several studies suggest that activity of the place cells relies primarily on visual information (Etienne et al., 1996; Maaswinkel and Whishaw, 1999; Save et al., 2000). Moreover, distal visual cues were shown to be of primary importance in the control of the firing fields (O'Keefe and Conway, 1978). Rotation

of a single cue card attached to the wall causes a similar rotation of place fields (Muller and Kubie, 1987). A similar control was observed when the only available cues were three objects placed *at the periphery* of the cylindrical watermaze so as to form a triangular configuration (Cressant et al., 1997, 1999). However, when the same objects were placed *at the center* of the maze, their rotation (as a rigid set) did not result in a corresponding rotation of place fields for most of the cells, suggesting poor cue control by the configuration of intra-maze objects.

Non-visual external sensory input. When visual cues are not available, rats can rely on other sensory modalities to drive the place cells firing. Olfactory cues have been observed to contribute to the stability of place fields (Lavenex and Schenk, 1996; Save et al., 2000). Furthermore, when exploring an environment containing three-dimensional objects as local cues, blind rats display an exploratory pattern that led them to make contact with the objects more often than sighted rats (Save et al., 1998). Presumably, this behavior allows the animal to calibrate its internal estimations (i.e. path integrator) using tactile information.

Idiothetic cues. Hippocampal place cells exhibit location-sensitive activity in absence of visual cues (e.g. in darkness), suggesting that they may be driven by movement related internal signals. For instance, removing visual cues does not alter the activity of hippocampal place code (O'Keefe and Conway, 1978; Hill and Best, 1981; Pico et al., 1985; Muller and Kubie, 1987; O'Keefe and Speakman, 1987; McNaughton, Leonard, and Chen, 1989; Quirk et al., 1992); and place cells in visually symmetric environments have asymmetric visual fields (Sharp et al., 1990). Moreover, when the place cells are established in darkness, they persist in subsequent light conditions (Quirk et al., 1990; Markus et al., 1994).

Save et al. (1998) recorded place cell activity in early blind rats, and found place field similar to those recorded in sighted rats. It suggests that motion-related information (and possibly non visual sensory information) may be sufficient to form a stable place code in the hippocampal formation.

Interaction between internal and external information. Despite the fact that internal motion-related information may be used to update place cell firing (i.e. by path integration, M. L. Mittelstaedt and Mittelstaedt (1980); Etienne and Jeffery (2004)), this information is prone to accumulate errors over time. This requires a process of re-calibration based on external sensory input to take place in order to maintain an accurate estimation of position (H. Mittelstaedt, 1983; Gothard et al., 1996; Etienne et al., 1996; Save et al., 2000; Redish et al., 2000).

Gothard et al. (1996) studied the nature of interaction between internal and external information in the place cell activity. They observe that, in case of mismatch

between the information provided by external and internal cues, the population activity changes in order to align itself with one of the two. Gothard et al. (1996) conclude that the dynamics of these changes were determined by the degree of the perceived mismatch. Using a similar protocol Redish et al. (2000), conclude that in addition to the mismatch, a temporal delay (different from an animal to another, but consistent within animal) was required to make the transition.

This data suggest that both types of information compete in a dynamical process to control place cells firing.

Direction of movement

Experimental data have shown that the firing of place cells does not depend on the heading direction when the animal is foraging freely in an open environment. In contrast, on radial mazes or linear tracks the firing of these cells is becomes strongly directionally selective (Muller et al., 1994; Gothard et al., 1996). Furthermore, place directionality also appears in open environments when the animal is constrained to follow the same path between points of special significance (Markus et al., 1995).

Influence of environmental geometry

Several reports suggest that the shape of the surrounding environment influences the location and shape of the place fields of hippocampal cells. Muller and Kubie (1987) first recorded place cells in a gray cylinder with a white cue card on the wall, and then in a gray square-shaped box with the same visual appearance (i.e. with the cue card on the same location relative to the laboratory). Many cells that were active in the cylinder stopped firing in the square box and the fields of the cells active in both environments were markedly different in shape location and size.

O'Keefe and Burgess (1996) measured CA1-CA3 pyramidal cells of rats exploring four different boxes (a small square; a horizontal rectangle; a vertical rectangle; and a large square) located within a rectangular room. The location of peak firing in different boxes was found to depend on environmental features such as the distance to one or several walls, or the ratio of the distances to two opposite walls. Furthermore, the place fields changed their shape according to manipulations of the environment. In some cases, in boxes differing along one dimension the place fields either stretched or doubled their place fields along the changing direction.

Geometry of an arrangement of objects may also influence place field stability. Firing fields are more poorly controlled by three objects if their arrangement is an equilateral triangle then if it is an isosceles triangle (Cressant et al., 1997, 1999). The distinction between geometry of the environment and single visual cues may be viewed as the distinction between configural versus single landmarks (Poucet et al., 2003). Importance of configural cues suggests filtering out high-frequency cues (like

small objects) in favor of coarse-grained cues, allowing for faster spatial learning and higher resistance to unreliable cues. These advantages have previously been suggested to characterize cognitive mapping abilities of animals (O'Keefe and Nadel, 1978).

In our model, presented in the next chapter, location-sensitive activity of place cells results from the feed-forward projection of the upstream grid cells. We will show that the feed-forward input hypothesis can explain many properties of place cells, including their reliance on distal configural cues, firing in the darkness, place-field rotation following rotation of visual cues, rapid development in a novel environment and dependence of place-field shapes on the environmental layout (see Chapter 6).

4.4 Modeling space representation: state of the art

The ability of animals to navigate in complex task-environment contexts has been the subject of a large body of research over the last decades. Due to its spatial representation properties reviewed above, the hippocampus has been studied and modeled intensively. Below we review the principal theories attempting to explain the hippocampal role, and we describe some models of the mechanisms beneath place cell firing.

Recent discovery of grid cells provided a possibility that place cells inherit some of their properties from a downstream population of the entorhinal neurons. In particular, neurophysiological properties of grid cells suggest that they may perform integration of self-motion information over time (i.e. path integration) (Hafting et al., 2005). In Section 4.4.2 we review two models that address the issue of how the grid-cell network might perform path integration.

4.4.1 Models of place cells

Sharp (1991)

The model of place cell activity proposed by Sharp (1991) implements a 3-layer competitive learning scheme of Rumelhart and Zipser (1986) (Fig. 4.4a). Input layer includes binary sensory cells of two different types that encode the agent's distance and bearing to one or more landmarks. Type 1 neurons fire whenever the agent is within a certain range of its preferred landmark (or landmarks). The size of this range varies among cells. Type 2 cells are also sensitive to the landmark distances, but in addition they are sensitive to the landmark bearings. The bearing range varies between cells as well. The tuning of these cells (which landmarks at what distance and bearing range activate a given cell) of both types of cells is random and remains fixed throughout the experiments.

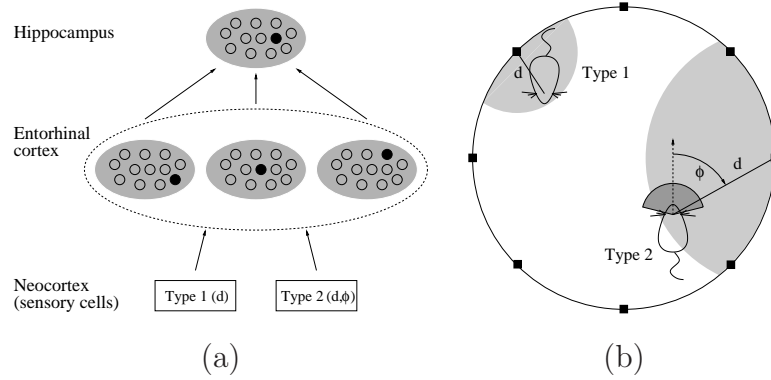


Figure 4.4: Place cell model proposed by Sharp (1991): (a) system architecture. Shaded areas mean winner-take-all competition. (b) Environment with eight landmarks. Sensory cells encode the view considering only the distance d (type 1), or the distance d as well as bearing ϕ to dedicated landmarks (type 2).

The intermediate layer is comprised of three populations (clusters) of 20 neurons. Each cell j receives input $h_j = \sum_i w_{ji}$ from all sensory neurons i of the first layer. In each cluster, the cell j^* with the largest input $h_j^* = \max_j h_j$ is the winner with activity 1, whereas all other cells within the cluster are silent (i.e. implementing a winner-take-all (WTA) scheme). The three active cells in the second layer are eligible for Hebbian-type learning in their input synapses w_{ji} .

The three active cells of the second layer project their activity onto the third layer, which consists of one cluster of 20 neurons. The same WTA mechanism as in the intermediate layer is applied here, and again, the winner-neuron adapts its weights using Hebbian learning. In this layer, which is proposed to be located in the hippocampus, place cells with omni-directional place fields are reported by Sharp for simulations in the circular environment with eight landmarks evenly spaced along the wall (Fig. 4.4b). When the movement of the agent in this environment is restricted to follow paths like in an eight-arm-maze, simulated place cells are unidirectional, in agreement with experimental data (McNaughton et al., 1983).

As many subsequent models, this model relies on an abstract visual system where the exact distances to the eight landmarks are available. All eight landmarks are also perfectly distinguishable by the sensory cells. Since the place cells in this model are purely visual, they can not maintain spatially selective activity in the dark, in contrary to experimental data (Quirk et al., 1990; Markus et al., 1994; Save et al., 2000).

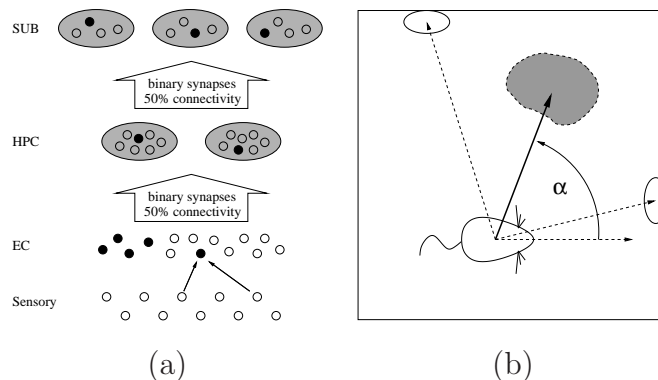


Figure 4.5: Place cell model proposed by Burgess *et al.* (1994): (a) system architecture. Shaded areas mean winner-take-all competition. EC: Entorhinal cortex, HPC: Hippocampus, SUB: subiculum. (b) θ Phase precession: Firing of EC neurons is ‘late’ when the angle $|\alpha|$ between agent heading and place field center is $< 60^\circ$, ‘middle’ when $60^\circ < |\alpha| < 120^\circ$ and ‘early’ when $|\alpha| > 120^\circ$. The shaded area is the place-field center, which is, by construction, located between the two landmarks.

Burgess *et al.* (1994)

Burgess *et al.* (1994) offer a model of place cells consisting of four layers of neurons, as depicted in Figure 4.5a.

Sensory cells in this model encode distances to external landmarks. A set of 15 sensory cells is attributed to each landmark of the environment. Per theta cycle, sensory cell i fires a number of spikes n_i which depends on the difference between the actual distance to the landmark and its preferred distance d_i . The tuning curves are large and of triangular shape, and the preferred distances uniformly cover the environment.

One layer above, each cell in entorhinal cortex (EC) receives input from two predefined sensory cells i and j and fires $\lfloor n_i \cdot n_j / 2 \rfloor$ spikes. The two afferent sensory cells are chosen such that each is coding for a different landmark and the location of their peak firing activities coincides with the center of the entorhinal cell’s receptive field. The angle α between the agent’s heading and the egocentric orientation of the place-field center determines the phase (with respect to the theta rhythm) at which spikes are fired (Fig 4.5b): If $|\alpha| < 60^\circ$, the cell fires at a ‘late’ phase, if $60^\circ < |\alpha| < 120^\circ$, the phase is ‘middle’, and else the cell fires ‘early’ in the theta cycle. Burgess *et al.* (1994) postulate that phase precession as seen in hippocampal place cells is generated in EC, which forwards this information to its target structure.

Each neuron in the EC layer connects to half of the cells in the hippocam-

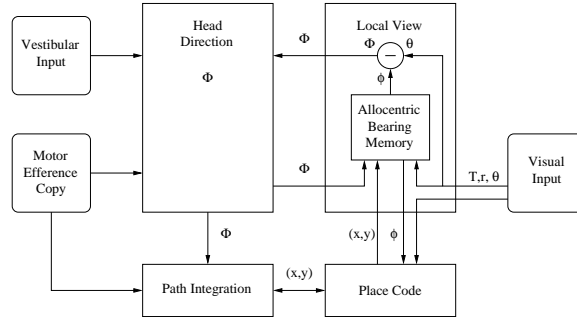


Figure 4.6: Architecture of the model proposed by Wan, Redish and Touretzky. During exploration, landmark information (type T , distance r and egocentric bearing θ) is combined with head direction Φ to produce allothetic landmark bearing ϕ . The allothetic bearing memory stores (T, r, ϕ) . Path integration updates position (x, y) . Place cells use all this information to tune their receptive fields.

pus (HPC). The synaptic weights are binary (0 or 1). Initially, most connections are turned off. A Hebbian-type learning rule allows these synapses to be switched on if the pre- and postsynaptic cells are both maximally active. The input to each place cell in HPC is proportional to the sum of presynaptic spikes at active synapses. Neurons in the HPC layer are clustered into five groups of 50 neurons. In each group, only the four cells with largest inputs are allowed to fire spikes (Rumelhart and Zipser, 1986).

Each HPC place cell projects to half of the cells in the subicular layer (SUB) of the model. The same Hebbian learning procedure as between EC and HPC is implemented here. The only difference is that in SUB, cells are arranged in ten groups of 25 neurons. As a consequence, each cell has to compete with less cells, which results in larger place fields as in HPC.

In addition to the abstract vision model (i.e. distances to landmarks), the mechanism which determines the phase of firing with respect to the theta rhythm depends on the bearing to the cell's center of receptive field. It is not clear how the rat can compute this bearing. Similarly to Sharp (1991), the place cells in the model are purely visual, i.e. they can not maintain firing in the absence of visual cues

Wan, Redish and Touretzky (1994, 1996, 1997)

The model by Wan, Redish and Touretzky (Wan et al., 1994; Touretzky and Redish, 1996; Redish and Touretzky, 1997a, 1997b) consists of separate populations for the local view, head direction, path integrator and place code (Fig. 4.6). All populations interact with each other in order to form a consistent representation of space.

The visual input provides the system with the following information about each

landmark: its type T_i , distance r_i and bearing angle θ_i . The compass bearing ϕ_{ik} of landmark i , viewed from place (x, y) is then calculated and stored. This calculation also requires information about the agent's current heading Φ which is provided by the head direction system.

The head direction system keeps track of the compass bearing Φ of the agent by integrating angular velocity signals from vestibular cues and efferent motor copies of motor commands. If the agent is disoriented, the current heading can be reset by the local view system by comparing the egocentric and compass bearing of landmarks.

The path integrator updates the agent's position (x, y) within the environment by summing up motor efference copies. When reentering a familiar environment, the internal state of the path integration system may be incorrect. It can, however, be recalibrated using visual input. This is done via the place code module.

The place code population combines information about the local view and the internal path integration system. Each newly recruited place unit tunes to the following parameters: (i) Type T , distance d and compass bearing ϕ of two randomly chosen landmarks, (ii) retinal angle difference $\alpha = \theta_i - \theta_j$ between two (possibly different) randomly selected landmarks, (iii) position information (x, y) given by path integration. Place units compute a fuzzy combination of these parameters discarding missing or unreliable inputs.

In contrast to previous models, the model of Wan, Redish and Touretzky include path integrator explicitly into the calculation of place cell activity allowing for spatial firing in darkness. The model is still highly abstract since it relies on distances and bearing to landmarks, and, moreover, requires a predefined set of landmark types.

McNaughton et al. (1996)

McNaughton et al. (1996) emphasize the importance of idiothetic inputs for place cell activity, by proposing that hippocampus itself performs path integration. According to this idea, exteroceptive information is a second order correlate, and is used to initialize and calibrate path integration by associative learning.

The core of the theory is the multi-chart hippocampal hypothesis: the synaptic matrix of recurrent CA3 connections provides a large set of preconfigured quasi-independent reference frames. Each of these reference frames can be imagined as a two-dimensional surface (a chart) consisting of a random subset of the total CA3 place cell population. Neighboring cells in each chart are defined by synaptic strength of recurrent connections, such that cells that are strongly mutually connected are considered neighbors. At any time, only one chart can be active, representing the currently used reference frame (i.e. the currently used representation of the environment). Which chart is selected depends on the collection of cells that are active: a chart with a well localized activity pattern will be more likely selected than a chart exhibiting a

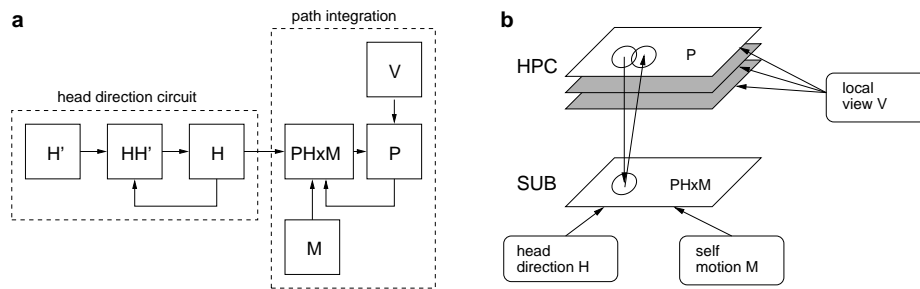


Figure 4.7: McNaughton et al. (1996) model. (a) Model architecture. Head direction circuit performs integration of angular motion and produces the estimate of current heading H . This estimate together with displacement information is used to perform path integration. (b)

scattered activity. Under this assumption, a disoriented animal entering an unknown environment would select an arbitrary preconfigured chart. In subsequent visits to the same environment the same chart will be chosen as a consequence of learned associations between external sensory information and activity of cells belonging to this chart.

The cell activity within a chart is based on an attractor dynamics producing a Gaussian-like blob of activity. Within the active chart, a blob of activity tracks the animal's position over time. The mechanism for shifting this activity blob over the network is an extension, from one to two dimensions, of the head-direction model proposed by Skaggs et al. (1995). The path integrator circuit (Fig. 4.7) involves, beyond the CA3 layer (P), a population of PHxM cells coding for (i) the animal's current position (P), (ii) the animal's current heading (H), and (iii) the current self-movement information (M). The firing activity of each cell i PHxM is correlated with all three variables simultaneously in agreement with experimentally observed neurons in the subicular complex which exhibit conjunctive coding of place, speed and head direction (Sharp and Green, 1994). In the model, PHxM cells and CA3 cells form a loop to update the spatial map: CA3 cells store the current position, while PHxM cells signal the displacement due to self-motion and head-direction information.

Samsonovich and McNaughton (1997) have validated the above path integration model through numerical simulation. Their results fit several experimental data including doubling, reshaping, and vanishing of place fields in distorted environments (O'Keefe and Burgess, 1996; Gothard et al., 1996), directionality of place fields during linear motion (Gothard et al., 1996) and slow place field rotation after animal disorientation (Knierim et al., 1995).

In this model, similarly to previous models, the local view information is represented as a sum of Gaussian components tied to important environmental features

(e.g. walls of recording apparatus or feeding locations), and are thus abstracted from the question of how the importance of these particular features is learned by the animal. Moreover, no mechanism is proposed of how the associations between the path integrator and external cues is learned. In addition, new experimental data (Fyhn et al., 2004; Hafting et al., 2005) suggest that path integration might be performed by the entorhinal neurons upstream from the hippocampus.

Gaussier and colleagues (1998, 2000, 2002)

The models by Gaussier and colleagues (Gaussier et al., 1998, 2000, 2002) rely on landmark detection from real panoramic camera images. For each detected landmark in turn, its type and compass bearing (the agent has a built-in compass) are represented in a merged “what” and “where” matrix. The landmark-type neurons form a winner-take-all network, whereas the landmark-bearing network supports generalization by “spreading” activity to neighboring neurons.

When a place seems interesting (e.g. close to a goal location), a place cell of the place recognition layer is recruited and units from the view-matrix connect to it. In contrast to most of the models, place recognition is assumed to take place before reaching CA3/CA1 fields, i.e. either in the EC or DG. At each time step, the activity of place cells is calculated in two steps: first, the initial activation is determined according to the similarity between stored and currently perceived landmark information (i.e. the what-where matrix); second, a winner-take-all mechanism resets the activities of all but the winning cell to zero.

The cells in the downstream layer, attributed to CA3/CA1 fields, learn *transitions* between places as identified by the sequence of cell activations in the place recognition layer.

Although visual input in the model is provided by a real camera, the camera images are aligned using an artificial compass. In addition, the winner-take-all mechanism in the place recognition layer suppresses all but one neuron. This is in contradiction with experimental data suggesting distributed and redundant nature of the hippocampal place code. Finally, in the absence of visual input, this model does not work due to the lack of a path integration component.

Arleo *et al.* (2000, 2001)

Arleo *et al.* (Arleo and Gerstner, 2000a, 2000b; Arleo et al., 2001; Arleo and Gerstner, 2001) propose a spatial learning system based on low-level feature extraction of real camera images from a miniature robot. Idiothetic representations are calibrated using visual stimuli (figure 4.9).

The feature extraction module transforms the high-dimensional camera image into a filter-based representation. Two alternatives are described: (i) linear vision

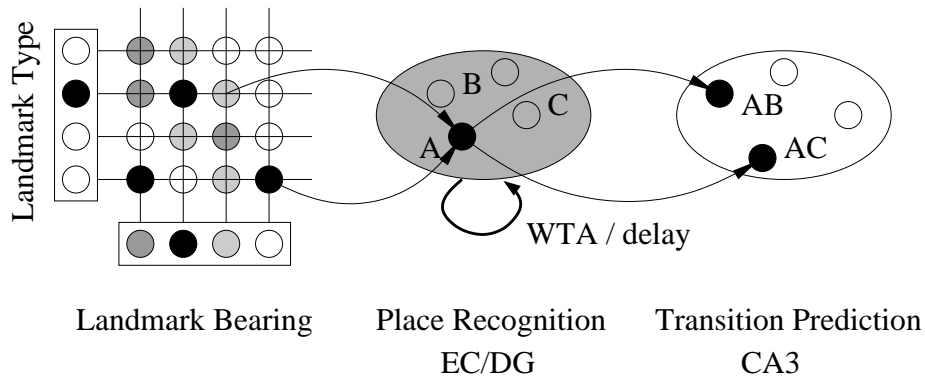


Figure 4.8: Architecture of the model proposed by Gaussier and colleagues. Landmark type and bearing are extracted and merged in a recognition matrix. Place cells compete with each other implementing a winner-take-all (WTA) mechanism. Place cells allow the following layer to predict potential future places by associating the delayed place of the previous time step (e.g. place A) with the current place. After transition learning, possible future places (e.g. B or C) can be predicted.

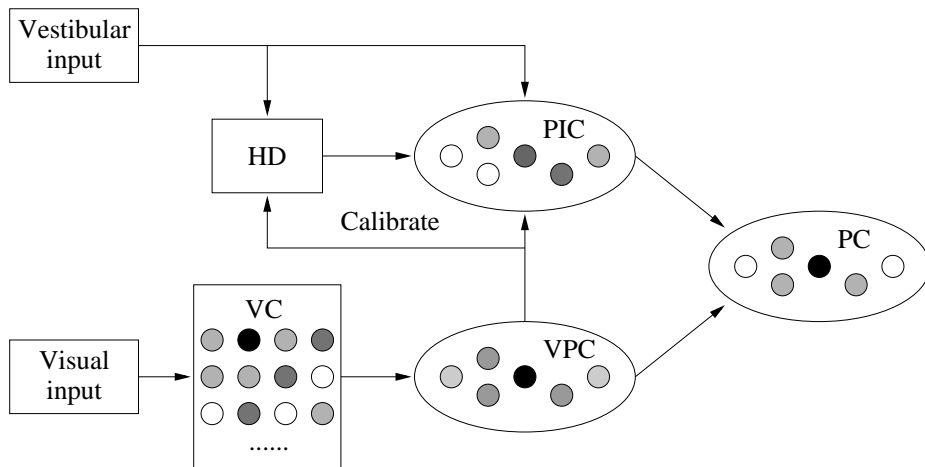


Figure 4.9: Architecture of the model proposed by Arleo *et al.* Low-level visual features are extracted and stored in view cells (VC) which drive visual place cells (VPC). Vestibular cues update the head direction (HD) system as well as a population of path integration cells (PIC). VPC and PIC converge onto a population of place cells (PC). Synapses are modified using a Hebbian learning. HD and PIC are constantly recalibrated by VPC to keep the representations consistent.

camera: Walsh-like filters are tuned to various patterns and spatial frequencies. (ii) 2d camera: A set of modified Gabor filters are tuned to different orientations and spatial frequencies. A log-polar retinotopic sampling grid is placed on the image and the filter set applied to each “retina” point.

At each time step, the agent takes four “snapshots”, one in each cardinal direction. For each orientation, the filter activities are stored in a population of “snapshot cells” (SC). An unsupervised growing network scheme is employed which recruits visual place cells (VPC) when necessary. Synapses from SCs to VPCs are initialized and modified using a Hebbian-type learning rule. VPCs are suggested to occupy superficial lateral entorhinal cortex.

Vestibular input drives populations of head direction (HD) and path integration (PIC) cells. PIC is postulated to be located in superficial medial entorhinal cortex, whereas the HD system is distributed across ante- and laterodorsal thalamic nuclei, lateral mammillary nuclei and postsubiculum. Position information from VPC is used to recalibrate path integration. Similarly, the bearing angle to a salient landmark (a lamp) in conjunction with VPCs are used to recalibrate the head direction system.

PIC and VPC project to place cells in the hippocampus proper (PC). The same unsupervised growing network scheme and Hebbian learning is applied to PCs. Realistic place fields are reported for both visual systems.

In this model, four real camera snapshots provide visual stimulus at each location. However, the images must always be taken in the four cardinal directions, which is equivalent to having a high-precision compass.

4.4.2 Models of grid cells

Discovery of grid cells in the dMEC (see Section 4.2) inspired two different lines of research, the first one investigating the mechanisms underlying the spatial firing of the grid cells themselves (Fuhs and Touretzky, 2006; McNaughton et al., 2006), and the second one looking at implications of the grid-like spatial representation for existing theories of hippocampal activity (Solstad et al., 2006; Rolls et al., 2006).

There are two main theories of how a network of neurons can produce hexagonal spatial activity patterns. The computational model by Fuhs and Touretzky (2006) relies on the fact that in a two-dimensional sheet of neurons a hexagonal activity pattern can emerge spontaneously if the mutual connections are local with longer-range inhibition and shorter-range excitation. Each subpopulation of grid cells is modeled as such a two-dimensional sheet of neurons. Path integration is performed in this network by shifting the activity patterns along the corresponding sheets on the basis of velocity input. The translation of the activity pattern is performed on the basis of neuronal interaction within the same sheet without involving additional populations of neurons.

The second model of grid-cell activity is proposed by McNaughton et al. (2006). In their model, each grid-cell subpopulation is represented by a single two-dimensional sheet of neurons similarly to the model by Fuhs and Touretzky (2006). However, the periodic activity pattern is achieved through a circular symmetry of the recurrent weight matrix. Although periodic weight matrix is mathematically equivalent to the repeating patches of locally connected neurons, a possible biological implementation and predictions of these two models are different (e.g. problems due to border effects in the Fuhs & Touretzky's model are eliminated by periodic connectivity, but existence of circular weights in biological networks is questionable). Path integration in this model is performed by translation of the activity pattern as well, but requires an additional population of cells with conjunctive coding of place, speed and direction. Existence of such cells in deeper layers of the dMEC was experimentally proven by (Sargolini et al., 2006).

Although both models discuss how path integration might be performed by the grid-cell network, none of them discusses in any detail how the cumulative error is corrected. Any system that updates its position estimate solely on the basis of self-motion signals is subject to the cumulative error, i.e. drift of position estimate from the true position over time.

The two models described above and ones by Solstad et al. (2006) and Rolls et al. (2006) suggest that single-peaked Gaussian-like place field of downstream CA1 neurons might result from a weighted summation of grid-like spatial patterns. However, no attempts have been made to see whether such a scheme is compatible with other place field properties like, e.g., their dependence on the shape of the room.

Chapter 5

A new model of spatial learning and navigation in the rat

Our model of goal-oriented behavior consists of two separate pathways capable of generating motor actions (Fig. 5.1). The first, direct, pathway associates visual input directly with motor actions and implements stimulus-response, or *taxon*, behavior. We think of this pathway as a simplified model of the anatomical connections between the cortex and the dorsal striatum (caudate putamen in the rat) thought to be involved in the development of stimulus-response associations (Packard and McGaugh, 1996a; White and McDonald, 2002). The second, indirect, pathway generates actions based on a learned representation of space and drives a *locale* navigation strategy. The spatial representation is stored in a simplified model of place cells in the hippocampus and modulates motor actions through the nucleus accumbens (Brown and Sharp, 1995; Redish, 1999). The model hippocampus receives input via dorsal entorhinal cortex (dMEC) where integration of self-motion cues is performed in a network of grid cells (Fyhn et al., 2004; Hafting et al., 2005). Path integration is influenced by the visual input. Goal-directed movements through the environment, generated by the taxon or locale strategy, are encoded by two populations of action cells that model movement-related functions of either the caudate putamen (CP) or the nucleus accumbens (NA).

In this chapter we give detailed description of the model components and learning equations. The illustration and analysis of model performance in various tasks are presented in Chapters 6 and 7.

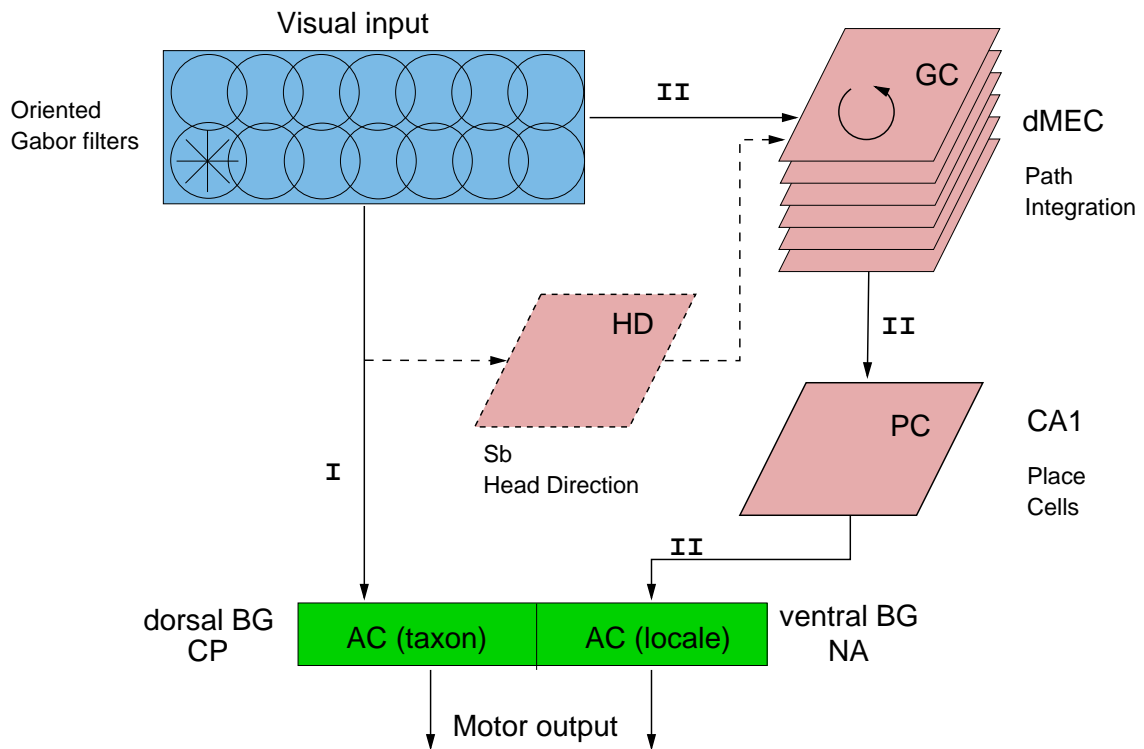


Figure 5.1: Model overview. Motor actions of the simulated are controlled via two pathways: direct (I) and indirect (II). Colors represent different brain areas: cortex (blue), hippocampal formation (pink), basal ganglia (green). Full lines represent neural projections in the model, dashed lines symbolize an algorithmic implementation of a particular function. GC - grid cells, PC - place cells, HD - head direction, AC - action cells, dMEC - dorsocaudal medial entorhinal cortex, BG - basal ganglia, CP - caudate putamen, NA - nucleus accumbens, Sb subiculum.

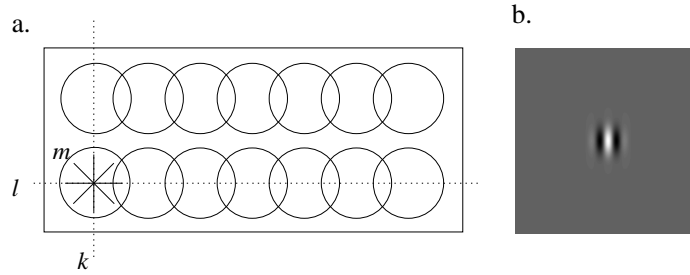


Figure 5.2: Model of visual input. *a*, Input image (rectangle) is sampled by a set of overlapping orientation sensitive filters (circles, an example of a real filter is shown in *b*). Filters are arranged in a rectangular grid and 8 filters of different orientations are placed at each point of the grid. The number of filters drawn is less than the model actually uses, for simplification. *b*, Example of a Gabor filter (Eq. 5.1) sensitive to orientation 90° .

5.1 Model of visual input

The rat visual system was modeled by processing the input images using a large set of orientation-sensitive visual filters with localized receptive fields, described as Gabor wavelets. Experimental evidence suggests that in the rat (i) the variation in ganglion cell density is relatively small across the retina; (ii) the receptive field size of the cells is approximately constant (Dean, 1990; Goodale and Carey, 1990); (iii) a vast majority of cells ($\sim 90\%$) in the primary visual cortex are orientation sensitive; and (iv) the size of the center of their receptive field (e.g. of the ON center) is $3\text{-}13^\circ$ in diameter (Girman et al., 1999). As a simplification, we modeled the output of the primary visual processing system as responses of a set of overlapping orientation-sensitive complex Gabor filters of width $\sigma_g = 1.8^\circ$ (spatial wavelength $1/2\sigma_g$) distributed uniformly across the view field of 300° . More specifically, a rectangular sampling grid of 96×12 locations is used and 8 filters of different orientations are placed at each point of the grid as schematically shown in Fig. 5.2a. An example of a two-dimensional Gabor filter sensitive to vertical lines in the image is shown in Fig. 5.2b. Such a Gabor filter is a two-dimensional complex wavelet defined in the space domain as:

$$g(\vec{x}_{kl}, \vec{w}_m) = \exp\left(-\frac{\|\vec{x} - \vec{x}_{kl}\|^2}{2\sigma_g^2}\right) \cdot \exp(i\vec{\omega}_m \cdot (\vec{x} - \vec{x}_{kl})) \quad (5.1)$$

where $\vec{x}_{kl} = (x_{kl}, y_{kl})$ is the coordinate of the grid point (k, l) at which the filter is centered in visual space, $\vec{w}_m / \|\vec{w}_m\|$ defines the filter orientation, $\|\vec{w}_m\|/2\pi$ is the frequency of the modulating sinusoidal wave, σ_g is the width of the circular receptive

field and \vec{x} is running over all pixels in the image. Sampling is sufficiently dense so that the distance between grid point is $2\sigma_g$.

A response of the filter to the corresponding portion of the image \mathcal{I} perceived at time t is characterized by its amplitude:

$$G_{klm}(t) = \sqrt{\left(\Re[g(\vec{x}_{kl}, \vec{w}_m)] * \mathcal{I}(t)\right)^2 + \left(\Im[g(\vec{x}_{kl}, \vec{w}_m)] * \mathcal{I}(t)\right)^2} \quad (5.2)$$

where $\Re[\cdot]$ and $\Im[\cdot]$ are the real and imaginary parts, respectively, and $\langle * \rangle$ denotes integration over visual space. The set of the filter amplitudes $G_{klm}(t) = G(\vec{x}_{kl}, \vec{w}_m, t)$ serves as the internal representation of the visual snapshot observed at time t , i.e. the *local view*. In a non-symmetric environment every combination of place and orientation would cause different activations of the filter set so that different places and gaze directions can be distinguished on the basis of the difference between the filter response amplitudes. The description of visual input by the responses of filters avoids the definition of cues or landmarks, so that the model can work in enclosures with rich or scarce visual cues. We will show that the activity of the set of filters represents measures like distances to walls or landmarks *implicitly* without the need to define them.

5.2 Action selection model

Our model implements two different goal-navigation strategies, taxon and locale navigation. As suggested by the review of animal navigation in Chapter 3 the two navigational strategies can be characterized by the following properties:

- Locale strategy uses an allocentric frame of reference frame, while taxon strategy uses an egocentric one.
- The two strategies are supported by distinct memory systems. Whereas the taxon strategy can be mediated by the dorsal striatum, the locale strategy depends on the hippocampus.
- The two strategies can be learned simultaneously in a single task. Reward-based learning of the two strategies may be performed in the basal ganglia where the reward signal is represented by phasic dopamine input.
- The two strategies compete for controlling behavior.

According to these assumptions, the two strategies are encoded in the model by two different populations of action cells (Fig. 5.3). The first set of action cells, considered as a simplified model of caudate putamen (CP), implements taxon navigation;

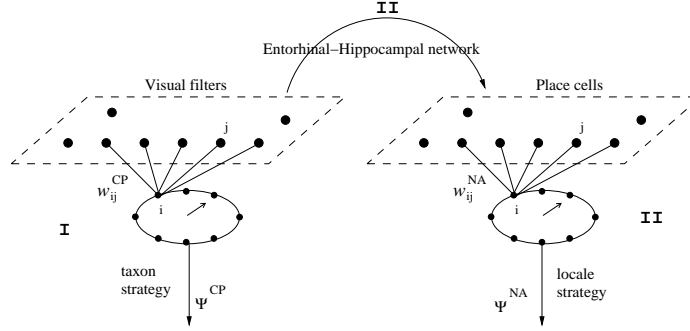


Figure 5.3: Navigation model.

the second set of action cells models navigation-related functions of the nucleus accumbens (NA) and implements locale navigation. Each population consists of $N_{ac}=360$ cells. Cell k in CP codes for egocentric turn by angle $\psi_k^{CP} = 2\pi k/N_{ac}$, while cell k in NA codes for a movement in an allocentric direction $\psi_k^{NA} = 2\pi k/N_{ac}$. Action cells are driven by presynaptic input and fire at rate

$$r_i^{CP} = \sum_j w_{ij}^{CP} r_j^{pre} \quad (5.3)$$

where the index j runs over all presynaptic cells. For the taxon strategy the rate of the presynaptic cells is given by the response amplitude of the visual filters to the current visual image G_j , where j runs over all positions \vec{x}_{kl} in the image and all filter orientations \vec{w}_m . For the locale strategy Eq. (5.3) describes analogously the activity of cells in NA, but the presynaptic cells are the place cells $r_j^{pre} = r_j^{pc}$ (Eq. (5.18), see Section 5.3).

Given the activities of the action cells in population CP, the optimal action according to the taxon strategy is given by the maximally active action cell:

$$\hat{\Psi}^{CP} = \operatorname{argmax}_{\psi_i^{CP}} r_i^{CP} \quad (5.4)$$

In the case of locale strategy, the optimal action is given by the population vector of the action-cell activities:

$$\hat{\Psi}^{NA} = \arctan \frac{\sum_i r_i^n \sin(\psi_i^n)}{\sum_i r_i^n \cos(\psi_i^n)} \quad (5.5)$$

Actions $\hat{\Psi}^{CP}$ and $\hat{\Psi}^{NA}$ are encoded in different reference frames and are assumed to be recoded by the motor system into actions Ψ^{CP} and Ψ^{NA} defined in the egocentric frame of reference of the organism. For the CP no conversion is necessary, whereas for the NA it takes into account the current head direction Φ (Section 5.3.1):

$$\Psi^{\text{CP}} \equiv \hat{\Psi}^{\text{CP}} \quad (5.6)$$

$$\Psi^{\text{NA}} = \hat{\Psi}^{\text{NA}} - \Phi \quad (5.7)$$

Values Ψ^{CP} and Ψ^{NA} represent optimal predictions of the egocentric goal direction according to the taxon and locale strategy, respectively. These predictions have to be *exploited* in order to get to the goal as fast as possible, given the current level of knowledge about the outcomes of the actions. However, in a novel environment a set of available actions has to be *explored* first in order to learn the outcomes of different actions. A possible way of balancing the exploration and exploitation is to choose the optimal action most of the time, while choosing a random action with a small probability ϵ , thus following an ϵ -greedy policy (see Chapter 2). This procedure was adopted in the simulations with $\epsilon = 0.1$.

We apply a simple algorithmic approach for the readout of the action cell activities and their conversion into a unified reference frame Eqs. (5.4 - 5.7). However, in a more biologically plausible setting both operations can in principle be performed by using lateral interactions between actions cells (Deneve et al., 1999, 2001).

The two navigation strategies are implemented as follows.

1. Taxon strategy. In this scenario the simulated rat learns the associations between the configuration of cues visible from the starting position (i.e. a local view) and the direction towards a goal (Eichenbaum et al., 1990; Da Cunha et al., 2003; Cunha et al., 2006). Experimental data suggest that animals with hippocampal lesions follow stereotyped trajectories (O'Keefe and Nadel, 1978), hence we assume here that for a purely taxon strategy the initial choice of movement direction from the starting position determines whether the model rat hits the goal or not in the current trial. A simulation of one trial consists then of presenting a snapshot of the environment taken from the starting position and subsequent rotation by angle Ψ^{CP} calculated according to Eq. (5.6). The trial ends after the animal performs the rotation.
2. Locale strategy. When the model rat is placed into a familiar environment, activities of place cells signal the current location. This location signal propagates to the action cell population and the next action consists of turning by angle Ψ^{NA} (Eq. (5.7)) and then moving by distance $\vec{v}\Delta t$, where \vec{v} is the constant speed of the model rat. This movement changes the position of the animal in the maze, thereby changing the internal position estimate, generating the next action and so on. The trial ends when the animal reaches the goal.

Learning of behavior

Appropriate synaptic weights w_{ij}^{NA} or w_{ij}^{CP} in Eq. (5.3) for both strategies are learned according to Q-learning, an online temporal-difference (TD) update rule (see Chapter 2). In our model the estimate of the Q-value of a movement in direction ψ_i in state s_t is identified with the firing rate of the corresponding action cell (Arleo and Gerstner, 2000b; Strösslin et al., 2005), i.e.

$$Q^n(s_t, a_t = \psi_i^n) \equiv r_i^n \quad (5.8)$$

where r_i^n is calculated according to Eq. (5.3) according to the current strategy ($n = \text{NA}$ or $n = \text{CP}$). This value is updated after each time step by changing weights w_{ij}^n according to:

$$\Delta w_{ij}^n(t) = \eta \delta^n(t) e_{ij}^n(t) \quad (5.9)$$

where $\eta = 0.0001$ is the learning rate, $\delta^n(t)$ is the TD error and $e_{ij}^n(t)$ is the eligibility trace of past state-action pairs. The eligibility trace of a synapse is increased each time the synapse has participated in generating a movement and decays with a constant $\gamma\lambda$

$$e_{ij}^n(t+1) = \exp[-(\psi_i^n - \Psi^n)^2 / 2(\sigma_\psi^n)^2] r_j^n + \gamma\lambda e_{ij}^n(t) \quad (5.10)$$

The exponential term ensures that actions ψ_i^n similar to the actually performed action Ψ^n (Eqs. (5.4,5.5)) are also eligible for learning, thereby providing generalization in the action space (Strösslin et al., 2005). The generalization width σ^n has been tuned to provide fast convergence separately for NA and CP populations (see Table 5.1 for parameter values). Since a taxon trial is finished after a single orientation step (see above), we eliminate memory of previous trials by setting $\lambda = 0$ for the taxon strategy.

Equation (5.9) can be interpreted as a Hebbian learning rule that depends on joint pre- and postsynaptic activity conditioned on the presence of a ‘success’ signal δ . As reviewed in Chapter 3, this signal is likely to be related to phasic activity of dopamine neurons in the SNc and VTA of the basal ganglia (Schultz et al., 1997).

Competition between strategies

The fact that a single learning trial of the taxon strategy always consists of a single step, does not permit to perform competition between strategies on a timestep-by-timestep basis in the present model. Hence, a simplified competition scheme was adopted. For each experimental trial both strategies are simulated in separate runs

with identical starting conditions and weights w_{ij}^{NA} and w_{ij}^{CP} are updated according to the outcome of each strategy for this trial.

The preferable, or the *winner* strategy for each trial is determined from the history of the outcomes of both strategies *after* all trials have been performed. Thus, the locale strategy is considered a winner for a particular trial, if it was more successful during preceding trials than the taxon strategy. More specifically, let n be the number of the current trial and $N_n^l, N_n^t \leq N$ denote the number of successful trials when driven by the locale and taxon strategy, respectively, among the N trials that preceded trial n (i.e. $n - N, n - N + 1, \dots, n - 1$). Then the winner strategy for trial n is defined as follows:

- If $N_n^l > N_n^t$ then locale strategy is the winner in trial n .
- If $N_n^t \geq N_n^l$ then taxon strategy is the winner. The equality is included in this case since the direct (taxon) pathway is assumed to require less effort for producing an action (or, alternatively, produce the next action faster) than the indirect (locale) one.

Successful trials are defined based on the aim of the learning task, separately for each experiment (see Chapter 7).

Thus, an *a posteriori* analysis of the model (i.e. after all trials have been completed) is able to characterize both the behavior of an ‘intact’ animal, i.e. the one which always chooses the winning strategy, as well as that of a ‘lesioned’ animal. In the lesioned animal only one strategy is always used, so no competition occurs.

5.3 Space representation model

Recent experimental data suggest that sensory information about the environment is transformed into an accurate location signal already in the dorsal band of the medial entorhinal cortex (dMEC), the structure upstream from the hippocampus (Fyhn et al., 2004). In addition, direct projections from the dorsal entorhinal cortex to the CA1 field of the hippocampus are sufficient to produce place cell activity in this area, bypassing dentate gyrus and CA3 areas (Brun et al., 2002). Hence we model the place cell activity as a result of feedforward input from the upstream population of cells with periodic spatial firing fields (grid cells), similar to the neurons observed in the dMEC.

5.3.1 Path integration in the network of grid cells

The dorsal band of the medial entorhinal cortex (dMEC) contains neurons with periodic hexagonal spatial firing fields (Fyhn et al., 2004) (see Section 4.2). The fact

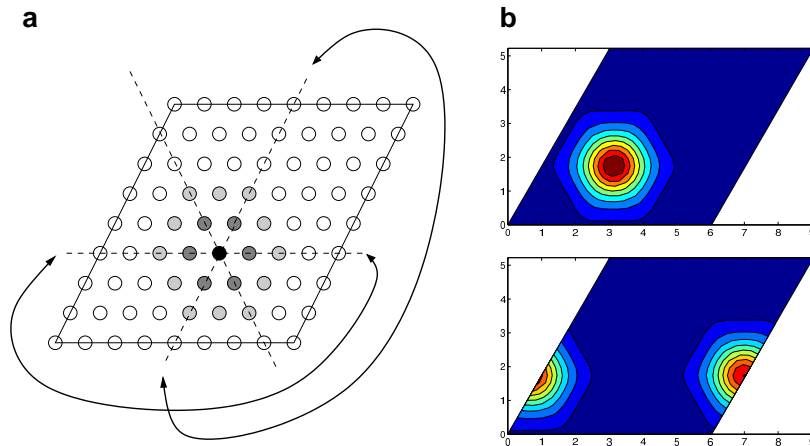


Figure 5.4: a. Organization of a modeled grid-cell population that produces hexagonal firing pattern. The population consists of N_{gc}^2 cells and each cell has six equidistant neighbors. Black arrows show how the cells near the edges of the chart are connected. b. Two examples of population activity plotted in the chart coordinates.

that grid-like firing fields persist in darkness suggests that grid cells are driven by self-motion information. Since grid cells in different layers have different spatial frequencies and orientations, the population of all grid cells together can represent spatial position with a high degree of accuracy and could perform path integration, i.e. integration of self-motion information over time (Hafting et al., 2005).

Our model of the grid-cell network consists of Q populations of cells. Each population can be represented as a two-dimensional chart consisting of cells with lateral connections. The organization of a chart is schematically shown in Figure 5.4a. Each circle in this chart represents one dMEC cell and the spatial arrangement of the circles reflects the *connectivity* between the corresponding cells. There are three essential properties of the connectivity pattern which give rise to the hexagonal firing patterns of each individual cell. First, the closest neighbors of each cell form a regular hexagon, the vertices of which define three principal directions of the chart (shown by the dashed lines). Second, each cell is connected with non-zero weights only to the cells along these principal directions, e.g. the cell shown in black in the figure has connections to the cells along the dashed lines only. Third, the cells near the edge of the chart are connected to the cells on the opposite edge (‘periodic boundary condition’) as shown by the arrows in the figure. The size of the chart is defined as the number of cells along a principal direction denoted by N_{gc} (i.e. the number of cells in the chart is N_{gc}^2).

Given a two-dimensional population of cells organized as shown in Figure 5.4,

each cell can be assigned an index along each of the three principal directions. Then the weight between cells with indices i and j along the same direction is given by:

$$w_{ij}^{\text{gc}} = \exp\left(\frac{\cos(2\pi(i-j)/N_{\text{gc}}) - 1}{\sigma_{\text{gc}}^2}\right) \quad (5.11)$$

where $\sigma_{\text{gc}} = 1.2$ defines the lateral spread of the weights and $N_{\text{gc}} = 25$ is the number of cells along one principal direction of the chart. If two cells do not lie along one of the principal directions, the weight between them is set to 0. Note that the actual spatial distribution of the cells in the brain is irrelevant, as long as the connections between them are as given by Eq. (5.11).

Evolution of activities $o_i(t)$ in the recurrent network are described by two coupled equations:

$$u_i(t+1) = \sum_j w_{ij}^{\text{gc}} o_j(t) \quad (5.12)$$

$$o_i(t+1) = \frac{u_i(t+1)^2}{1 + \mu \sum_j u_j(t+1)^2} \quad (5.13)$$

where the constant $\mu = 0.015$ controls the height of the activity peak in the stable state (Deneve et al., 1999). Presented with a nonzero input, the network stabilizes after a few iterations and the activity in the stable state can be approximately described by a Gaussian function (see Fig. 5.4b). Movements of the model animal through the environment cause corresponding shifts of the activity packets in each grid cell population as described by the update rules below.

In this model, the hexagonal grid-like spatial layout of the firing fields is due to the periodic structure of lateral connections, which are identical for all grid-cell populations. The difference in spacing and field size between cells belonging to different populations is caused by differences in the update rules that convert the movement of the animal into the movement of the activity packet across the charts (McNaughton et al., 2006). An alternative connection scheme that avoids periodic boundary conditions has been described in Fuhs and Touretzky (2006). We note here that simulation results presented in Section 6.2.1 do not depend on the actual implementation of the grid-cell dynamics as long as the resulting firing pattern is periodic.

Integration of self-motion information

Since the form of the activity packet in the stable state is constant over time, its position in the q -th chart can be described by a vector, denoted by $\vec{P}^q(t)$, defined in the chart coordinates. Assuming that the speed of the animal is constant and described by the vector \vec{v} , the update of the activity packet position in the q -th

population due to internal estimates of speed and direction (i.e. proprioceptive and vestibular inputs) is modeled as

$$\vec{P}_{\text{pi}}^q(t) = \vec{P}^q(t-1) + \nu_q \mathbf{R}_q \vec{v} + \vec{\eta}_q \quad (5.14)$$

where $\vec{P}^q(t-1)$ is the activity packet position at the previous time step, $\vec{\eta}_q$ is a zero-mean Gaussian noise term describing errors in internal estimations of speed and direction (with standard deviation equal to 5% of the displacement since the previous time step), ν_q defines the mapping of the absolute value of the speed vector from spatial coordinates to the coordinates of the q -th chart and \mathbf{R}_q is the rotation matrix

$$\mathbf{R}_q = \begin{vmatrix} \cos(\xi_q) & -\sin(\xi_q) \\ \sin(\xi_q) & \cos(\xi_q) \end{vmatrix} \quad (5.15)$$

that defines the mapping of the animal movement direction to the direction of the activity packet. The parameter $\xi_q \in [0, \pi]$ is fixed for a given chart and $\xi_q = 0$ is chosen such that the animal movement along the horizontal spatial axis corresponds to movement of the activity packet along the horizontal axis of the q -th chart. As an example, consider a population with $\xi_q = 0$ and assume that the animal is running along a horizontal spatial axis. If the value of ν_q is such that running over spatial distance L causes the activity packet to make a full cycle across the chart, then the observed distance between the maximal firing locations (i.e. the grid spacing) will be equal to L and grid orientation will coincide with the horizontal axis of space. According to Hafting et al. (2005) grid spacings of different dMEC populations vary from 300 mm to 800 mm and grid orientations cover 360° . Hence, in the model we set ν_q and ξ_q as

$$\nu_q = 2\pi/L_q, \text{ where } L_q = 300 + 500 \cdot \frac{q-1}{Q-1} \quad (5.16)$$

$$\xi_q = \pi \cdot \frac{q-1}{Q-1} \quad (5.17)$$

where $q = 1, 2, \dots, Q$. Distinct values of parameters ξ_q imply that movement of the animal along a spatial direction corresponds to movements of activity packets in different directions in the corresponding charts, allowing for a large number of locations being represented uniquely by the combined activity of all grid-cell layers (Fuhs and Touretzky, 2006).

As reported in Hafting et al. (2005), grid spacings increase along dorsoventral location in the dMEC, whereas no such relationship were observed for the grid orientations. For simplicity, we take the same index q for both spacings and orientations and note that in order to be fully consistent with the data, grid orientations should be distributed randomly between 0 and π (which amounts to a random permutation

of orientations in Eq. (5.17)). Such a change will not, however, change principally any of the results.

Upon the entry into a novel environment, the activity packets are assigned random positions \vec{P}^q in the corresponding charts and current gaze direction Φ is initialized by an arbitrarily chosen direction, which also defines the ‘horizontal’ spatial axis.

We do not model explicitly the head-direction system (Arleo and Gerstner, 2001; Skaggs et al., 1995). After initialization, the head direction estimate is updated according to the egocentric angular rotations of the simulated rat. Cumulative errors in the head-direction estimation are modeled via the noise term η in Eq. (5.14).

5.3.2 Place cells

A single grid cell population can represent the animal position uniquely only over a limited area defined by the grid spacing (Eq. (5.17)). However, since different spatial frequencies and orientations are represented in different grid-cell populations, their combined activity can encode a unique spatial position over a large space. Hence, we model the activity r_i^{pc} of a CA1 hippocampal place cell as a consequence of feedforward projections from the grid-cell population (Brun et al., 2002; Solstad et al., 2006):

$$r_i^{\text{pc}} = [u_i^{\text{pc}} - \theta_{\text{pc}}]^+ = \left[\sum_j w_{ij}^{\text{pc}} r_j^{\text{gc}} - \theta_{\text{pc}} \right]^+ \quad (5.18)$$

where $u_i^{\text{pc}} = \sum_j w_{ij}^{\text{pc}} r_j^{\text{gc}}$ is the potential of cell i , r_j^{gc} is the activity of grid cell j , w_{ij}^{pc} is the connection weight, θ_{pc} is the activity threshold, $[x]^+ = x$ if $x > 0$ and $[x]^+ = 0$ otherwise.

The weights w_{ij}^{pc} are not fixed but learned during the initial exploration of the environment and readjusted by Hebbian learning later on. During exploration, a place cell is ‘recruited’ from a pool of cells on each time step, provided that the current location is represented by less than $T = 20$ sufficiently active place cells, i.e.

$$\sum_k \mathcal{H}(r_k^{\text{pc}} - \theta_{\text{u}}) \leq T \quad (5.19)$$

where $\mathcal{H}(x) = 1$ if $x > 0$ and $\mathcal{H}(x) = 0$ otherwise. This condition limits the cell growth after sufficiently long exploration. The same cell can be occasionally chosen more than once for the same or different environments. This is consistent with experimental evidence that a place cell can have multiple place fields in one environment as well as place fields in different environments (Muller et al., 1987; Kubie and Ranck, 1983).

Once cell i is recruited, the weights w_{ij}^{pc} of the cell are set equal to the current activity of the grid cells, i.e., $w_{ij}^{\text{pc}} = r_j^{\text{gc}}(t)$ where t represents the time step of exploration at the moment of recruitment. On subsequent time steps the weights are updated using competitive Hebbian learning in the form:

$$\Delta w_{ij}^{\text{pc}} = \begin{cases} \eta u_i^{\text{pc}} (r_j^{\text{gc}} - w_{ij}^{\text{pc}} u_i^{\text{pc}}), & \text{if } u_i^{\text{pc}} > \theta_u \\ 0, & \text{otherwise} \end{cases} \quad (5.20)$$

which yields normalized weight vectors such that $\sum_j w_{ij}^2 = 1, \forall i$ (Oja, 1982). The normalization ensures that maximal output firing rate is bounded by the norm of the inputs, i.e. $r_i^{\text{pc}} \leq M = \sum_j (r_j^{\text{gc}})^2$. We note that M is constant since the bump of activity in a grid-cell population has a fixed size and amplitude. The thresholds in Eqs. (5.18,5.20) are fixed at the values $\theta_{\text{pc}} = 0.4M$ and $\theta_u = 0.6M$.

In standard competitive learning (see, e.g. Hertz et al. (1991)) the inputs and outputs are binary and only the weight vector of one output unit, the winner, is updated after the presentation of a pattern (Sharp, 1991). Here we use a soft version of the competitive learning where many output units are updated at each time step and the strength of the update depends on the output unit activity. This allows for faster learning and is biologically more plausible.

In order to use the place cell activity for goal navigation an explicit decoding of position signal is not required (Section 5.2). But in order to analyze the results, it is convenient to calculate explicitly the position encoded by the place cell population. Here we apply the population vector for this purpose:

$$\vec{p}^{\text{pc}} = \frac{\sum \vec{p}_i^{\text{pc}} r_i^{\text{pc}}}{\sum r_i^{\text{pc}}} \quad (5.21)$$

where $\vec{p}_i^{\text{pc}} = (x, y)^T$ is the position where the cell i was recruited during exploration.

5.3.3 Head direction and visual input

The representation of the animal location described so far is updated using only self-motion input and is therefore subject to a cumulative error due to noisy estimates of the movement speed and direction (Eq. (5.14)). This cumulative error can be corrected by using associations between external stimuli and path integration (McNaughton et al., 1996). Since these associations have to be learned during exploration, there is an initial period during which only path integration is available; however, once enough visual information has been accumulated, vision may influence the path integration estimates.

In the model, the visual information at each time step is represented by a local view (i.e. a set of visual filter activities G_{klm} , Eq.(5.2)). During exploration, the local views are stored in memory together with the current estimates of the gaze direction (initially derived from the path integration). After enough local views have been memorized, they can be used to provide an estimation of the allocentric head direction and position – which can then be used to readjust the path integrator implemented in the model grid cells.

Each local view in the model is represented by a hypothetical ‘view cell’. Similar to the recruitment of place cells described in the previous subsection, we recruit ‘view cells’ by the following procedure. If the current view at time t does not lead to a strong activity of at least $T = 20$ view cells, a new view cell i is recruited and initialized with a basis function center $\rho_{ij}^{\text{vc}} = G_j(t)$ that represents the current view at time t . Here $G_j(t)$ denotes the activity of a visual Gabor filter with index j at time t , j runs over all filters. We think of the ‘view cells’ as a simplified model of the memory of local views outside of the hippocampus (Gillner and Mallot, 1998; Spiers et al., 2001).

Instead of modeling the head direction system explicitly we use the following algorithmic procedure to estimate the gaze direction from stored local views. Suppose that a local view i taken from a location x has been stored in memory together with the gaze direction Φ_i . At a later time the model animal returns to the same location but with unknown head orientation. In order to estimate the gaze direction $\hat{\Phi}$, we determine the angle $\Delta\Phi = \hat{\Phi} - \Phi_i$ that leads to the best alignment of the current local view with the stored one (Fig. 5.5). Given the discrete sampling grid of the visual filters, we define an index $u = \Delta\Phi \cdot N_{\text{cols}}/V$ where $V = 300^\circ$ is the total angle of the horizontal view field and $N_{\text{cols}} = 96$ is the number of columns in the filter grid. The goodness of an alignment with shift $\Delta\Phi$ can be formally defined as the normalized cross-correlation $C_i(\Delta\Phi)$ between the current view and the stored view i (Lewis, 1995):

$$\tilde{C}_i(u) = \frac{\sum_{klm} \left(G_{klm}^i - \langle G^i \rangle \right) \left(\hat{G}_{k-u\ lm} - \langle \hat{G} \rangle \right)}{\sqrt{\sum_{klm} \left(G_{klm}^i - \langle G^i \rangle \right)^2} \sqrt{\sum_{klm} \left(\hat{G}_{k-u\ lm} - \langle \hat{G} \rangle \right)^2}} \quad (5.22)$$

where summation is over the indices of the overlapping filters¹ (see Fig. 5.5b), $\langle \cdot \rangle$ is the average filter activity and u is the amount of the relative shift between the local views.

Searching for the maximum of C_i across all possible shifts $\Delta\Phi$ yields the correct angle

$$\hat{\Phi} = \Phi_i + \underset{\Delta\Phi}{\operatorname{argmax}} \left(C_i(\Delta\Phi) \right). \quad (5.23)$$

where $C_i(\Delta\Phi)$ is the cross-correlation function (Eq. (5.22)) with the corresponding change of variables. Generalizing this idea to all the views taken from all different locations yields the gaze direction estimate

¹Since the view field is circular, the shifts in (5.22) are circular and take into account the width of the view field

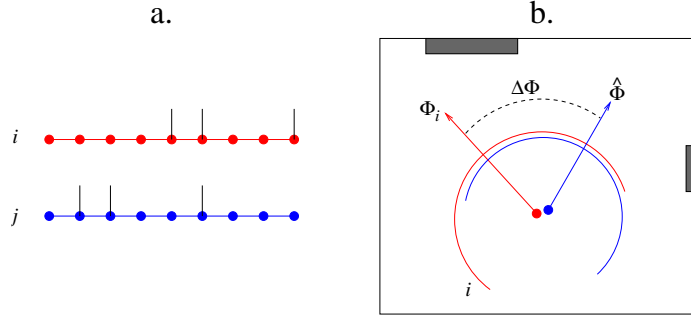


Figure 5.5: Estimation of gaze direction and position from alignment of local views. a. Alignment of one-dimensional local views. Dots denote the filters and black lines denote the filter amplitudes. The local view i has to be shifted left to coincide with local view j . b. A more detailed illustration of the same concept. The large square represents the top view of a room with two landmarks. The two arcs represent two local views as in a (arc widths denote the view field size and arrows represent the corresponding gaze directions). The new gaze direction $\hat{\Phi}$ can be predicted from the old one by estimating the difference $\Delta\Phi$ that corresponds to the best alignment between the filter responses.

$$\Phi_{\text{vis}} = \underset{\Phi}{\operatorname{argmax}} \left(\sum_i C_i(\Delta\Phi) \Big|_{\Phi_i + \Delta\Phi = \Phi} \right) \quad (5.24)$$

Angle Φ_{vis} represents an algorithmic estimation of the allocentric head direction from the set of stored local views and is used to initialize internal head direction estimate Φ upon the entry into a familiar environment (see below). While our model is algorithmic (Franz et al., 1998), rather than ‘neuronal’, it captures the fact that head direction cells are anchored to visual cues of the environment (S. J. Y. Mizumori and Williams, 1993).

Readjustment of path integration

As mentioned above, each stored local view i is represented by a view cell which is modelled as a radial basis function with center ρ_{ij}^{vc} . Given the estimation of the gaze direction Φ_{vis} , the activity of a view cell given by

$$r_i^{\text{vc}} = \exp \left(-\frac{1}{2\sigma_{\text{vc}}^2} \left[\frac{1}{\Omega_i} \|\mathbf{G} - \bar{\rho}_i^{\text{vc}}\| \right]^2 \right) \cdot \exp \left(\frac{\cos(\Phi_{\text{vis}} - \Phi_i) - 1}{\sigma_{\Phi}^2} \right) \quad (5.25)$$

where $\vec{\rho}_i^{\text{vc}}$ is the center of the radial basis function after shifting by an amount $\Phi_{\text{vis}} - \Phi_i$, \mathbf{G} is the set of responses of the visual Gabor filters to the currently perceived view, $\|\cdot\|$ is the Euclidean norm and $\Omega_i = V - (\Phi_{\text{vis}} - \Phi_i)$ is a normalization factor that accounts for the overlap of the the two visual fields. The second exponential term gives more weight to the comparisons with larger overlap, i.e. similar direction of gaze. The value of the parameter σ_{vc} controlling the sensitivity of the visual system was chosen separately for each testing environment such that the average difference between two stored views for that environment causes $r_i^{\text{vc}} = 0.3$. The resulting values were $\sigma_{\text{vc}} = 0.16$ for environments N-I and B-I and $\sigma_{\text{vc}} = 0.08$ for environments N-II, N-III and B-II. The cell directionality is controlled by the parameter $\sigma_{\Phi} = 1.3$.

Readjustment of the path integration network is performed via associative connections between view cells and grid cells. Connection weights w^{vis} projecting from view cells to the grid cells are learned using associative Hebbian learning with weight decay:

$$\Delta w_{ij}^{\text{vis}} = \gamma_0(1 - w_{ij}^{\text{vis}})r_i^{\text{gc}}r_j^{\text{vc}} - \gamma_1 w_{ij}^{\text{vis}} \quad (5.26)$$

where $\gamma_0 = 0.1$ is the learning rate and $\gamma_1 = 0.01$ a decay factor. The first term represents the standard Hebbian rule with a soft bound to implement a maximum weight value of 1 and the second term prevents saturation of all weights.

Because of the Hebbian learning procedures, a view cell j develops strong connections to those grid cells that code for the corresponding location. After learning, the stimulation of the visual system alone will cause a ‘location’ signal \vec{P}_{vc}^q in all grid cell populations:

$$\vec{P}_q^{\text{vc}} = \frac{\sum_j \vec{p}_i^q w_{ij}^{\text{vis}} r_j^{\text{vc}}}{\sum_j w_{ij}^{\text{vis}} r_j^{\text{vc}}} \quad (5.27)$$

where \vec{p}_i^q is the position of the grid cell i on its chart. This position estimate resulting from vision alone is used to update the path integrator

$$\vec{P}^q(t) = \vec{P}_{\text{pi}}^q(t) + \alpha(\vec{P}_{\text{vc}}^q(t) - \vec{P}_{\text{pi}}^q(t)) \quad (5.28)$$

where \vec{P}_{pi}^q is the estimation of the new position due to integration of speed and direction signals (Eq. (5.14)) independent of visual input and α controls the importance of visual input. Its value is chosen according to the following scheme:

$$\alpha = \begin{cases} 0.1, & \text{if } \sum_i \mathcal{H}(r_i^{\text{vc}} - \theta_{\text{vc}}) \geq T \\ 0, & \text{otherwise} \end{cases} \quad (5.29)$$

where $\theta_{\text{vc}} = 0.4$. This scheme ensures that in the beginning of exploration when not enough local views are stored in memory, no readjustment of path integration takes place. To avoid large drift of the path integration estimate when exploring novel

areas the exploration strategy was chosen such that the modeled animal learns the connections w^{vis} in a small localized area, before it moves on to the next one.

If an animal is put back into a *known* environment (i.e. with existing place cell population) the following reorientation procedure is performed. First, the current gaze direction is reset by the allocentric estimate (Eq. (5.24)); second, view cell activities are calculated according to Eq. (5.25). Third, the view cell activities are propagated via the connections to all grid cell populations; and finally activity packet positions are set to \vec{P}_q^{vc} (Eq. (5.27)) in all Q populations of grid cells.

Number of columns in the filter grid	N_{cols}	96
Number of rows in the filter grid	N_{rows}	12
Number of filter orientations	N_{orie}	8
Gabor filter spatial width, degrees	σ_g	1.8
View field of the model rat, degrees	V	300
Size of the action cell population	N_{ac}	360
Probability of a random action	ϵ	0.1
Future discount factor	γ	0.8
Eligibility trace decay factor	λ	0.8
Width of generalization profile in the action space, degrees	$\sigma_{\psi}^{\text{NA}}$	20
	$\sigma_{\psi}^{\text{CP}}$	5
Learning rate	η	10^{-4}
Size of the grid cell population	N_{gc}^2	625
Number of grid cell populations	Q	6
Lateral spread of the weights	σ_{gc}	1.2
Divisive normalization constant	μ	0.015
Place cell activity threshold (relative to the max.)	θ_{pc}/M	0.4
Competitive learning threshold (relative to the max.)	θ_{u}/M	0.6
Number of active cells to consider a location as familiar	T	20
View cell directionality	σ_{Φ}	1.3
Learning rate for calibration weights	γ_0	0.1
Decay rate for calibration weights	γ_1	0.01
Activity threshold for calibration	θ_{vc}	0.4

Table 5.1: Model parameters. The value of parameter σ_{vc} controlling the sensitivity of the visual system is chosen depending on the testing environment (see Section 5.3.3), and thus not shown here.

5.4 Latent *vs* motivational learning

Following O’Keefe and Nadel (1978) we distinguish two learning regimes: latent learning and motivational learning.

In the typical latent-learning situation an animal is put in a novel environment and allowed to explore. The animal is neither hungry nor thirsty, and the location of food or water within this environment is not the source of motivation for the animal’s exploration. If the animals are subsequently made hungry or thirsty, they learn to go to the reward location faster than if there was no such a ‘pre-exposure’ session, suggesting that some information is acquired even during an unrewarded exploration. Such demonstrations of *latent learning* (Blodgett, 1929; Tolman and Honzik, 1930; Tolman, 1948) suggest that during the pre-exposure sessions rats might acquire information specific to the spatial layout of the environment, i.e. its spatial map (White, 2004).

The ability of latent learning has also been related to the question of the overall aim of spatial exploration. Early behavioral data suggest that environment exploration is not observed in the animals with hippocampal lesions and that hippocampal rats tend to produce repetitive, stereotyped behaviors (see Chapter 6 of O’Keefe and Nadel (1978) for a comprehensive review of the role of hippocampus in exploration).

In our model, learning in the entorhinal-hippocampal network is considered to be an instance of latent learning. Several properties of this network make this consideration possible: (i) learning in the modeled network results in acquisition of a spatial map of the environment expressed in population activity of modeled hippocampal neurons (ii) learning equations (5.20,5.26) do not depend on the presence of reward, (iii) exploration (or pre-exposure) phase is required for learning place fields.

The second learning regime requires positive ‘motivation’ in order to learn, i.e it depends on the presence of reward (Eq. (5.9)). Motivational learning may depend or not on the space representation. In fact, we will show that in certain tasks the model learns location of the goal faster after the pre-exposure session (i.e. when the place fields were already learned), than without the pre-exposure, in agreement with experimental data mentioned above. Therefore, before proceeding to the analysis of motivational learning in the model, we examine properties of the latent learning system, i.e. spatially-selective cells in the hippocampal formation.

Chapter 6

Properties of spatial representation in the model

In the previous chapter a new model of goal-oriented behavior was presented. This model describes two different types, or strategies, of goal navigation. The first strategy performs actions associated directly with currently perceived sensory stimuli and represents an instance of a stimulus-response, or taxon, behavior (e.g. approaching a visible goal). The second, locale, strategy, uses a memorized representation of relative positions or surrounding sensory cues. The goal location is remembered with respect to this representation such that it can be approached even in the absence of sensory cues, provided that the current position and orientation with respect to this representation are known. The current chapter examines the properties of the space representation in the model.

Behavioral data suggests that learning of such a representation does not depend on the presence of reward, a type of learning referred to by early researches as *latent learning* (Blodgett, 1929; Tolman and Honzik, 1930). Lesion data suggest that the hippocampus is involved in latent learning and is necessary for tasks where an internal representation of the environment is necessary (O'Keefe and Nadel, 1978). The behavioral and lesion data are complemented by a large number of neurophysiological studies showing that activity of neurons in different parts of the hippocampal formation is highly correlated with a spatial position of the animal. In particular, grid cells in the dorsal entorhinal cortex (Fyhn et al., 2004) and place cells in the CA fields of the hippocampus (O'Keefe and Dostrovsky, 1971) have been thought to play a major role in mediating spatial behavior.

In the set of computer simulation described below we examined firing properties

of grid and place cells that encode the spatial representation in the model, focusing on the following issues:

- How does a self-motion information influence activity of grid and place cells?
- What is the role of visual information during spatial exploration?
- What is the mechanism of interaction between the two types of input?

To address these questions we conducted four computer experiments. Section 6.1 describes the experimental setup, Section 6.2 analyzes firing fields of place and grid cells during unrewarded exploration, Section 6.3 examines an interaction between path integration and visual input in changing rectangular environments and, finally, in Section 6.4 the experimental results are discussed.

6.1 Experimental setup for latent learning

Four different experiments were conducted. In Experiment 1 firing fields of grid and place cells were analyzed while the simulated rat explored a square area 1×1 m. located in the middle of a large room with multiple visual features (environment N-I, see Chapter 2). Cell activities were analyzed in three different conditions:

Open field exploration. The simulated rat was allowed to explore the testing arena by performing movements in random directions. Upon the first entry to the environment, the path integration network was initialized as described in Section 5.3.1 and subsequently updated according to the update equations (5.14) and (5.28).

Darkness was simulated by turning off visual input to the grid cells after an initial exploration period. After 10 min. (4800 time steps) of exploration in darkness the visual input was turned back on.

Cue-rotation condition was subsequently simulated by interrupting the exploration, rotating the walls of the experimental room 90° clockwise, and restarting the simulation from a different location. Upon the re-entry into the environment a reorientation procedure was performed as described in Section 5.3.3.

In the next three experiments the influence of geometric manipulations on the place-cell activity was analyzed. For that purpose two additional sets of rectangular environments were used.

In Experiment 2, a set of shrinking rectangular environments (N-II, see Chapter 2) was used, and the simulated rat was running back and forth along a line parallel to the northern wall of the enclosure, simulating movement along a linear track. During the *training phase*, the simulated rat explored the linear track in the original environment (N-IIa) until a sufficient number of place cells were created. The path integration network was initialized differently at the two ends of the linear track. This was done

to be consistent with the evidence that place cells are directional in linear mazes (Gothard et al., 1996). In the second, *testing phase*, the simulated rat was exposed to each of the shrinking environments (N-IIb – N-IIe) in turn; place-cell activities were analysed while the simulated rat was moving along the track in these novel environments.

In Experiment 3 a similar procedure was repeated, but this time in the set of stretching rectangular environments (N-III, see Chapter 2). The training and testing phases were identical to the ones in the second experiment.

In the last experiment (Experiment 4) environments N-IIIa and N-IIIe from Experiment 3 were used, and the simulated rat was allowed to move in two dimensions. The path integration network was initialized once before the experiment. During the training phase the simulated rat explored randomly the area of the original box (N-IIIa) until a sufficient number of place cells were created. During the testing phase, it moved in a zigzag fashion through the wide box such that directional dependence of place fields could be assessed.

6.2 Experiment 1: learning spatial representation

For all experiments described below the number of grid-cell populations in the model was $Q = 6$. This was enough to produce single localized peak of activity in the place-cell population, in all experimental environments.

In Experiment 1 the activities of grid cells and place cells were analyzed during exploratory behavior of the simulated rat.

6.2.1 Grid cells

An analysis of cell activities in the conditions of Experiment 1 shows that the modeled dMEC cells exhibit grid-like activity pattern from the beginning of exploration, generated by hardwired lateral connections in the model (Fig. 6.1a). Similarly to biological grid cells, the simulated cells have hexagonal firing fields extending over the whole area of the testing environment, due to periodic lateral connections in the grid-cell subpopulations (Fig. 6.1b-d). Cells that belong to different grid-cell populations differ by grid spacing and orientation as well as by the sizes of the peak firing locations (Hafting et al., 2005). The difference in spacing and orientation is due to the mapping of speed and direction of the animal movement into the speed and direction of the movement of activity packets in different populations (Eq. (5.17)).

The firing fields of the grid cells in the model persist in darkness (Fyhn et al., 2004), but drift slowly due to the noise in the path integrator (Fig. 6.1e,f). To examine the drift of the path integration update, grid-cell activities were analyzed separately during the first and second halves of the darkness period and the difference map was

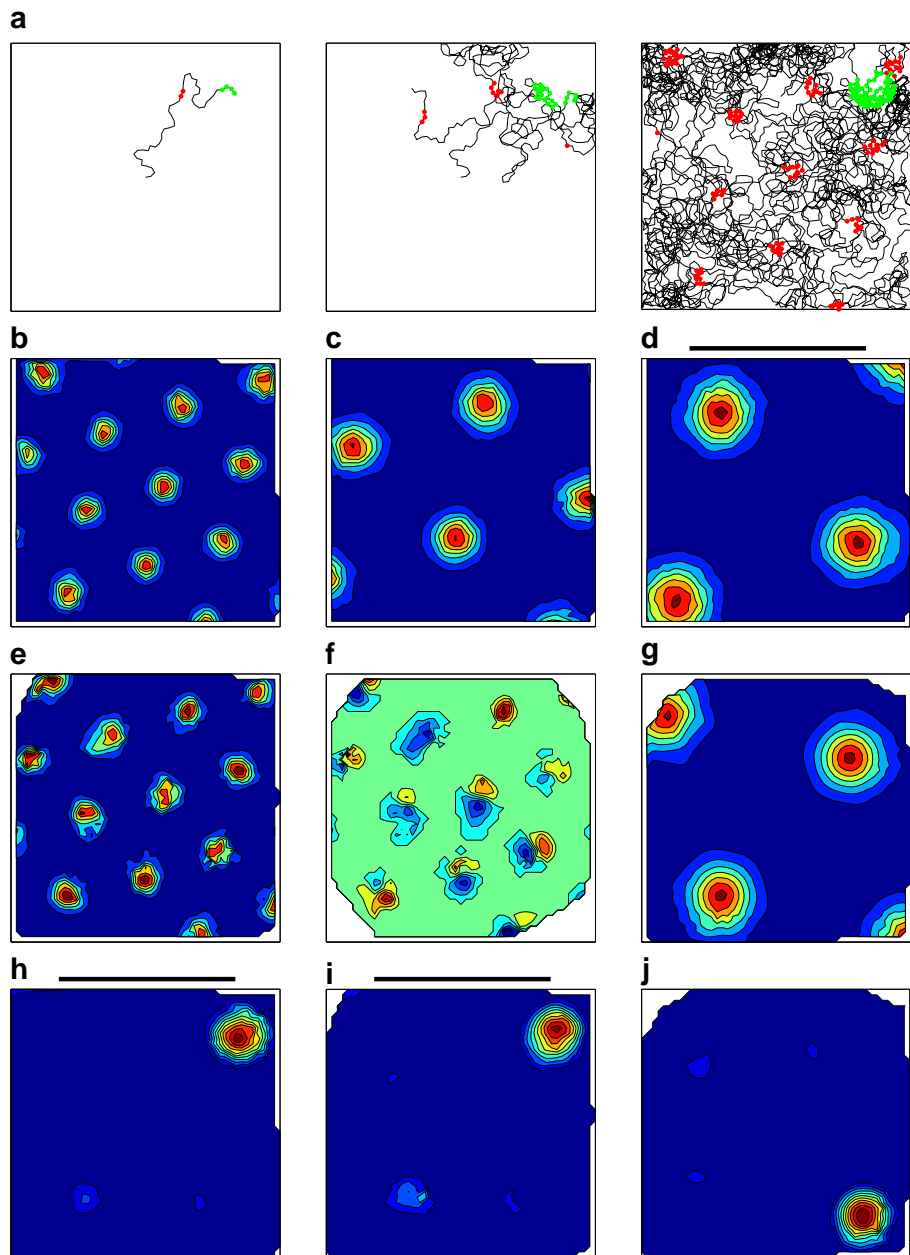


Figure 6.1: Firing field properties of modeled grid and place cells. (a) Trajectory of the modeled rat at three subsequent moments during exploration. Red (green) dots mark the locations where the firing rate of an example grid (place) cell was higher than 0.7 of its maximum over the whole environment. (b-d) Color coded rate maps of three grid cells from different populations (blue - minimum rate, red - maximum rate). (e) Rate map of the cell shown in b measured during 10 min (4800 time steps) exploration in the absence of visual input. (f) Rate difference map between the first half and second half of the darkness period for the cell shown in e. Difference in the locations of the red and blue peaks expresses the drift of the firing grid (green color corresponds to zero difference). (g) Rate map of the cell shown in d measured in the environment with rotated visual cues (the black bar denotes cues on the northern wall in the non-rotated environment). (h-j) Firing rate maps of the place cell shown in a in the original environment (h), in darkness (i) and with rotated visual cues (j).

calculated (Fig. 6.1f). The difference in locations of positive and negative peaks in the difference map corresponds to the amount of drift. Note that in the combined map (Fig. 6.1e) this drift is expressed as a weak dispersal of locations of peak firing (Hafting et al., 2005).

In the cue-rotation condition the firing fields of the modeled grid cells rotated together with visual cues (Hafting et al., 2005) (Fig. 6.1d,g). In the context of the model this is explained as follows. Since the model represents and stores local views as responses of a set of orientation-sensitive filters, a view taken, e.g., in the northern direction corresponds to a view taken in the eastern direction after cue rotation. This has two consequences: first, the current gaze direction is incorrectly estimated as ‘north’ during the reorientation procedure, (Eq. (5.24)); second, since the grid-cell network is influenced by the view upon the entry (Section 5.3.3), rotation of visual cues causes a corresponding rotation of the grid-cell firing patterns.

We emphasize here the crucial influence of the head direction estimation (Eq. (5.24)). Rotation of the firing fields is a direct consequence of the error in the estimation of an allocentric gaze direction. This error is caused by the fact that currently perceived view in the rotated environment is correlated maximally with the snapshots that were taken in the northern direction and stored during exploration.

Rotation of all visual cues in the present experiment is equivalent to rotation of a single controlling cue card (Hafting et al., 2005). Note here that the model avoids definition of what is a cue card or a landmark. The maximum correlation estimation gives a most likely amount of rotation on the basis of similarity between local visual features in the visual field.

6.2.2 Place cells

Each place cell in the model represents a subset of most active grid cells at a certain location in the environment, as a result of competitive learning. Therefore, in the conditions of Experiment 1, the simulated place cells (*i*) exhibit location sensitive firing from the first time the simulated rat passes through the field (Hill, 1978); (*ii*) have place fields that persist in darkness (Quirk et al., 1990); and (*iii*) rotate their firing fields following a rotation of visual cues (O’Keefe and Conway, 1978) (Fig. 6.1h-j).

The results of Experiment 1 show that the place cells in the model depend on the path integration as well as on the visual input. However, contrary to most previous models, this dependence is inherited from the upstream population of grid cells.

In the simple scenario of the Experiment 1 the dependence on the visual input is expressed as a rotation of firing fields following the rotation of visual cues, while dependence on the path integration follows from the ability of these cells to fire in the absence of visual cues. These two phenomena, observed in biological place cells as well, served as a reason to think that place cells perform a combination of the two

types of sensory signals (i.e. internal and external) (Quirk et al., 1990; O’Keefe and Conway, 1978; Jeffery and Keefe, 1999).

Further insights into the mechanism of this combination come from experiments in which place cells were recorded while the geometry of the surrounding environment was manipulated. O’Keefe and Burgess (1996) were first to observe a sensitivity of the place-cell activity to changes in the geometric layout of a rectangular testing arena. Their results suggested that the activity of place cells depends on distances to the nearby walls and were interpreted in favor of the hypothesis that geometry of space plays an important role for spatial orientation, presumably mediated by the hippocampal place cells (Wang and Spelke, 2003; Cheng and Newcombe, 2005). However, when Gothard et al. (1996) investigated the mechanism of interaction between vision and path integration when rats were running on a shrinking linear track, they realized that such interaction might explain the dependence of place-cell activity on distances to walls observed by O’Keefe and Burgess (1996)

In a set of experiments below we show that our model is consistent with experimental data of Gothard et al. (1996) and O’Keefe and Burgess (1996) and hence explains the influence of environmental geometry by the process of correction of path integration using learned associations between visual snapshots and grid cells.

6.3 Dynamics of place fields in geometrically manipulated environments

6.3.1 Experiment 2: Shrinking linear track

Before presenting results of Experiment 2, we briefly describe the setup of the experiment of Gothard et al. (1996). In this experiment, rats were trained to shuttle back and forth along a linear track with a movable box on one end and a fixed reward site on the other (Fig. 6.2). The box remained at the same location throughout the entire training period (Box 1). During testing, the track was shortened on some trials by moving the box towards the reward site, when the box was behind a rat and presumably outside of its visual field. On these testing trials the box was randomly moved between five different locations (Box 1 to Box 5).

Cell recordings show that in all five conditions, cells located near the ends of the track kept their place fields at fixed distances to the nearby walls. In contrast, cells located near the middle of the track lost their place fields in the shortest-box condition (Box 5). Similar experimental results were also reported by Redish et al. (2000).

We tested the effect of shrinking of the environment on the place field activity in our model. The simulation reveals that cells that had firing fields near the walls in the original environment (N-IIa) kept their fields close to the same walls in the shrunk environments (Fig. 6.3). This is explained in the model by the inertia of the

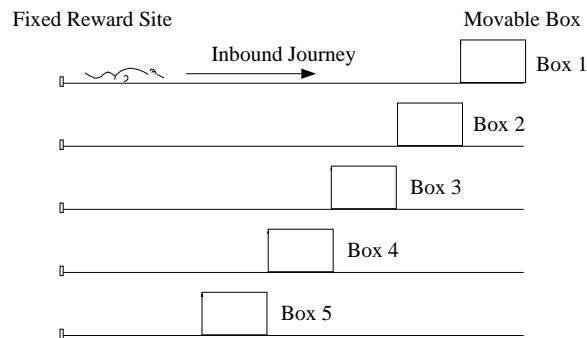


Figure 6.2: Experimental setup used by Gothard et al. (1996) The rat is trained in a linear track to alternate between a fixed site and a movable box (Box 1). The rat is later tested in the same track, but with the box moved between five different positions (Box 1 to Box 5) on some trials.

path integration network, represented by parameter α in Eq. (5.28). Even for big mismatches between visually estimated position and the path-integration estimate, correction signal to the grid-cell populations during the first several steps after path integration reset is small, but accumulates with time.

This accumulated correction signal can have two consequences, depending on size of the mismatch:

- For a small mismatch (N-IIb and N-IIc, Fig. 6.3) place cells in the middle of the track have narrower place fields and the position of the place fields shifts in a direction opposite to the direction of movement.
- For a large mismatch (N-IId and N-IIe, Fig. 6.3), place cells near the middle of the track lose their place fields.

Figure 6.4 explains these effects in the framework of our model. Suppose that two grid cell populations labeled $q = 1$ and $q = 2$ are mapped onto the real space as shown by two parallelograms in Figure 6.4b. Suppose further that at the moment the activity packet positions in both populations correspond to the actual position A of the rat, while visual input predicts a different position B . If the mismatch between A and the visual estimate B is small (Fig. 6.4b) then the cross-talk between vision and path integration (Eq. (5.28)) makes the two activity peaks merge at an intermediate position between A and B , indicated by the cross in the figure. Thus, visual input in a slightly shortened track ‘pulls’ the grid-cell activity packets forward, and this forward movement of the activity packets causes a forward movement of the corresponding subset of active place cells. Place cells near the middle of the track shift their place

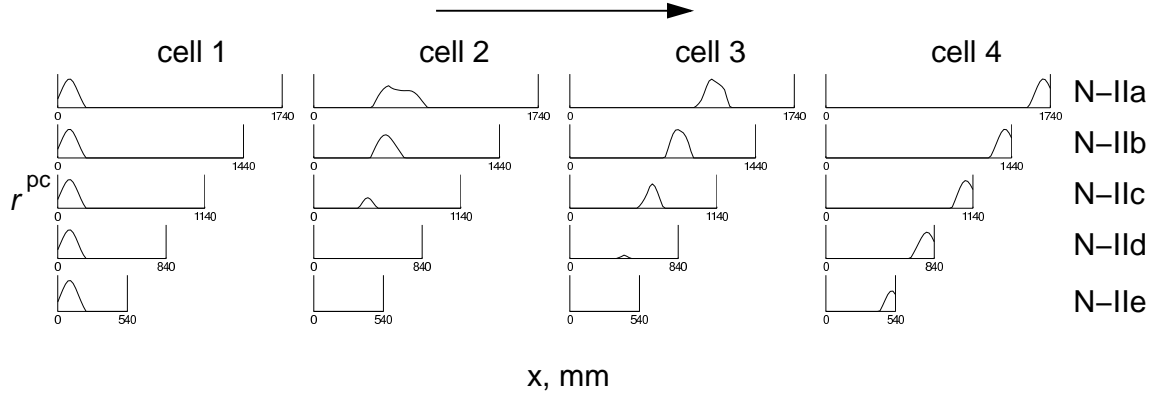


Figure 6.3: Place fields (r^{pc} as a function of the model rat’s position on the track) of four modeled CA1 cells in the original (N-IIa; top graph) and shrunk (from top to bottom: N-IIb, N-IIc, N-IId, N-IIe) environments during the rightward movement. Note that cell 2 has a large field in the original environment, that shrinks and finally disappears in shrunk environments.

fields backwards, since in this case they are activated in advance compared to the position where they would have been active on the basis of a pure path-integration update. This effect is similar to the one described by Samsonovich and McNaughton (1997) for a single activity packet, but generalized to the case of the multi-layer path integrator.

However, for a large mismatch (Fig. 6.4c) the activity packets in different charts are shifted in different directions due to the periodicity of the lateral connections (or, equivalently, to the periodicity of the firing fields). Hence, the superposition of several grid-cell activity packets (Eq. (5.18)) is not coherent with the superposition learned during training, so that the place-cell stimulation remains subthreshold. In this case, place cells with preferred positions between A and B lose their place fields.

In order to characterize the dynamics of the whole population of cells, the vector of place-cell firing rates measured in each location of the shortened track was cross-correlated with the firing rate vectors corresponding to each location on the original track (Gothard et al., 1996). More specifically, let x be the position of the simulated rat along the original track, x' the position of the rat along a shrunk track and $r_i^{pc}(x)$ the vector of place-cell firing rates (Eq. (5.18)) when the rat is in position x . Then the cross-correlation matrix between the firing rates in the original and shrunk tracks is calculated as:

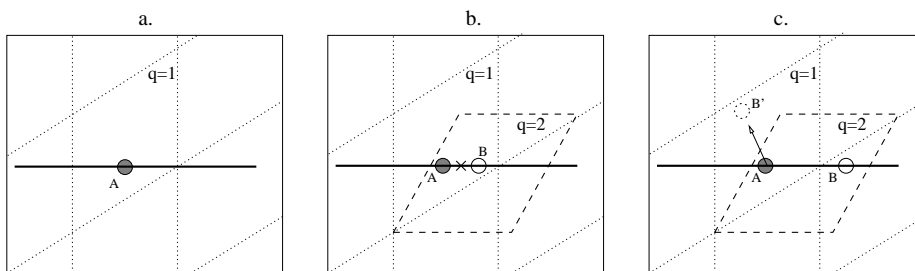


Figure 6.4: Schematic illustration of mismatch correction in the grid-cell populations. In all plots, the large square is the top view of the room and the black line is the linear track. a. Dotted lines show a possible mapping of the grid-cell chart corresponding to a population labeled $q = 1$ onto the floor of the room, A is the current position of the rat on the track. b. Same graph as in (a) but the mapping of the grid cell chart corresponding to another population ($q = 2$) is added (dashed line). Activity packets in both charts are in positions that correspond to A . Suppose that B is the visually estimated position. Due to the influence of vision both activity packets move towards B , leading to a coherent signal sent to place cells in the hippocampus, so that place cells between A and B fire. c. If the mismatch between A and B is too big, the activity packet in the first population moves in the direction of B' , while that of the second population moves in the direction of B . Summation of the grid cell activities is no longer coherent so that the place cells between A and B lose their place fields.

$$c_{xx'} = \sum_i \frac{r_i^{\text{PC}}(x)r_i^{\text{PC}}(x')}{\sqrt{\sum_j (r_j^{\text{PC}}(x))^2 \sum_k (r_k^{\text{PC}}(x'))^2}} \quad (6.1)$$

Figure 6.5 shows the cross-correlation matrices between firing rates in the original track (vertical axis) and each of the shrunk track (horizontal axes) when the rat was moving from left to right (top row) and from right to left (bottom row). The band of a strong correlation along the diagonal on the full track (N-IIa, Fig. 6.5) expresses the fact that the population vectors were similar for nearby locations. Since place fields were larger in the middle of the track (e.g., cell 2, Fig. 6.3), the correlations extend over a broader band on both sides of the diagonal. Small deformations of the environment were tracked by the grid-cell activity packets due to the influence of visual input. These deformations result in shifted and narrowed place fields of cells near the middle of the track (environments N-IIb,c). For larger deformations, however, these place cells lose their place fields (N-IId,e). The disappearance of the place fields is a consequence of the fact that a combination of the grid-cell activity packets from different populations was no longer coherent, due to the strong influence of the visual input as explained above.

6.3.2 Experiments 3 and 4: Stretching rectangular rooms

In the last two experiments, we analyzed place field dynamics in a stretching rectangular box (environment N-IIIa – N-IIIe, see Chapter 2). In order to highlight the relation to the shrinking track experiment, we first considered the case of linear movement and then turned to movement in two dimensions.

In the linear case (Experiment 3), similarly to the previous simulation, population vectors near the two ends of the linear track correlated strongly with the population vectors near the two ends of the track seen during training (i.e. cells near the walls keep their size and distance to the nearby wall approximately constant, Fig. 6.6a). In contrast, a decrease in the slope of the high cross-correlation band suggests that place cells with preferred position near the middle of the original environment extended their place fields. Moreover, in the widest box, cells with preferred position *between* the two bands corresponding to different directions of movement (e.g. exactly in the middle of the original environment) had different peak firing locations depending on the direction of movement (Fig. 6.6a,b environment N-IIIe).

These results are in agreement with data from (O’Keefe and Burgess, 1996) who report that when place fields were learned in a narrow rectangular room with gray walls and later recorded in a wide rectangular room, those in the middle of the environment have stretched together with the room. Furthermore, the stretched fields consisted of two directional subcomponents that were activated depending on the direction of movement.

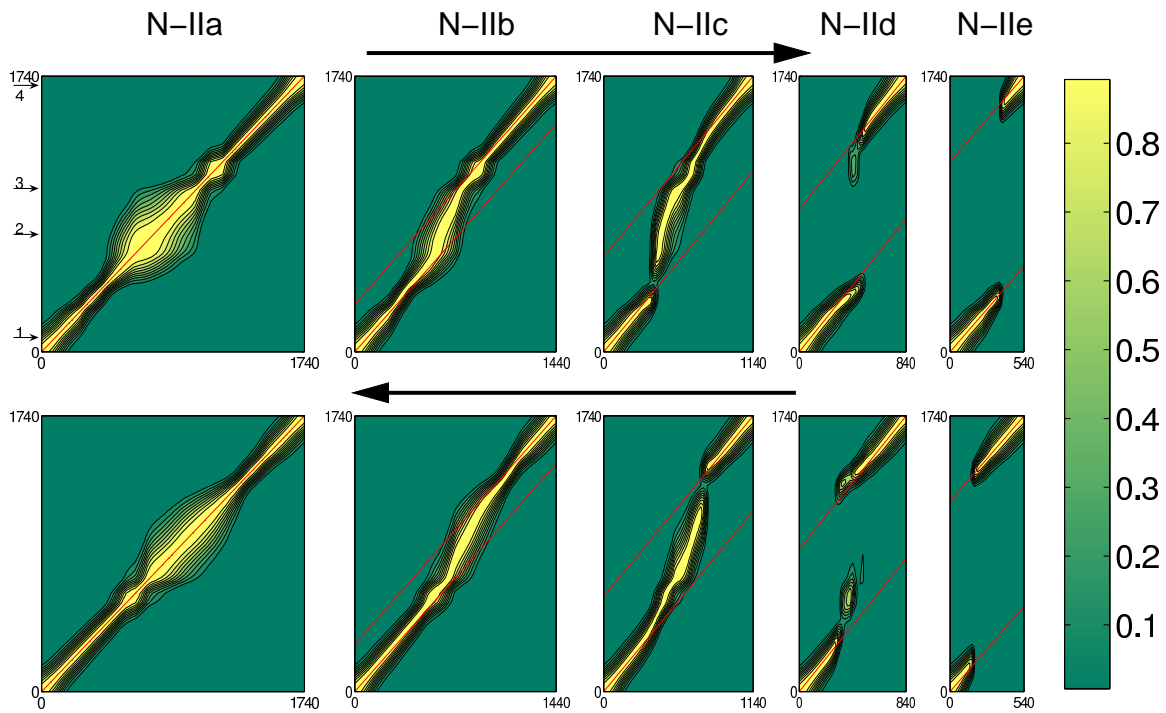


Figure 6.5: Cross-correlation matrices between place-cell firing rates in the shrunk environments (horizontal axis) and the original environment (vertical axis) for the five environments and two directions of movement (shown by the black arrows). The red lines correspond to the locations of the cross-correlation maxima when the position of the rat is measured with respect to the left (lower line) or right (upper line) wall. Small arrows in the upper-left plot mark the locations of maximal firing in the original environment of the four cells shown in Figure 6.3.

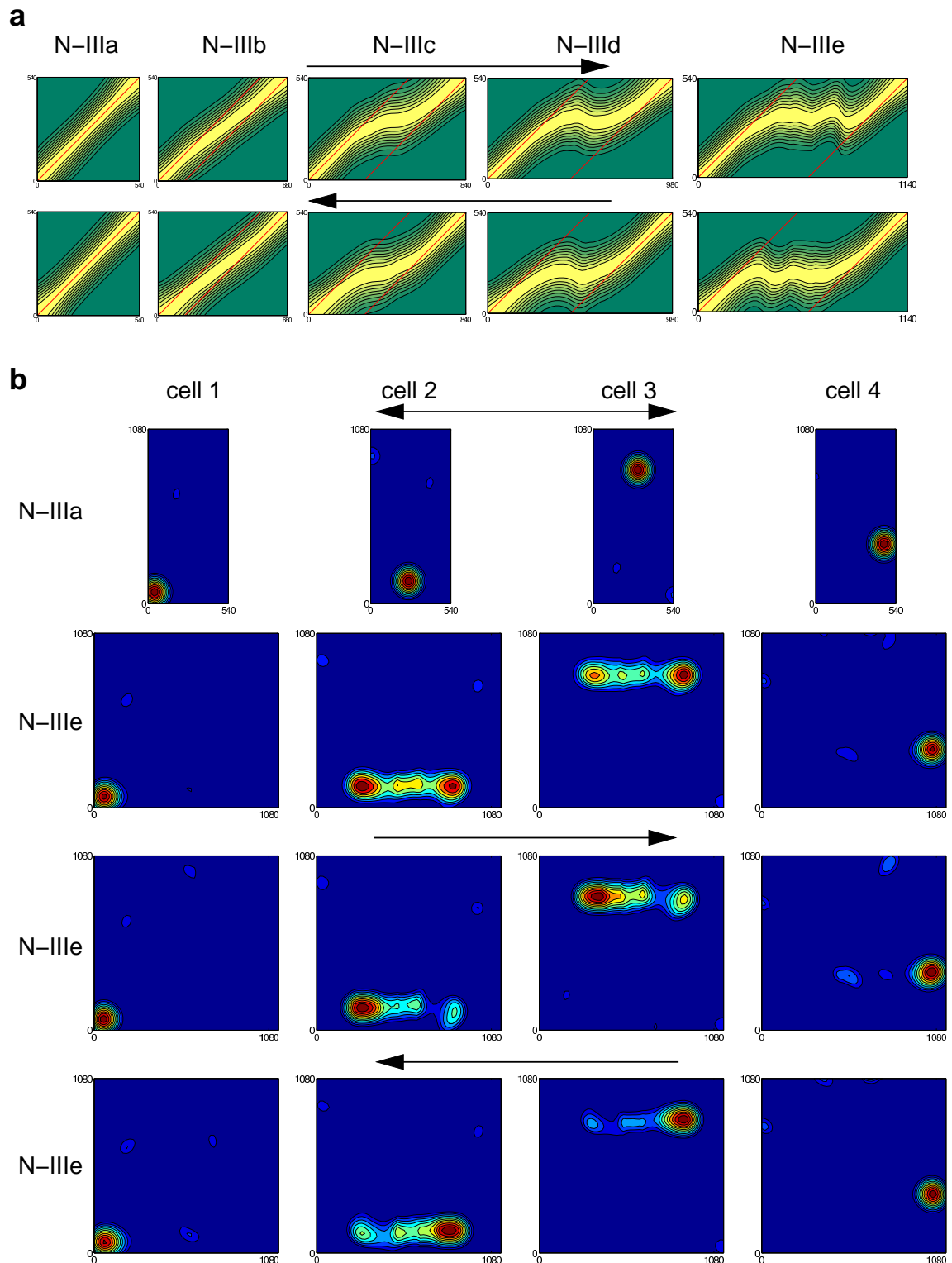


Figure 6.6: Place-field deformation in a stretching environment. (a) Cross-correlation matrices in the original (N-IIIa; top row) and stretched (N-IIIb-e) boxes when the model rat was moving along a linear trajectory in two different directions (shown by the black arrows) (b) Two-dimensional place fields of four different place cells for the original (N-IIIa) and stretched (N-IIIe) versions of the box for leftward movement (bottom); rightward movement (2nd from bottom) and averaged across directions (3rd from bottom).

In order to show that the same effect is preserved in the two-dimensional environment, we conducted Experiment 4, in which the simulated rat was allowed to move in two-dimensions, similarly to the rats in the experiment of O’Keefe and Burgess (1996). Figure. 6.6b shows firing fields of four cells in the narrow (N-IIIa) and wide (N-IIIb) boxes for different directions of movement. Cells 1 and 4 with preferred positions near walls in the original environment (Fig. 6.6b, top row) retained their field sizes and distances to the closest walls in the stretched box (second row). Their peak firing locations did not depend on the direction of movement (two bottom rows). In contrast, cells 2 and 3 with preferred positions near the middle of the original box extended their place fields in the stretched box. Furthermore, the peak firing locations depended on the direction of movement (Fig. 6.6b, two bottom rows) such that when moving from left to right the left part of the field is more active, whereas when moving from right to left the right part of the field is active, in agreement with data of O’Keefe and Burgess (1996).

6.4 Discussion

Results of the simulations demonstrate that the model is able to capture a number of neurophysiological properties of grid and place cells: (1) CA1 and dMEC cells exhibit spatially-localized firing fields (O’Keefe and Conway, 1978; Muller et al., 1987), (2) anatomical topology is not observed in the CA1 population, but cells in the dMEC are organized in several subpopulations with different frequencies and orientations (O’Keefe and Conway, 1978; Kubie and Ranck, 1983; Muller and Kubie, 1987; Hafting et al., 2005), (3) cells in the CA1 and the dMEC exhibit localized firing from the first time the rat passes through their place fields (Hill, 1978; Wilson and McNaughton, 1993; Hafting et al., 2005), (4) both cell types retain their location sensitivity in the absence of visual input (i.e. in darkness) (O’Keefe and Conway, 1978; Hill and Best, 1981; Muller and Kubie, 1987; O’Keefe and Speakman, 1987; Quirk et al., 1992; Fyhn et al., 2004) (5) firing fields of both cell types rotate following rotation of visual cues (Muller and Kubie, 1987; Cressant et al., 1997, 1999; Hafting et al., 2005) (6) CA1 cells stretch their fields if the environment is stretched and some place fields disappear when the environment is shrunk (O’Keefe and Burgess, 1996; Gothard et al., 1996; Redish et al., 2000).

We note that Gothard et al. (1996) were first to propose the idea that interaction between visual input and path integration can explain results of O’Keefe and Burgess (1996). This suggestion was later tested by Samsonovich and McNaughton (1997) in their model. The key contributions of our model in this respect are (i) reproduction of the same results using interconnected network of grid cells and place cells, and without an explicit representation of walls in the model and (ii) an implementation of a correction mechanism by means of which the path integration, performed in the

model by the grid-cell network, is updated using two-dimensional local views of the environment.

In this work we do not propose a new model of grid cell activity (Fuhs and Touretzky, 2006; Solstad et al., 2006; Rolls et al., 2006; McNaughton et al., 2006). Rather, we try to answer the question whether the feed-forward projection hypothesis for the development of place fields of the hippocampal CA1 cells is consistent with the known properties of place cells, e.g. dependence of their place-field shapes on the geometric layout of the environment (O'Keefe and Burgess, 1996) and dynamics of the place fields during movement along a shrinking linear track (Gothard et al., 1996). The results of the simulations in this chapter suggest that the answer is positive.

We would like to stress the two important points that distinguish our model from other models of place cells (including those that model place cell activity as a result of feed-forward projections from grid cells (Solstad et al., 2006; Rolls et al., 2006)): *(i)* visual input is represented in the model by the activities of a large set of orientation-sensitive filters applied to input visual images and *(ii)* visual information influences grid-cells directly, but place cells only indirectly via the grid cells.

Although many properties of place cells mentioned above were reproduced by other models (see Section 4.4.1), most of these models used the abstract notions of distances and bearings to walls or landmarks. However, it is not clear how a landmark or a wall are represented in the rat's brain, and so these models rely on abstract human notions when trying to explain cell activities. In contrast, our model suggests that many of these properties can be explained, at least to some extent, by simply considering local visual features that constitute local views of the environment, and their interactions, without artificial separation of these features into belonging to a wall or to a landmark.

For example, neurophysiological data suggest that distal visual cues exert stronger control over place fields than nearby cues (Poucet, 1993; Poucet et al., 2003). In a watermaze study of Cressant et al. (1997), when the only visual cues in the environment were three objects located in the periphery of the maze close to the walls, their rotation (as a whole) was followed by rotation of place fields. However, when the same objects were placed near the center of the watermaze, they failed to control place field locations after rotation.

In the context of our model these results can be explained as follows. When the objects are located at the periphery, their rotation controls place-field locations in the same way as did visual cues in Experiment 1 (Fig. 6.1i,j). In this case, local views in the rotated state look exactly the same as in the non-rotated state, since they are simply rotated as a whole relative to each other. In this case the place fields will look rotated, due to the correlation-based algorithm of the head-direction estimate. In contrast, when the objects are located near the center of the maze, the estimation of a reference direction from the set of local views is difficult, because the left-right relationship between the object positions on different snapshots could be

reversed (Cressant et al. (1997)). As we will see in the next section, snapshot-based estimation of the reference direction, in the case when different objects can occupy the same positions relative to the rat, results in orientation errors due to inability to extract detailed differences between the objects based on limited number of snapshots.

Chapter 7

Simulation of rat goal-oriented behavior

As the complexity of the task and perceptual capabilities of biological organisms increase, an explicit spatial representation of the environment appears to be employed to support navigation (Tolman, 1948). It has been hypothesized that such a representation is encoded by hippocampal place cells during a process of unrewarded exploration of a novel environment (O'Keefe and Nadel, 1978). In the previous chapter we examined properties of the modeled spatial representation, stored in the simulated populations of location-sensitive cells. In this chapter we proceed to the question of how such a representation can be used for goal-oriented behavior.

Our review of animal navigation in Chapter 3 suggests that animals can use locale and taxon strategies depending on the task. Thus, the first major goal of the present chapter is to analyze the reward-based learning algorithms that implement locale and taxon strategies in the model. Our analysis is focused on the advantages and limitations of the two strategies as well as on the conditions under which one or the other strategy is preferable.

The second major goal of the chapter is to examine the model behavior in a set of tasks in which rats exhibited a preference for the geometric cues (i.e. the shape of the environment) over non-geometric visual features (see Section 3.3.1). We believe that understanding of the surprising behavior of rats in these tasks might provide an insight into the processes underlying the rat's perception of the surrounding environment.

We focus on the experimental paradigms: Morris watermaze task with hidden platform (Morris, 1981) and rectangular room with hidden food source (Cheng, 1986). The two paradigms were chosen for two reasons. First, the watermaze task has

been used in numerous studies to demonstrate the rats' ability to use extra-maze cues for goal navigation in both the locale and taxon regimes; hence it provides an experimental paradigm that allows for comparison between the two strategies in exactly the same sensory environment. Second, none of these studies suggested that the spatial layout of the surrounding environment might be of primary importance for navigation. In contrast, experiments of Cheng performed in the task conditions, which can be thought of as a dry-land variant of the watermaze task, have lead to a surprising conclusion that the geometry of a surrounding space is the primary factor during the goal-oriented behavior. By modeling the goal oriented navigation in these two paradigms we aimed at understanding the distinctions and similarities in the task conditions and rat behaviors that have lead to such different conclusions.

Each section in this chapter presents results from a different set of simulations. Section 7.1 investigates learning of a hidden goal in the watermaze by the two navigation strategies; Section 7.2 proposes a view-based reorientation hypothesis that explains results of Cheng (1986) without invoking the 'geometric module' concept; Section 7.3 explores further the distinction between geometric and non-geometric cues in the context of the experiment of Pearce et al. (2004). Finally, we conclude with general discussion of our results in Section 7.4.

7.1 Locale and taxon navigation strategies in the watermaze

To study properties of the two goal-navigation strategies we have chosen the experiments of Morris (1981) for the locale navigation and Eichenbaum et al. (1990) for the taxon navigation. In both experiments rats had to find a submerged platform in a circular pool filled with milky water. In the standard Morris task the rats are placed into the pool in a different location on each trial. In these conditions, rats with hippocampal lesions were impaired compared to normal rats.

In contrast, in the experiment of Eichenbaum et al. (1990) the same starting position was used in all trials. In this case, lesions of fornix (connecting hippocampus with NA) did not prevent rats from learning, suggesting that different navigation strategies could be used by rats in these experiments. To study further the consequences of fornix lesions, the rats were released from a novel starting position, not used during training (Eichenbaum et al., 1990). Whereas intact rats swam directly to the platform, fornix-lesioned rats failed to do it. Hence the impairment was related specifically to the ability of the lesioned rats to generalize their knowledge of the platform position to novel starting locations.

We tested our model in the computer versions of the two tasks. We then analyzed the effects of 'lesions' (i.e. inactivation of either locale or taxon pathways in the

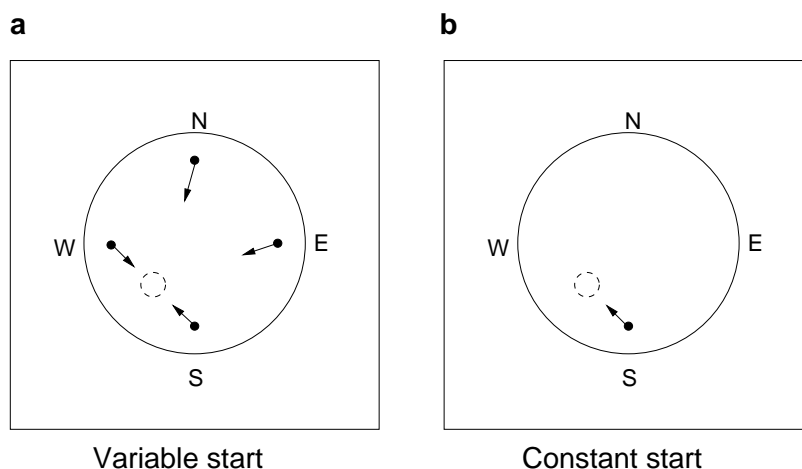


Figure 7.1: Experimental setup and simulation results for the two watermaze tasks. (a) Four starting positions (black circles) in the circular maze were used in the variable start task. (b) In the constant start task only the starting position S was used during training. Arrows show the direction to the invisible target platform in each condition.

model) on the model performance for the two tasks and during the novel-start tests.

7.1.1 Experimental procedures

Computer simulations consisted of two parts: simulations in the *variable-start* condition were designed by analogy to the experiment of Morris (1981), whereas the *constant-start* condition corresponded to the experiment of Eichenbaum et al. (1990). In both conditions the same virtual environment was used (environment B-I, see Chapter 2).

Before the training trials started, the simulated rat was given a *pre-exposure session*, during which it explored the area of the watermaze without any rewards given, until a sufficient number of place fields were learned. Hence, during the training trials the simulated rat could either learn the goal location using the representation of the environment built during the pre-exposure (i.e. use locale strategy), or use taxon strategy. During the training, platform 6 cm in diameter was located in the SW quadrant of the simulated watermaze (Fig. 7.1).

In the variable-start condition, a training trial started by placing the simulated rat in one of the four starting positions shown in Fig. 7.1a, chosen at random in the beginning of the trial. In the constant-start condition, the simulated rat was placed always in the S position at the start of a trial (Fig. 7.1b). Initial orientation of the simulated rat in both condition was randomly chosen between 0° and 360° .

Competition between strategies and performance comparison

As described in Section 5.2, the competition between the two strategies was modeled trial-by-trial, rather than timestep-by-timestep. On each trial the simulated animal performed two separate runs, one using locale strategy and the second one using the taxon strategy (see below). The performance of a particular strategy on a trial was coded by binary value (success/failure). The winning strategy for each trial was determined *after* all training trials were completed as the one having more successes during $N = 10$ preceding trials. An intact animal was assumed to always use the winning strategy, and a lesioned animal could only use the available strategy. Hence after all training trials completed, performance of intact animals could be compared with that of lesioned animals.

For visualization purposes, performance of a particular strategy on each trial was assigned either value 0 (if it was a success) or 1 (failure). After all trials were completed, the two binary vectors, corresponding to the two strategies were smoothed with a running average filter with N -trial kernel, resulting in smoothed *performance curves*.

Simulation of locale navigation. From the starting position the simulated rat was allowed to move around the watermaze according to locale strategy rules (see Section 5.2) until the platform was hit. At this moment the rat received a positive reward. Wall hits were negatively rewarded. At the end of the trial the weights between place cells and action cells in NA were updated according to (Eq. (5.9)).

The outcome of the locale strategy run on this trial was considered as a success, if the time to reach the platform (i.e. the escape latency) was not higher than predefined threshold τ , which was calculated as

$$\tau = \mu_{\text{asym}} + \sigma_{\text{asym}}$$

where μ_{asym} and σ_{asym} are the average values of the escape latency and its standard deviation after the performance stabilized (in the present simulations after 20 trials). Otherwise the locale strategy was considered a failure.

Simulation of taxon navigation. At the starting position the simulated rat performed an egocentric turn according to the taxon strategy rules (see Section 5.2). If the resulting heading direction was not more than 10° off the direction to the center of the platform, the rat was given a positive reward (success). Otherwise no reward was given (failure). At the end of the trial the weights between visual filters and action cells in CP were updated according to (Eq. (5.9)).

Novel-start tests for the constant-start condition

As mentioned before, experimental data suggest that after training in the constant start condition, intact rats are able to swim directly to the hidden platform from novel starting positions, whereas rats with fornix lesions are impaired in this task (Eichenbaum et al., 1990).

In order to compare model performance with these results, we performed a set of novel-start tests. After training in the constant-start condition, all weights in the model were fixed, and the simulated animal was given 100 testing trials from positions W and E, not used during training. As before, each testing trial consisted of two runs, one according to locale strategy and the second one according to taxon strategy.

7.1.2 Results

Ten different animals were simulated for each condition. Each of the animals had a different spatial map learned during the pre-exposure session. Results presented below are averaged over the ten animals.

Figure 7.2a shows the two performance curves corresponding to the locale (red) and taxon (blue) strategies across 200 training trials in the variable start condition. In this graph, performance close to 1 for trial n means that most of preceding 10 trials were not successful (according to the corresponding strategy), whereas performance close to 0 means that most of the preceding trials were successful. In this case the locale strategy was more efficient than the taxon strategy across all training trials.

The effect of lesions of either HPc/NA (the locale system) or CP/SNc (the taxon system) in the model can be determined from Figure 7.2a by considering only one of the two curves corresponding to non-lesioned system. Hence, the model predicts that intact animals, as well as animals with damage of the CP or SNc, are able to learn the variable start task in, whereas animals with damaged hippocampus (or NA) are impaired in this task. This is consistent with several experimental studies (Cunha et al., 2006; Morris et al., 1982; Eichenbaum et al., 1990; Sutherland and Rodriguez, 1990).

Considering the locale strategy alone, the performance stabilized after approximately 10-15 trials as shown by the evolution of average escape latency (Fig. 7.2a), in agreement with animal data (Morris et al., 1982; Cunha et al., 2006). At the asymptote of the performance the simulated rat adopted approximately direct paths from any starting position to the hidden platform as shown by the learned action map (Fig. 7.2c,d).

In the constant start condition the situation was different (Fig. 7.3a). In the taxon regime the simulated rats were able to learn the task due to the presence of a stable association between the starting position and the goal (Eichenbaum et al., 1990; Cunha et al., 2006). The locale strategy was preferable over the taxon strategy

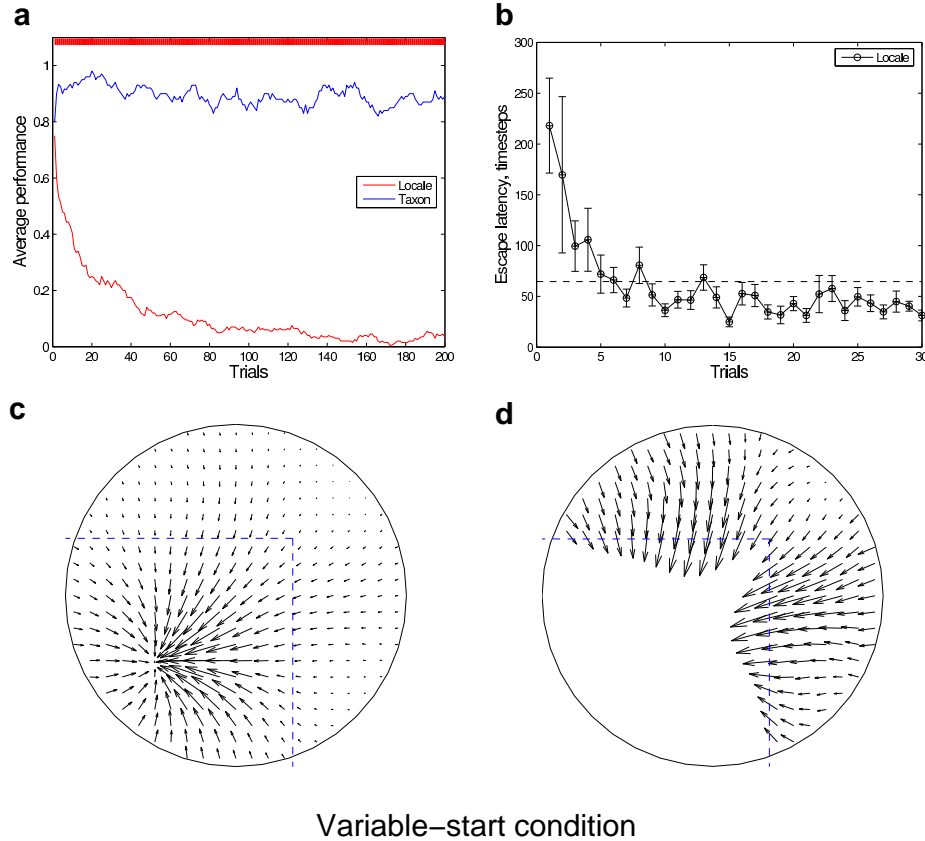


Figure 7.2: Results of simulation in the variable start condition. (a) Performance curves for locale (red) and taxon (blue) strategy for 200 training trials. The colored bar at the top of the graph shows the winning strategy, i.e. the strategy that was more successful in $N = 10$ preceding trials (red - locale, blue - taxon). (b) Evolution of the escape latency (time to reach the platform) across trials, averaged over all animals. Dashed line marks the threshold τ for a successful trial (see text). (c) Navigation map of animal 1 after training 30 trials (locale strategy). Arrows show learned directions towards the platform (i.e. Ψ^{NA} at the sample location, (Eq. (5.5))) and arrow lengths correspond to the value of the optimal action (Eq. (5.8)). (d) Since the arrow lengths in c are proportional to the action value, arrows near the periphery of the maze far from the starting location are hardly visible. Here the same plot was redrawn excluding the arrows from the well explored part of the maze so that the arrows near the periphery had a larger visible length.

in the beginning of training, while this relationship reversed after a longer training, as shown by the colored bar at the top of the plot (Fig. 7.3a). The speed of learning in the locale regime was similar to that in the variable start condition, as seen from the comparison of the escape latencies (Fig. 7.3b and Figure 7.2b).

Considering lesion effects in this case, the model predicts that (i) neither HPC/NA nor CP/SNc lesions prevent animals from learning this task and (ii) hippocampal animals might learn slower than intact animals in the beginning of training. Both effects have been observed in animals with lesions of fornix (the fiber bundle connecting HPC and NA) in the constant start version of the watermaze task (Eichenbaum et al., 1990).

Novel starts

Performance curves for the novel-start tests suggest that the taxon strategy was not successful during the novel-start tests, in contrast to the locale strategy (Fig. 7.4a). In other words, the results are consistent with the evidence that animals with hippocampus lesions were not able to solve the task, while intact animals were not impaired in this case. In addition, there was no difference in the escape latencies between the simulated rats trained in the variable-start and constant-start conditions (Fig. 7.4b), similarly to the rats in the experiment of (Eichenbaum et al., 1990).

The latter effect can be understood by looking at the navigation map formed during training in the constant start condition (Fig. 7.3c,d). Direction of the arrows near the periphery of the maze towards the goal location (Fig. 7.3d), suggests that although during training the simulated rats were always released from the same starting position, they had a chance to explore the whole area of the maze as a consequence of exploration/exploitation tradeoff adopted in the model (Section 5.2).

In order to see why the taxon strategy was so inefficient, we analyzed the heading directions separately at the starting positions W and E (Fig. 7.4c,d). The doubly-peaked heading histograms suggest that two different sets of visual cues controlled the behavior.

An analysis of the model revealed that the first set of cues was given by the images on the walls of the room seen in the direction of the platform during training, whereas the second set of cues was induced by the upper edge of the watermaze wall, which had a constant relationship with the direction to the platform during training. To make this point clear, consider a snapshot of the environment taken from the starting position towards the hidden goal (i.e. from position S in the direction of 135° , Fig. 2.2, environment B-I). During training this snapshot was associated with the turning angle of zero degrees (i.e. in this case the animal has to swim straight ahead to hit the platform). Imagine that during a novel-start trial the simulated rat is placed at position W, looking in direction 45° . In this case, the image of the extra-maze wall is changed accordingly, but the contour of the wall remains the same,

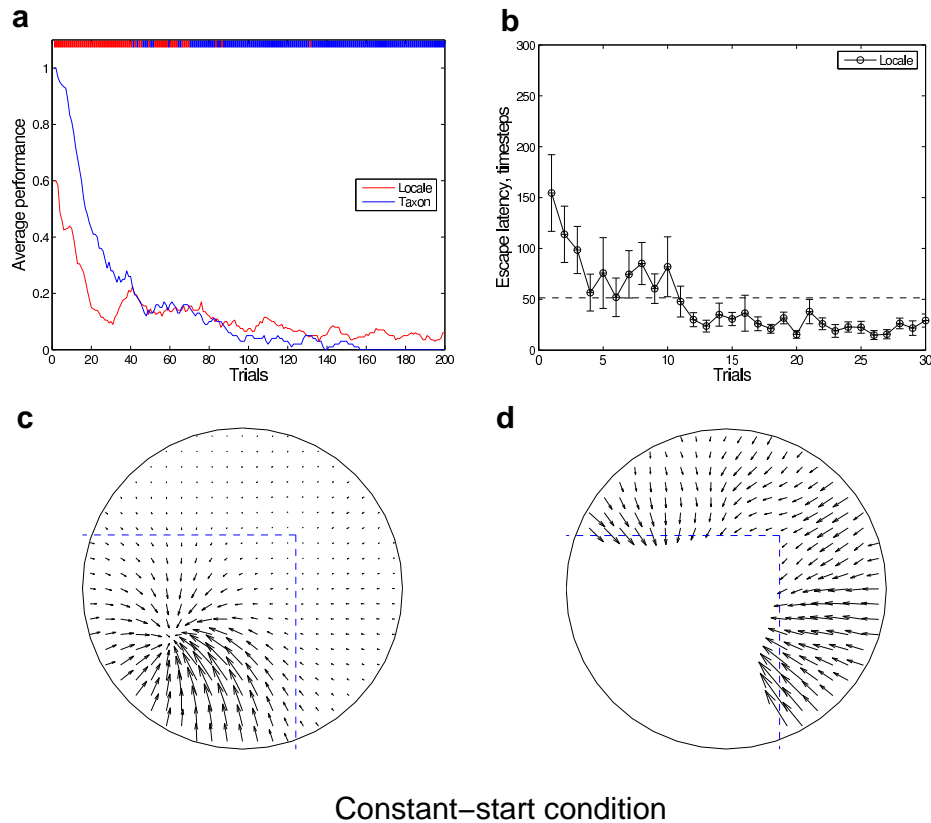


Figure 7.3: Results of simulation in the constant start condition. (a) Performance curves for locale (red) and taxon (blue) strategy. (b) Evolution of escape latency across trials, averaged over all animals. Dashed line marks the threshold τ for a successful trial. (b,c) Example of a navigation map learned after 30 trials in the constant start condition. In c the arrow lengths are rescaled for better visibility

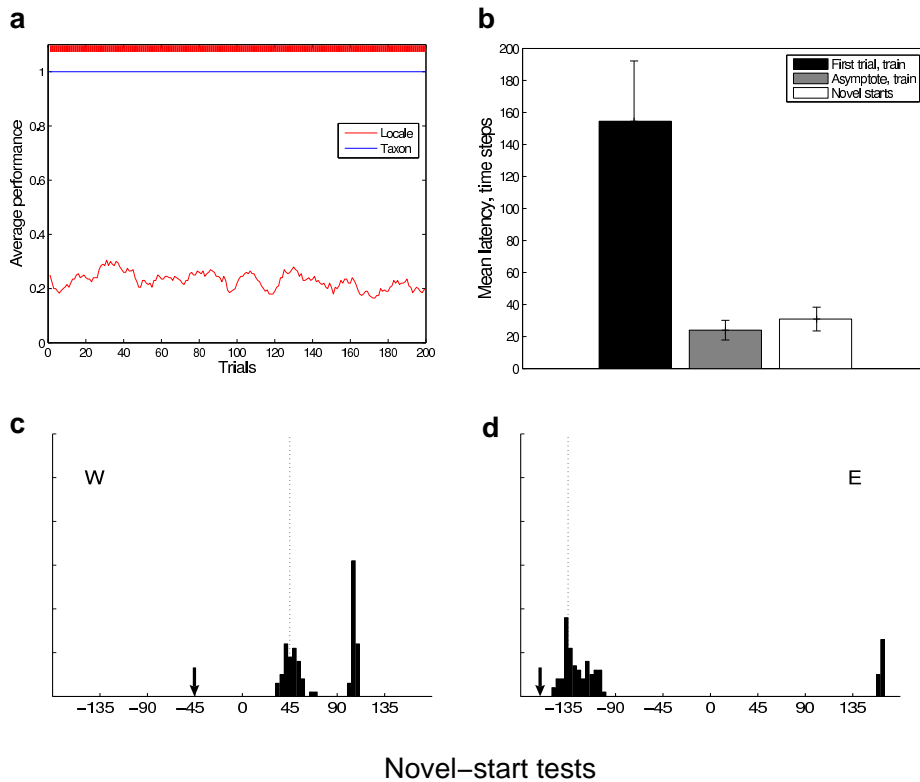


Figure 7.4: Performance in the novel-start tests. (a) Performance curves for the locale (red) and taxon (blue) strategies in 200 testing trials from starting positions W and E. (b) Mean escape latency \pm SE during novel-start tests using locale strategy in comparison to the latency of first training trial (random search) and at asymptote of training performance. (c,d) Distributions of headings (taxon strategy) during novel-start tests from W (c) and E (d) positions. The dotted lines indicate the direction defined by cues from the watermaze wall (see text for details). Arrows indicate correct direction to the platform. Bin size is 1° .

due to circular shape of the pool. Depending on the saliency of visual features of the wall contour *vs* features from the wall images, the rat will either rotate in agreement with extra-maze cues, or not rotate at all. Hence, based solely on the cues from the wall of the pool, the platform direction would be (incorrectly) estimated as 45° from the W position and -135° from the E position (dotted lines in the figure).

To summarize, the simulated rats in this experiment had no difficulties to reach the platform if they were using locale strategy; in contrast, when using taxon strategy the model rats *(i)* never took the right direction to the platform, since the two sets of controlling cues gave wrong predictions; *(ii)* sometimes chose a direction consistent with the cues from the watermaze wall, discarding the extra-maze cues; *(iii)* sometimes chose the direction consistent with extra-maze cues; A similar range of behaviors was reported for the rats in the constant-start watermaze (Eichenbaum et al., 1990).

7.1.3 Discussion

In this set of simulations the model was tested in the watermaze task with variable and constant starting positions. The results of these simulations are consistent with the following experimental evidence:

(i) Lesions of hippocampus prevent animals from learning the variable start version of the reference memory watermaze (RMW) task (Morris et al., 1982; Da Cunha et al., 2003; Sutherland et al., 1983); however, lesions of taxon subsystem (e.g. SNc) do not produce any impairment in this case (Cunha et al., 2006)

(ii) Constant start version of the RMW task can be solved by intact animals, as well as animals with either fornix or SNc lesions (Eichenbaum et al., 1990; Cunha et al., 2006), however hippocampal animals learn slower, especially in the beginning of training (Eichenbaum et al., 1990).

(iii) Locale strategy was preferable over the taxon strategy in the beginning of training, while this relationship reversed after longer training. This is in agreement with the data showing that animals gradually shift from place-learning to response-learning when given extensive training (Packard and McGaugh, 1996a; Chang and Gold, 2003). The taxon strategy in the model learns associations between snapshots of the environment taken in a particular direction and the rotation angle resulting in the correct heading. Hence, in the beginning of training, i.e. when the simulated rat has seen only a small amount of all possible snapshots from the starting position, its performance is low. However, when progressively more snapshots are experienced, it gets more and more accurate until each snapshot corresponds exactly to the optimal rotation angle (i.e. approximately until trial 160, Figure 7.3a). In contrast, the locale strategy associates place fields with movement directions and hence already after the first trials can reduce the escape latency significantly (Fig. 7.3b)

(iv) Inactivation of the locale pathway in the model resulted in the inability of the simulated rat to choose the direction to the platform during the novel-start tests

(Figure 7.4a). In contrast, intact (or CP/SNc-lesioned) simulated rats were as fast as the simulated rats trained in the variable start condition. These results are consistent with evidence that fornix-lesioned, but not intact, rats were impaired in the novel start tests after constant-start training (Eichenbaum et al., 1990). In the model this is due to the fact that learning of locale strategy involves random exploration of surrounding area (the amount of exploration in the model is controlled by parameter ϵ , Section 5.2 and Chapter 2). The parts of the environment that were later used as novel starting positions were visited in the process of exploration, and thus participated in learning of goal-directed actions. This is exactly the type of process observed by Sutherland et al. (1987) who concluded from their experiments that rats must (1) be familiar with the distal cues viewed from the region of the novel starting location, and (2) swim through the vicinity of the novel starting location as part of a swim path associated with an invisible goal. However, simulated rats that were using taxon strategy were learning associations between snapshot taken from the starting positions with corresponding swimming direction, and hence were not able to this information when the set of snapshots was different (due to difference in position).

Concerning the latter point, we note that in a significant part of testing trials from the novel starting positions (Fig. 7.4c,d) the simulated rats chose swimming direction relative to featureless watermaze wall and discarding visual pattern on the extra-maze walls. As explained before this is due to the fact that in certain snapshots the edge of the watermaze wall on the snapshot was more informative about the platform direction than other cues.

However, an alternative interpretation of rat's choices in these trials is that the rats oriented with respect to the circular wall of the pool, i.e. its geometric *shape*. Although this might seem as a valid interpretation, the explanation of this effect in our model does not depend on the geometry of the environment *per se*, i.e. the shape of the room, but rather on the structure of incoming visual inputs which are not by themselves sensitive to the geometric properties (i.e. whether the feature is coming from a wall that forms a part of the room's shape, or from another object).

In the next set of simulations we focus on reproduction of experimental data that addressed directly the question of influence of environmental geometry for spatial orientation tasks.

7.2 Is there a geometric module in the rat brain?

Cheng (1986) observed that when disoriented rats tried to relocate food buried in a rectangular room with visual landmarks in the corners, they often searched in a location that was rotationally opposite to the correct location (i.e. exhibited *rotational errors*, see Fig. 7.5a). The rotational errors may be explained by suggesting that in a disoriented state rats ignore visual landmarks and orient themselves using

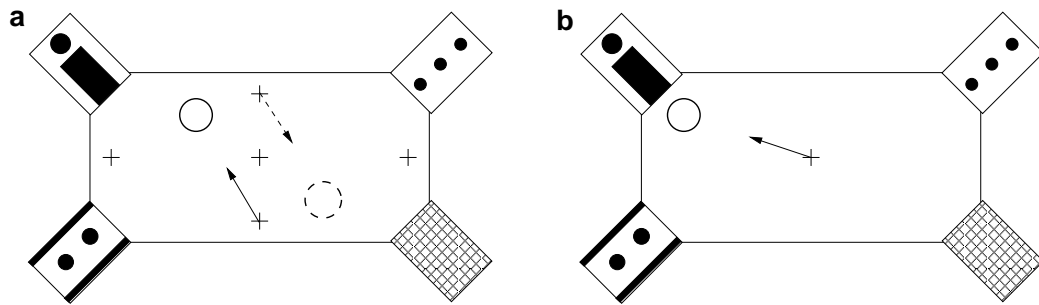


Figure 7.5: Experimental setup of Cheng (1986) (a) Working memory task. The large rectangle is the environment, corners contain distinct landmarks. Crosses mark starting positions. On the first part of a trial rats searched for food hidden at the location marked by the solid circle (solid arrow shows an example of path stored from the learning phase). Once the food was found and partially eaten, the rat was removed, disoriented and placed at a different starting position from which it had to find the remaining food. Dotted circle marks the location rotationally opposite to the correct food location, and dashed arrow shows a path corresponding to the rotational error. Different food locations and starting positions were used in different trials. (b) Reference memory task. The starting position (the small cross) and food location (circle) are constant from trial to trial.

solely the rectangular shape of the room, with respect to which the correct and its diagonally opposite locations are indistinguishable (Gallistel, 1990). Cheng suggested further, that extraction of the shape information from the sensory input might be a function of the geometric module, i.e. a mind module responsible for reorientation (see Section 3.3.1 for a short review). An evolutionary argument was proposed in favor of the existence of such a geometric module by Gallistel (1990).

It turned out that a crucial feature of this experiment was that starting positions and hidden food locations were different in each trial, since when the rats were trained in the same environment but with fixed starting position and food location (Fig. 7.5b), the number of rotational errors decreased significantly (although they were still systematic (Cheng, 1986)). An interpretation of these results suggested by Cheng was that although non-geometric features could be detected (as suggested by decreased number of errors in the experiment with fixed starting position), they are discarded during reorientation, presumably because the reorientation is based solely on the shape information. This is consistent with the property of impenetrability of a mind module for the information irrelevant for the module function (Gallistel, 1990; Wang and Spelke, 2003).

Results of the simulations performed in the previous section suggest a different

interpretation of these data. Since in the working memory experiment of Cheng different starting positions were used in each trial, our model suggests that the only successful strategy is the locale one. Taxon strategy can not be applied in this case, due to the lack of stable sensory-response associations linked with reward. Hence the rotational errors in this case are likely to be caused by the application of the locale strategy. This conclusion is supported by the fact that in the second experiment of Cheng, when such a stable association was possible, the rats did less rotational errors, presumably because the taxon strategy was used in this case.

What is the difference between the locale and taxon strategies that could explain rotational errors when the former strategy is used? As discussed in Chapter 3, the locale strategy encodes actions in an allocentric frame of reference, while the taxon strategy in an egocentric one. In order to be able to use an action encoded in an allocentric frame of reference, the animal must determine its allocentric heading from the alignment between the currently perceived visual cues and a representation of the environment stored in memory. In contrast, actions encoded in an egocentric frame of reference do not need to know the allocentric heading, since they are associated directly with the visible cues. From that we may conclude that it is specifically the reorientation phase that causes the rotational errors (Wang and Spelke, 2003), in particular the allocentric heading estimation.

In our model, the reorientation is performed by matching a currently perceived snapshot with the snapshots stored in memory during exploration. In a rectangular environment with symmetrically arranged landmarks, the snapshots taken in opposite directions from rotationally opposite locations are highly similar. Hence, given the imperfect visual acuity of rats, the diagonal errors can be caused in our model by the ambiguity of visual cues in the process of snapshot matching, i.e. during reorientation.

We conducted a set of computer simulations in order to check the following two hypotheses: (A) rotational errors in the working memory experiment can be explained in the model by errors in the estimation of the allocentric direction; (B) decreased number of rotational errors in the reference memory experiment is a consequence of taxon strategy

7.2.1 Experimental procedures

Similarly to the previous case, the present task included constant-start and variable-start conditions. These two conditions corresponded to the working memory (Figure 7.5a) and reference memory (Figure 7.5b) experiments of Cheng (1986), respectively. These simulations were conducted in the virtual environment B-II designed by analogy to the rectangular box used in the Cheng's experiments (see Chapter 2).

Reorientation trials

In order to check hypothesis (A), we performed a set of 1000 reorientation trials in the variable-start and constant-start conditions.

In the variable-start condition the simulated rat was placed into one of the five starting positions inside the box (marked by the crosses in Figure 7.5a), while in the constant-start condition the center of the box was always chosen. Initial orientation was randomly chosen between 0° and 360° .

Once placed at the starting location, the simulated rat performed reorientation procedure as described in Section 5.3.3, i.e. current allocentric heading was estimated from the set of local views stored during the pre-exposure session (Eq. (5.24)) and path-integration network was reset accordingly.

The outcome of a reorientation trial was considered as correct when the absolute value of the difference between the estimated and a real allocentric headings was less than 10° , a rotation error when the difference was greater than 170° and a miss, otherwise.

We also estimated position errors after the reset of the path integration system using visual information. The estimated position was considered as correct, if the distance to the true position of the simulated rat was less than 10 cm; rotational error if the distance to the position, diagonally opposite to the true position, was less than 10 cm; and a miss otherwise.

Simulation of taxon strategy

In order to check hypothesis (B), taxon navigation was simulated in both the variable-start and the constant-start conditions analogously to the watermaze simulations.

7.2.2 Results

Reproduction of the working memory experiment

The results of the simulations show that rotational errors observed¹ by Cheng (1986) can be reproduced by our model (Fig. 7.6). In order to show that rotational errors were indeed caused by the properties of visual cues, we performed 1000 reorientation trials (with random starting positions) in a cue-rich environment (N-I, see Chapter 2) and a perfectly symmetric rectangular environment (N-IIIa). No orientation errors were observed in the cue-rich environment, since snapshots taken in different directions can be well distinguished by the visual system. In contrast, in a perfectly symmetric rectangular environment each snapshot corresponds to the two opposite orientations, making the number of rotation errors equal to the number of correct

¹Animal data combine rats choices in two versions of the working memory task, i.e. with and without the white wall (Cheng, 1986)

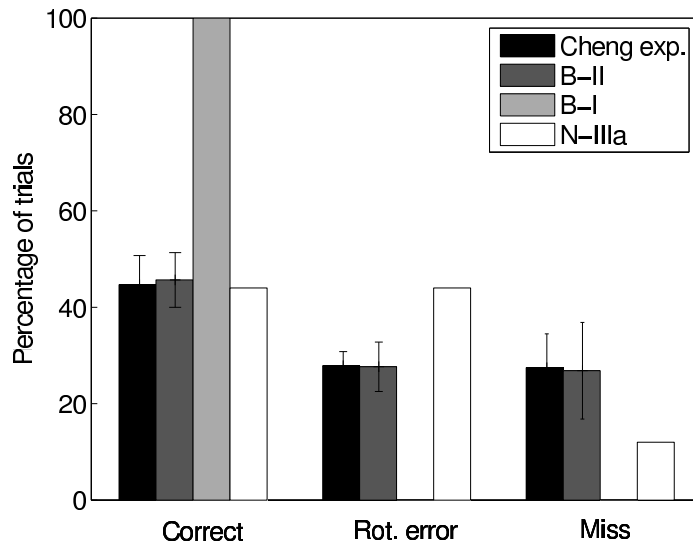


Figure 7.6: Bars show percentage of correct choices, rotational errors and misses for real (*black*) and simulated (*dark gray*) rats in the working experiment of Cheng (1986) and variable-start condition, respectively. In *light grey* and *white* the results of 1000 reorientation trials in the cue-rich (N-I) and symmetric (N-IIIa) environments, respectively, are shown.

rotations (Fig. 7.6a). Since in all three cases considered here the room was either rectangular or square, these results indeed suggest that the number of rotational errors might be controlled by the structure of visual features rather than the room geometry.

In the model, the allocentric direction, estimated during the reorientation phase, is used to reset the path integration network. Hence, rotational errors in the direction estimation should correspond to the rotational errors in the position estimation. Next we checked whether this is the case. Figure 7.7a shows the comparison between distributions of heading and position errors after reorientation. In this case significant difference between the heading and position estimates was observed only for rotational errors (t-test, $p < 0.05$).

To examine the reason for this difference, we plotted the heading and position error distributions separately for the starting position at the center of the box and starting positions at the periphery (Fig. 7.7b,c). At the central position both the correct turn and a rotational error should result in the same position estimate, resulting in the high number of rotational errors for the central position (Fig. 7.7b). There was also an increase in the number of correct answers, probably due to a smaller number of misses (see below).

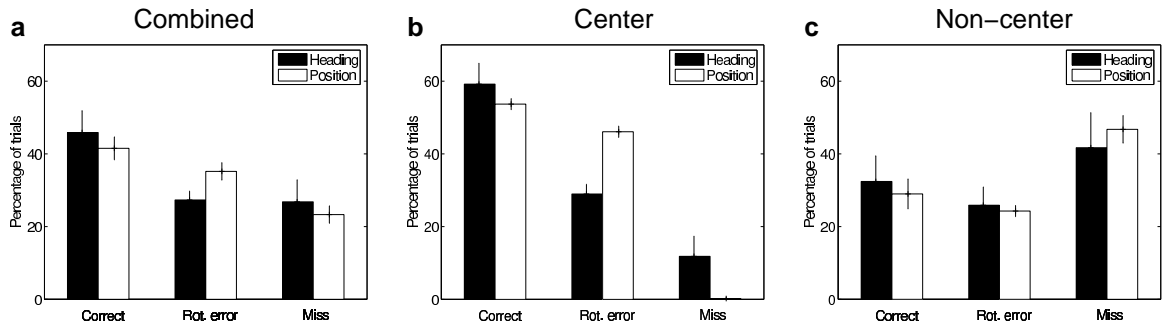


Figure 7.7: Distribution of errors in orientation and position when the simulated rat performed reorientation trials from all 5 starting positions (a), only the central starting position (b) and only the 4 starting positions in the periphery (c). Note that *a* and *b* correspond to variable-start and constant-start experimental conditions, respectively.

For the case of the non-central positions (i.e. near the middle points of the four walls) there was a good agreement between heading and position estimates (Fig. 7.7c). The high percentage of misses suggests that visual information is more ambiguous near the walls than in the center. An example of such an ambiguous situation is when the simulated rat is near a wall and looks directly toward it. In this case, the wall occupies a large portion of the view field and hence snapshots taken from this position may be similar to the ones taken towards the wall from other positions in the periphery.

Thus the discrepancy between the heading and position estimates observed for the rotational errors in Figure 7.7a is due to the effect of the central position. In conclusion, there was a good correspondence between heading and position estimates, but heading estimate was more precise, justifying its choice for performance measures in this simulation.

Reproduction of the reference memory experiment

We have proposed (hypothesis (B)) that decrease in the number of rotational errors in the experiment with fixed start can be explained by suggesting that rats in this experiment used taxon strategy.

Figure 7.8 shows an evolution of the ratio of the number of rotational errors and the number of correct turns across taxon training trials in the constant start condition. The number of rotational errors is as high as the number of correct turns in the beginning of training, but decreases with learning until ≈ 0.3 , reproducing qualitatively results of Cheng (1986).

A possible alternative explanation for the smaller number of rotational errors in

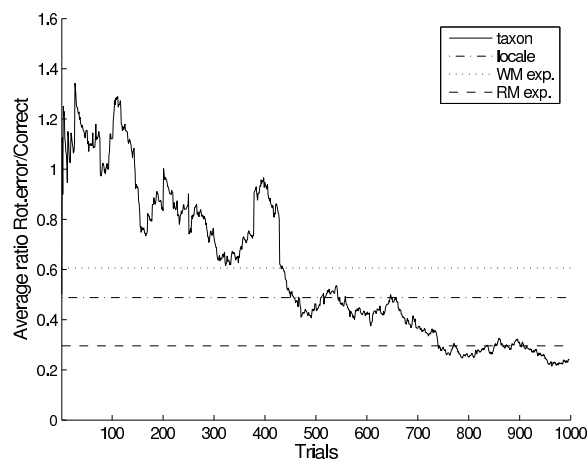


Figure 7.8: Evolution of the ratio of the number rotational errors *vs* the number of correct turns averaged over animals and smoothed by a running average with 10-trial kernel

this case is that when at the central position, the allocentric heading estimate is more precise than if all five starting positions are used (Figure 7.7a,b). In order to estimate the decrease of rotational errors due to this difference we calculated the mean ratio of rotational errors and correct answers for reorientation trials from the central position (0.48 ± 0.07 , dash-dot line in Fig. 7.8). From the comparison with the ratio calculated from the experimental data of Cheng (1986) (21 rotational errors *vs* 71 correct answers, dashed line), we may conclude that it is unlikely that the effect of central position can account for the decrease in the rotational errors.

To summarize, the results of our simulations confirmed our suggestions that the rotational errors may be caused by the ambiguity in visual input and that the decrease in the rotational errors in the fixed-start experiment can be a consequence of the change in navigational strategies (from locale to taxon).

7.2.3 Discussion

Simulated rats exhibited rotational errors in the testing environment, similarly to real rats in the experiments of Cheng (1986). Rotational errors in the simulations are caused by two main factors: ambiguous visual features and limited accuracy of the visual system.

To clarify this point, consider two sample snapshots taken by the simulated rat in opposite directions from the center of the box (Fig. 7.9a). In these snapshots large part of cues (e.g. wall edges) represent ambiguous information since they belong to

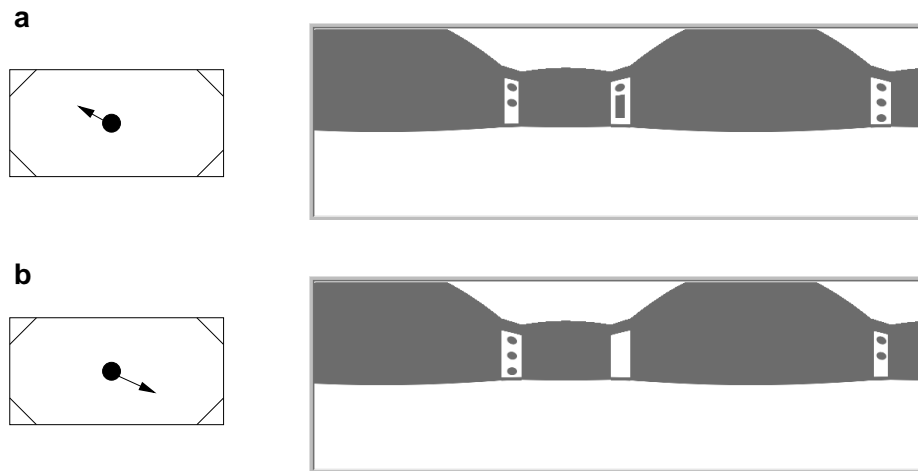


Figure 7.9: (a) Two snapshots taken from the central position in the direction of the north-west landmark (154°) and in the diagonally opposite direction. (b) Comparison between rat performance data in the experiment of Cheng (1986) and distribution of headings in reorientation trials in the variable start conditions.

both snapshots. Non-ambiguous information is represented by the visual pattern of the landmarks.

Depending on learning strategy, visual information is used differently during learning. During reorientation required by locale strategy (using Eq. (5.22) and Eq. (5.24)), a local view observed upon the entry to the box at the start of a trial is compared with local views stored in memory. Since there is a limited number of local views taken in the vicinity of the starting position, correlation will be sometimes higher for the correct orientation and sometimes for the rotationally opposite, depending on the exact position and orientation of the rat. The number of orientation errors can not be decreased by learning, since the representation of the environment stored in the grid cells and place cells is not updated during goal learning.

The situation is different during the taxon learning regime. In the beginning of learning, when the number of observed local views is low, the number of rotational errors is high (Fig. 7.8). However, as learning progresses, different local views become associated with the corresponding motor actions more and more accurately, leading to the decrease of rotational errors. As a conclusion, the model suggests that the decrease in the number of rotational errors is due to the switch between the navigational strategies.

Explanation for the rat behavior in Cheng's experiment given above is in contrast to the view that rotational errors are due to the insensitivity of the geometric module

to non-geometric information, i.e. its encapsulation (Cheng, 1986; Wang and Spelke, 2003) (see Section 3.3.1). In our model it is due to the assumption that the same information is acquired and processed differently depending on the learning strategy.

In addition to the issue of geometry discussed above, several behavioral studies suggested the preference for configural cues (i.e. sets of discrete cues) over single landmarks during navigation (Poucet et al., 2003). For example, S. Suzuki et al. (1980) trained rats to locate rewarded arms in an 8-arm maze, placed in a large cylindrical enclosure with multiple extra-maze stimuli. When the array of stimuli was rotated as a whole, the rats were choosing the arms in agreement with the rotated cues; however, when the cues were rearranged such that the relative positions of different stimuli changed, the performance was markedly disturbed. In another experiment (Benhamou and Poucet, 1998), rats were trained to find a hidden platform in a circular pool where the only cues were three different objects placed near the periphery of the pool. When the objects were arranged in the form of an isosceles triangle, the rats had no problem to remember the platform location; however, when the object arrangement was an equilateral triangle, the rats were unable to swim directly to the platform.

Although these results were not directly simulated here, it is easy to see that the model is consistent with them. In the first experiment, irrespectively of what strategy the rats actually used, rearrangement of cues would make local views *different* from those used during learning. Hence in the testing trials the model predicts that both strategies will be disrupted. This will not happen if the cues are rotated, since it will not change the local views, but simply change the directional reference, which either will not make any difference at all (in case of the taxon strategy) or will be taken into account during the head direction estimation (in case of the locale strategy)².

In the second experiment the situation is similar to the one in the Cheng's working memory task. The object arrangement in the form of an equilateral triangle makes the environment three-fold symmetric, and hence causes the orientation errors (but in this case they are not diagonal, as in the two-fold symmetric rectangular environment). In this case, the position *between* any two objects (which corresponds to the platform location in this experiment) is equivalent to the positions between any other two objects. Hence the model predicts that goal search will be concentrated near the middle points of the edges of the triangle, as it was observed in the experiment. The fact that rats in this experiment did not use object identities when released from different starting positions, but did use them when released from the center of the pool can be explained as above by the ambiguity of visual cues.

In conclusion, the approach to visual information processing adopted in the model suggests that the effects of both geometric (Cheng, 1986) and configural cues (Poucet, 1993; Poucet et al., 2003) can be explained on the basis of visual features that con-

²In a disoriented animal

stitute visual snapshots.

The following predictions can be made on the basis of the present results:

- Since rotational errors are mainly caused by a symmetric arrangement of visual features in the environment, their number can be decreased by either making the overall arrangement of landmarks non-symmetric or by making the landmarks sufficiently different.
- The model suggests that improvement in performance in the reference memory paradigm *vs* the working memory paradigm of Cheng is due to a switch from the locale to taxon strategy. Hence we predict that lesioning the taxon pathway (CP or SNc) will increase the number of rotational errors during the constant-start condition relative to controls, while not changing the performance in the variable-start condition.
- Sensory cues in the Cheng's experiments included distinct odors attached to the corner landmarks. Here we assume that visual cues, when they are available, override olfactory cues (Maaswinkel and Whishaw, 1999). If it is true that the rotational errors are caused primarily by the properties of visual input, switching off the lights during working memory experiment should result in decrease of rotational errors (at least on the trials in which the goal is hidden near the odor source).

In summary, the results of these simulations suggest that the dissociation between the geometric *vs* non-geometric cues (or configuration of cues *vs* identities of its constituent cues) is a consequence of competition between ambiguous and non-ambiguous visual features during reorientation. In environments in which the arrangement of walls is symmetric, the edges of walls represent ambiguous cues, whereas visual patterns attached to the walls (e.g. landmarks) represent non-ambiguous cues. We claim that behavioral decisions made on the basis of the ambiguous cues may *appear* to be caused by the room geometry, but could in fact be based on sets of local features, arranged in a symmetric and hence ambiguous configuration. Thus, there is no need in the concept of a 'geometric module' involved in the computation of the geometric shape congruence during reorientation. Moreover, behavioral data attributed to the encapsulation of the geometric module, i.e. the assumption that non-geometric information is encoded but not used during reorientation, can be explained by the switching between navigational strategies.

7.3 Transfer of goal information between environments

The issue of the geometric module can be considered from another, more general point of view, namely whether animals use global or local cues during goal search (Poucet, 1993; Learmonth et al., 2001; Pearce et al., 2004; Poucet et al., 2003). If an animal identifies the goal location based only on *local* cues situated next to the target (e.g. nearby landmarks), then the goal search consists of looking for a location with appropriate local features (Learmonth et al., 2001; Pearce et al., 2004). However, if the goal location is remembered with respect to a *global* cue, e.g., the geometric shape of the environment or its principal symmetry axis (Cheng, 1986, 2005), then the goal search implies (i) extraction of the global cue from the sensory input and (ii) going to the goal according to the extracted global cue. From this point of view, the behavior of rats in the experiments of Cheng is an instance of the global-cue behavior, where the global cue is extracted from the sensory input by means of the geometric module.

An experimental study aimed at a dissociation of the two types of search (i.e. local-cue vs global-cue) was conducted by Pearce et al. (2004). In this task rats were trained to swim to a target platform hidden in one corner of a featureless rectangular water pool (corner C, Fig. 7.10a). After several learning sessions, their corner choices were examined in a kite-shaped pool (Fig. 7.10b). The target corner in the rectangular training environment is defined up to the rotational error since no cues can be used to distinguish corner C from its diagonally opposite (C'). In the kite-shaped pool the bottom corner is geometrically equivalent to the corners C and C' of the rectangular training room, whereas the upper corner is equivalent to the corners I and I'. Rats' choices during three 4-trial testing sessions in the kite-shaped pool are shown in Figure 7.10c.

According to the local-cue hypothesis, rats remember the local properties of the target corner in the rectangular training pool, e.g. that the target corner is located to the left of the long wall (with respect to the rat inside the pool), or that it has the long wall to the right of the short wall (Pearce et al., 2004). The result of matching these local properties in the kite-shaped pool leads to identifying either corner C (since it lies to the left of the long wall and has a long wall to the right of the short one), or corner A (since it lies to the left of the long wall) as the correct corners. Hence the local cue hypothesis provides an explanation of the preference of the corners C and A over corners I and O, but fails to explain why corner A was chosen at least as often as corner C.

The global-cue hypothesis predicts that rats remember the location of the target corner with respect to a global characteristic of the environment, e.g. the environment shape (Cheng, 1986) or its symmetry axis (Cheng, 2005; Cheng and Gallistel, 2005). In the former case rats would be lost in the kite-shaped pool since the shapes are

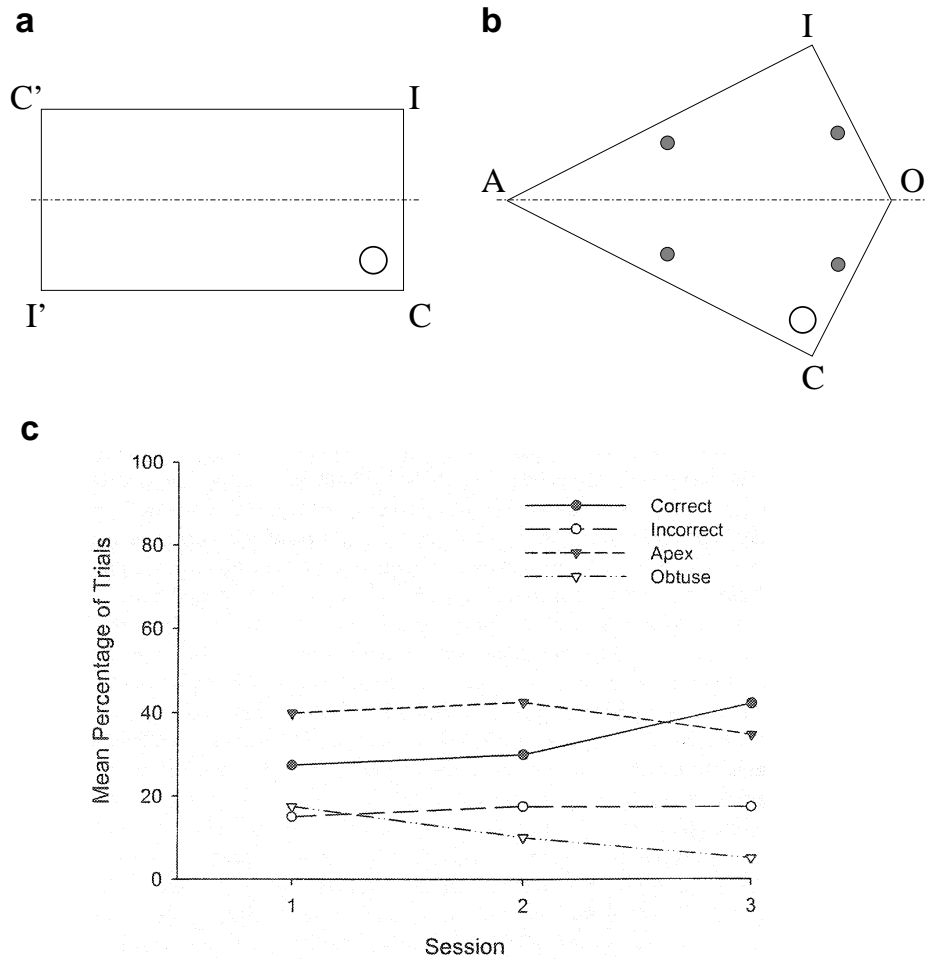


Figure 7.10: Setup and results of the experiment of Pearce et al. (2004). a,b. Training (a) and testing (b) environments used in the experiment. The target corner C in the training pool corresponds to the bottom corner of the kite-shaped pool (open circles). The black dots mark four starting positions in the kite shaped pool. The dotted lines show symmetry axes for the two environments. c. Percentage of trials on which rats swam directly to each of the four corners in the kite-shaped pool across three testing sessions, four trials each (reproduced with permission from Pearce et al. (2004)).

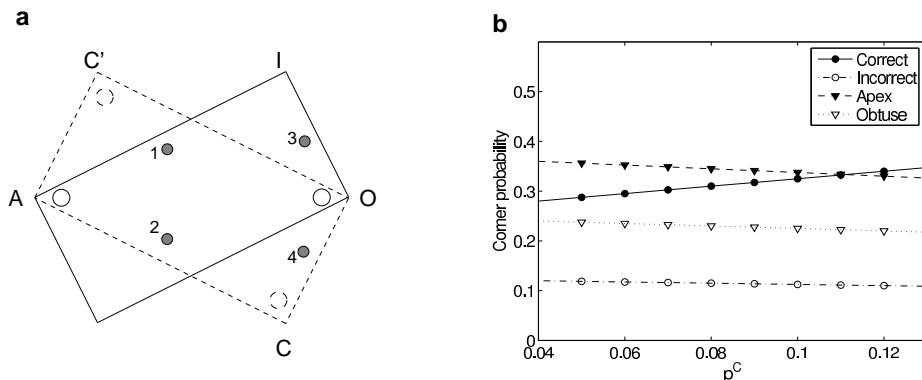


Figure 7.11: (a). Visual cues from the rectangle can be aligned with visual cues from the kite-shaped pool using either corners AIO (solid line) or corners ACO (dashed line). Each alignment is associated with the direction to the ‘target’ corner (circles) (b) Probabilities of choosing each to the four corners in the model as a function of p^C

different, i.e. no corner preferences should be observed. Hence, in this experiment rats should not be able to orient themselves by the shape of the environment. In the latter case the symmetry axis of the rectangle (i.e. the line that goes through the middle points of edges IC and I’C’) should be matched to the symmetry axis of the kite-shaped pool (i.e. line AO) and the authors suggest that rats would choose corners C and A of the kite-shaped pool equally often since their position roughly correspond to the position of the target corner (and it diagonally opposite) in the rectangular room (Cheng and Gallistel, 2005). The drawback of this explanation is that it is hard to put it to quantitative terms, since that would require knowledge of distances or angle magnitudes; even if such a quantification could be done it is not clear how well it would generalize to other similar cases.

We wondered whether our view-based reorientation mechanism can explain corner choices in the kite shaped pool (i.e. without any explicit representations of walls or symmetry axes). According to our hypothesis, the view-based reorientation procedure is performed upon the entry to the kite-shaped pool. The view-based reorientation in the model is performed by finding the best match between the local view observed upon the entry to the pool and local views stored during exploration. In environments where visual features are represented only by the edges of rectangular featureless walls, the outcome of the reorientation procedure can be predicted by a simple probabilistic algorithm described below.

First, consider the case when after learning in the rectangle, the simulated rat is placed at the starting position 1 (Fig. 7.11a). There are four possible cases:

1. the current local view contains corner AIO and the head direction is determined

(using Eq. (5.24)) from the alignment with corner C'IC of the rectangle. In this case the obtuse-angled corner O will be interpreted as the 'correct' corner (see Fig. 7.11a).

2. the current view contains corner AIO and is aligned with corner C'I'C of the rectangle. In this case the apex-angled corner is perceived as correct.
3. the current view contains corner ACO and is aligned with corner I'CI of the rectangle. In this case corner C will be chosen as the correct corner
4. the current view contains corner ACO and is aligned with corner I'C'I of the rectangle. In this case the direction towards C' (Fig. 7.11a) is interpreted as the direction to the correct corner. Since C' does not exist in the kite-shaped pool, we assume that one of the 'neighboring' corners A or I is chosen with probability $p^{ai} = 1/2$

In the limit of many trials the four possible outcomes are equally probable (because of the symmetry of the rectangular training environment), and the corner choices after reorientation can be described by a simple probabilistic model where each of the four outcomes is assigned probability 1/4. Starting position 2,3 and 4 can be analyzed in a similar way yielding the following corner probabilities

$$\begin{aligned}
 p_1^C &= p_2^C = 1/4 & p_3^C &= 0 & p_4^C &= 1/2 \\
 p_1^A &= p_2^A = 1/4 + 1/4 \cdot p^{ai} & p_3^A &= 1/2 & p_4^A &= 1/2 \cdot p^{ai} \\
 p_1^O &= p_2^O = 1/4 & p_3^O &= 1/2 & p_4^O &= 0 \\
 p_1^I &= p_2^I = 1/4 \cdot (1 - p^{ai}) & p_3^I &= 0 & p_4^I &= 1/2 \cdot (1 - p^{ai})
 \end{aligned} \tag{7.1}$$

where the subscript denotes the starting position. Note that from position 3 only corner AIO is perceived the same way as in the training room, so corners A and O are chosen with probability 1/2. A similar argument is applied to starting position 4.

Finally, at each starting position the 'rat' might have used some new information learned about the testing environment and go directly to the correct corner with probability p^C . The probabilities of going to each of the four corners are then given by:

$$\begin{aligned}
 p(C) &= p^C + (1 - p^C) \sum_i p^{st} p_i^C \\
 p(X) &= (1 - p^C) \sum_i p^{st} p_i^X
 \end{aligned}$$

where $X = A, O, I$, and probability of choosing a starting position is $p^{st} = 1/4$. Substituting numerical values from Eq. (7.1) we get:

$$\begin{aligned}
p(C) &= \frac{1}{4} + \frac{3}{4}p^C \\
p(A) &= \frac{3}{8} - \frac{3}{8}p^C \\
p(O) &= \frac{1}{4} - \frac{1}{4}p^C \\
p(I) &= \frac{1}{8} - \frac{1}{8}p^C
\end{aligned} \tag{7.2}$$

where letters C, A, O, I denote corresponding corners (Figure 7.11b).

In agreement with the experimental data (Figure 7.10c), the calculated probability of choosing corners C or A is higher than that for corners I and O for the values of the parameter p^C in the range $p^C \in [0.04, 0.13]$. Moreover, corner A is chosen more often than corner C for smaller values of p^C . A possible interpretation of this result is that in the beginning of testing rats used the goal information transferred from the training phase (which corresponds to smaller values of p^C), but as testing progressed they learned a representation of the testing environment that allowed them to approach the corner C directly (during testing trials a hidden platform was located at corner C of the kite-shaped pool).

7.3.1 Discussion

During testing in the kite-shaped pool, the rats in the experiment of Pearce et al. (2004) exhibited strong preference of the bottom corner over the top corner. This behavior can not be a consequence of random search (since the two corners are geometrically equivalent), suggesting that this preference was transferred from the training in the rectangular pool. In this section we considered a possible mechanism of this transfer, namely that the rats used local views stored from the training phase in order to direct their search during testing.

In this experiment, rats were released from different starting positions on different trials and the target platform was hidden, hence we assumed that they used locale strategy (see Section 7.1). The simulation of the working memory experiment of Cheng (Section 7.2) suggested that the outcome of a reorientation trial can be a good predictor of the rat's choice of the target location on this trial. The calculations performed above suggest that this might be the case for the experiment of Pearce et al. (2004) as well (Figure 7.11b).

The aim of this section was to show that the model is compatible with experimental data showing that rats are able to use local properties of the environment in order to direct their goal search Pearce et al. (2004). We note that in this case by local properties we mean geometric arrangement of walls near the target location.

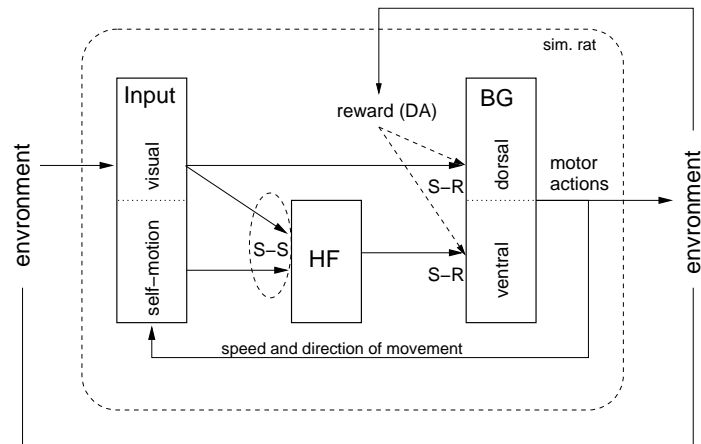


Figure 7.12: Sensory-motor loop implemented in the model. HF – hippocampal formation, BG – basal ganglia, S-S – stimulus-stimulus associations, S-R – stimulus-response associations.

Comparison with the simulation results of the previous section suggests that the model is consistent with data showing that rats can use global cues as well as local cues to drive their goal oriented behavior. The reason is that although visual features processed in the model are inherently local (since they belong to the snapshots taken at particular locations in the environment), reorientation on the basis of many snapshots produce behavior that may appear as driven by global cues (Section 7.2).

7.4 General discussion

In this thesis we proposed a model that implements the full sensory-motor loop (Figure 7.12). The simulated rat moves through a virtual environment, constantly receiving sensory inputs. The visual input is processed in the model by two parallel pathways: (I) the fast direct pathway from the visual filters to the action cells in the CP (that represents anatomical connections between cortex and the dorsal striatum) and (II) the slow indirect pathway from the visual filters to the action cells in NA, passing via grid cells and place cells (this pathway represents connections from cortex to the hippocampal formation and then to the ventral striatum). The readout of the action-cell activity and its conversion to the movement of the simulated rat represents output of the basal ganglia to cortical/subcortical motor structures.

If the environment produces rewards, the reward information is associated with movements through reward-based learning. In the model this is done in the synapses from visual filters and place cells to the action cells by means of reinforcement (TD)

learning, and reward information is assumed to be available in the form of phasic dopamine input from neuronal populations of the basal ganglia (i.e. SNc and VTA, (Schultz et al., 1997)).

Whereas actions cells perform reward-based stimulus-response (S-R) learning in the model, the cell populations in the modeled hippocampal formation learn stimulus-stimulus (S-S) associations in agreement with the role of hippocampus in latent learning (White and McDonald, 2002; Packard and McGaugh, 1992a, 1992b).

The model was tested in a set of computer simulations, that were designed analogously to the experiments performed on behaving rats. These tests demonstrated that (i) grid cells and place cells in modeled hippocampal formation have biologically plausible firing fields, with dynamical properties qualitatively similar to those of biological cells; (ii) the behavior of the model in navigation tasks is consistent with that observed in several animal studies, including basic lesion effects.

The present study focused on the importance of distal extra-maze cues for navigation (both locale and taxon). Modelling this type of navigation separately from object approaching behavior is appropriate, since several studies suggested that encoding and use of distal *vs* proximal cues for navigation might be distinct processes (see Poucet et al. (2003) for review); in addition, data from Cressant et al. (1997, 1999) suggest that place fields are controlled by distal, but not proximal cues, in agreement with our model (see Section 6.4).

One of the major goals of this study was to examine the effects of environmental geometry on the activity of spatially selective cells and goal-oriented behavior. Since our model is a neural network model which is largely built in agreement with anatomical and neurophysiological data, we expected that it might provide some insights into a possible implementation of abstract psychological theories of geometric processing, e.g. the theory of geometric module for spatial orientation.

In agreement with our expectations, the results presented in the study suggest that the influence of geometry of space observed in behavioral data can be a byproduct of visual information processing. The geometry of space is implicitly present in the visual input and hence influences cell activities as well as behavior. Hence our claim is that it is not necessary to invoke the geometric module concept to explain Cheng's data. In particular, (i) if the geometric module is viewed as a separate brain structure responsible for geometry-related calculations, then there is no need in such a structure, since our model can reproduce Cheng's results without it (ii) if the geometric module is meant to be a theoretical abstraction, then we question the utility of this abstraction. Our simulations suggest that rotational errors can be explained by the structure of visual inputs, rather than by room geometry.

We believe that our model offers a new approach to several issues in animal behavior, related to the processing of different types of visual cues. Experimental studies suggest that different visual cues exert different level of control over spatial behavior. In particular, configural cues seem to be used preferably to individual landmarks

(Poucet, 1993; Benhamou and Poucet, 1998; Poucet et al., 2003); similarly, environmental geometry (i.e. a global cue) has been suggested to override non-geometric (or local) cues (Gallistel, 1990; Benhamou and Poucet, 1998; Pearce et al., 2004; Cheng, 2005). As discussed previously (Sections 7.2.3, 7.3.1), from the point of view of our model these types of stimuli exert their control implicitly through their different appearance in the local views, so that an *a priori* separation of these cues into different types is misleading. In addition, the way the visual features are processed depends on the task that an animal is currently performing. Whereas during an unrewarded cognitive mapping of the environment a detailed information about small-scale visual features is not encoded (i.e. coarse, low-frequency coding is preferred in this case (O’Keefe and Nadel, 1978)), learning the details of a specific visual cue associated with food reward is important for a hungry animal.

Additional types of visual input, not implemented in the present model, e.g. encoding of the optic flow (Wylie et al., 1999) or direct distance estimation (Gallistel, 1990), are likely to be involved in the visual information processing. However, these types of cues are unlikely to provide more detailed information about visual stimuli than local views, and so they will not influence our principal results.

Chapter 8

Conclusions

As stated at the beginning of this document, the work here presented is aimed to address two fundamental questions: (i) How might different strategies be implemented in the brain? and (ii) What is the role of sensory stimuli during goal-oriented behavior? In this chapter we summarize the achievements of this work; we also analyze limitations of the current model, and suggest directions of future research.

8.1 Contributions

In this work we presented a system-level neural model of goal-oriented behavior in the rat. The model implements two navigational strategies: the first, taxon, strategy associates visual stimuli directly with motor actions; the second, locale, strategy uses a distributed representation of location encoded by grid- and place-cell activities. The representation of location is built incrementally through unrewarded exploration of environment, i.e. during a latent learning phase. During this phase internal estimation of position, encoded by the network of grid cells, is associated with visual input by means of Hebbian learning. Readout of position information is performed by the population of place cells. Activity of place cells can be then associated with motor actions using reward-based learning. Both the taxon and locale strategies are learned by linking reward information with pairs of stimuli and actions (in the taxon case) or place-cell activities and action (in the taxon case) by means of reinforcement learning.

An important property of the model is that it processes visual information by a large set of orientation-sensitive filters, akin to primary visual areas in the brain.

The model was tested in a large array of tasks that were designed by analogy

to real-world behavioral experiments. In particular, firing fields of location sensitive neurons were analyzed during exploration of the environment and compared with those of biological cells. In addition, dynamics of place-cell firing fields were examined during shrinking or stretching of experimental chamber. In both cases the results were in agreement with experimental data on place and grid cells. From this we may conclude that by employing a simple, but biologically plausible, visual system we were able to explain experimentally observed cell activities without *a priori* definition of such notions like ‘landmark’ or ‘wall’.

In a different set of computer experiments we examined the ability of the model to perform goal navigation in circular enclosures and rectangular boxes. In the circular environment with multiple visual cues the model was able to learn the location of a hidden goal. Moreover, it could use different navigational strategies depending on task conditions, similarly to real animals. Results of simulated lesion studies were consistent with those of real studies.

The computer experiments in rectangular boxes were aimed at reproducing results of (Cheng, 1986) who suggested that geometry of space plays a major role for spatial orientation. Although our model was able to reproduce the results, our conclusions concerning the influence of environmental geometry on behavior are different. In our model the geometry of space is represented implicitly in the visual features analyzed by the visual processing pathway in the model. In certain impoverished environments, like the ones used during Cheng’s experiments, the overall symmetry of the environment produces an effect that can be interpreted as geometric influence, due to ambiguity of visual information. This effect is eliminated once the ambiguity in visual input is removed. Hence we suggest that it would be misleading to emphasize the importance of geometry on the basis of these experiments, since a simpler, more general and more biologically explanation of these effects is possible, as demonstrated in this thesis.

8.2 Limitations and perspectives

Without doubt, the model uses many simplifications and assumptions. In particular, the following issues has to be addressed in future research:

Role of other hippocampal structures. The feed-forward architecture of the model is proposed to correspond to the entorhinal-CA1 pathway in the rodent hippocampus. While this pathway has been shown to be sufficient to maintain a stable place code (Brun et al., 2002; Fyhn et al., 2004), the question remains about the role of the other hippocampal structures for spatial navigation.

It has been suggested that dentate gyrus and CA3 might be responsible for the processes of orthogonalization and completion of incoming sensory patterns. Recurrent connectivity in the CA3 area of the hippocampus and neurogenesis in the den-

tate gyrus are consistent with these suggestions. Spatial information resulting from feed-forward projections from the entorhinal cortex to CA1 on one hand, and pattern completion/orthogonalization performed by the CA3 area on the other, might complement each other in a single comparison process. Such a comparison maybe important for deciding whether the environment is novel or not.

Relation to general memory functions of the hippocampus. A parallel has been drawn between the classification of locale and taxon strategies and the division between episodic (or declarative) and procedural memory (Redish, 2001). Both locale strategies and episodic memories are hippocampal-dependent and imply the flexible use of complex sensory stimuli. Taxon strategies and procedural memory, in contrast, depend on the dorsal striatum, are less flexible and require time to be developed. This analogy highlights the potential importance of studying navigation strategies in rodents as a model of multiple memory systems in mammals and their interactions.

The acquisition of stimulus-response strategies (similar to procedural memories) can be related to the development of habits. In navigational tasks, animals gradually shift from place-response (hippocampal dependent) to stimulus-response (striatum dependent) strategies when trained extensively training (Packard and McGaugh, 1996b; Chang and Gold, 2003). Such a transition has been interpreted as the basis for habit formation (Packard and McGaugh, 1996b; Packard and Knowlton, 2002).

Role of other brain areas. In this work we have only referred to the putative roles of the the hippocampal formation and the basal ganglia during goal-oriented behaviors. However, other brain areas are likely to be involved in these behaviors as well. In particular, the prefrontal cortex has been associated to the development of habits (Killcross and Coutureau, 2003), the execution of taxon strategies (Bruin et al., 2001), and learning and retrieval of goal information (Hasselmo, 2005). Its role in spatial navigation is a potential extension of the present model.

Robotic implementation. The model in its present form is in principal suitable for implementation on a robotic platform. In fact, it has been implemented in robot simulator software. Although the robotic implementation was not a goal of this study, such implementation will be advantageous for the model, since the use of real embodiment and agent-environment interactions constitutes a powerful test-bed for the robustness of the model.

References

- Alexander, G. E., and Crutcher, M. D. (1990, July). Functional architecture of basal ganglia circuits: neural substrates of parallel processing. *Trends Neurosci*, *13*(7), 266-71. 18
- Alexander, G. E., DeLong, M. R., and Strick, P. L. (1986). Parallel organization of functionally segregated circuits linking basal ganglia and cortex. *Annu Rev Neurosci*, *9*, 357-81. 18
- Amaral, D. G. (1993). Emerging principles of intrinsic hippocampal organization. *Current Opinion in Neurobiology*, *3*, 225–229. 36, 37
- Amaral, D. G., Dolorfo, C., and Alvarez-Royo, P. (1991). Organization of Ca1 projections to the subiculum: a PHA-L analysis in the rat. *Hippocampus*, *1*, 415–435. 37
- Amaral, D. G., and Witter, M. P. (1989). The three-dimensional organization of the hippocampal formation: A review of anatomical data. *Neuroscience*, *31*(3), 571–591. 34, 35, 36, 37
- Amaral, D. G., and Witter, M. P. (1995). Hippocampal formation. In G. Paxinos (Ed.), *The rat nervous system* (Second ed., pp. 443–493). Academic Press. 18, 34, 36, 37
- Annett, L. E., McGregor, A., and Robbins, T. W. (1989, Jan 1). The effects of ibotenic acid lesions of the nucleus accumbens on spatial learning and extinction in the rat. *Behav Brain Res.*, *31*(3), 231-42. 18
- Apicella, P., Scarnati, E., Ljungberg, T., and Schultz, W. (1992, September). Neuronal activity in monkey striatum related to the expectation of predictable environmental events. *J Neurophysiol*, *68*(3), 945-60. 20
- Arleo, A., and Gerstner, W. (2000a). Modeling rodent head-direction cells and place cells for spatial learning in bio-mimetic robotics. In J.-A. Meyer, A. Berthoz, D. Floreano, H. L. Roitblat, and S. W. Wilson (Eds.), *From animals to animats vi* (pp. 236–245). Cambridge MA: MIT Press. 49
- Arleo, A., and Gerstner, W. (2000b). Spatial cognition and neuro-mimetic navigation: A model of hippocampal place cell activity. *Biological Cybernetics, Special Issue on Navigation in Biological and Artificial Systems*, *83*, 287–299. 19, 27, 49, 59
- Arleo, A., and Gerstner, W. (2001). Spatial orientation in navigating agents: Mod-

- eling head-direction cells. *Neurocomputing*, 38–40, 1059–1065. 49, 64
- Arleo, A., Smeraldi, F., Hug, S., and Gerstner, W. (2001). Place cells and spatial navigation based on 2d visual feature extraction, path integration, and reinforcement learning. In T. K. Leen, T. G. Dietterich, and V. Tresp (Eds.), *Advances in neural information processing systems 13* (pp. 89–95). MIT Press. 27, 49
- Aston-Jones, G., Rajkowski, J., Kubiak, P., and Alexinsky, T. (1994, July). Locus coeruleus neurons in monkey are selectively activated by attended cues in a vigilance task. *J Neurosci*, 14(7), 4467–80. 20
- Baird III, L. C. (1995). Residual algorithms: Reinforcement learning with function approximation. In *International conference on machine learning* (p. 30–37). 9
- Baldassarre, G. (2002, Mar). A modular neural-network model of the basal ganglia’s role in learning and selecting motor behaviours. *Cognitive Systems Research*, 3(1), 5–13. 29
- Bao, S., Chan, V. T., and Merzenich, M. M. (2001, Jul 5). Cortical remodelling induced by activity of ventral tegmental dopamine neurons. *Nature*, 412(6842), 79–83. 20
- Bayer, S. A. (1982). Changes in the total number of dentate granule cells in juvenile and adult rats: a correlated volumetric and 3h-thymidine autoradiographic study. *Exp Brain Res*, 46(3), 315–23. 36
- Benhamou, S., and Poucet, B. (1998). Landmark use by navigating rats (*rattus norvegicus*) : contrasting geometric and featural information. *J Comp Psychol*, 112(3), 317–322. 105, 114
- Berns, G., and Sejnowski, T. (1996). How the basal ganglia make decision. In A. Damasio, H. Damasio, and Y. Christen (Eds.), *The neurobiology of decision making* (p. 101–113). Berlin: Springer-Verlag. 29
- Blodgett, H. C. (1929). The effect of the introduction of reward upon the maze performance of rats. *Univ. Cal. Pub. Psychol.*, 4(8), 113–134. 70, 71
- Blond, O., Crepel, F., and Otani, S. (2002, Mar 1). Long-term potentiation in rat prefrontal slices facilitated by phased application of dopamine. *Eur J Pharmacol*, 438(1–2), 115–6. 20
- Blum, K. I., and Abbott, L. F. (1996). A model of spatial map formation in the hippocampus of the rat. *Neural Computation*, 8, 85–93. 24
- Brandner, C., and Schenk, F. (1998, March). Septal lesions impair the acquisition of a cued place navigation task: Attentional or memory deficit? *Neurobiology of Learning and Memory*, 69(2), 106–125. 37
- Brown, M. A., and Sharp, P. E. (1995). Simulation of spatial-learning in the morris water maze by a neural network model of the hippocampal-formation and nucleus accumbens. *Hippocampus*, 5, 171–188. 19, 23, 53
- Bruin, J. P. de, Moita, M. P., Brabander, H. M. de, and Joosten, R. N. (2001, March). Place and response learning of rats in a morris water maze: differential effects

- of fimbria fornix and medial prefrontal cortex lesions. *Neurobiol Learn Mem*, 75(2), 164-78. 117
- Brun, V. H., Otnass, M. K., Molden, S., Steffenach, H. A., Witter, M. P., Moser, M. B., et al. (2002, Jun 21). Place cells and place recognition maintained by direct entorhinal-hippocampal circuitry. *Science*, 296(5576), 2243-6. 40, 60, 64, 116
- Burgess, N., Jeffery, K. J., and O'Keefe, J. (1999). Integrating hippocampal and parietal functions: a spatial point of view. In K. J. J. N. Burgess and J. O'Keefe (Eds.), *The hippocampal and parietal foundations of spatial cognition* (pp. 3-29). Oxford University Press. 37
- Burgess, N., Recce, M., and O'Keefe, J. (1994). A model of hippocampal function. *Neural Networks*, 7, 1065-1081. 19, 23, 37, 45
- Burwell, R. D., and Amaral, D. G. (1998, Aug 24). Cortical afferents of the perirhinal, postrhinal, and entorhinal cortices of the rat. *J Comp Neurol*, 398(2), 179-205. 34
- Buzsáki, G. (1984). Feed-forward inhibition in the hippocampal formation. *Progress in Neurobiology*, 22, 131-153. 37
- Buzsáki, G. (2002). Theta oscillations in the hippocampus. *Neuron*, 33(3), 325-340. 37
- Chang, Q., and Gold, P. E. (2003, Apr 1). Switching memory systems during learning: changes in patterns of brain acetylcholine release in the hippocampus and striatum in rats. *J Neurosci*, 23(7), 3001-3005. 96, 117
- Cheng, K. (1986, July). A purely geometric module in the rat's spatial representation. *Cognition*, 23(2), 149-78. 10, 21, 22, 87, 88, 97, 98, 99, 100, 101, 102, 103, 104, 105, 107, 116
- Cheng, K. (2005). Reflections on geometry and navigation. *Connection Science*, 17(1-2), 5-22. 107, 114
- Cheng, K., and Gallistel, C. R. (2005, April). Shape parameters explain data from spatial transformations: comment on pearce et al. (2004) and tommasi & polli (2004). *J Exp Psychol Anim Behav Process*, 31(2), 254-9; discussion 260-1. 107, 109
- Cheng, K., and Newcombe, N. S. (2005, Feb). Is there a geometric module for spatial orientation? squaring theory and evidence. *Psychon Bull Rev*, 12(1), 1-23. 22, 76
- Chrobak, J. J., and Buzsáki, G. (1996). High-frequency oscillations in the output networks of the hippocampal-entorhinal axis of the freely moving rat. *Journal of Neuroscience*, 16(9), 3056-3066. 38
- Chrobak, J. J., Lörincz, A., and Buzsáki, G. (2000). Physiological patterns in the hippocampo-entorhinal cortex system. *Hippocampus*, 10, 457-465. 37, 38
- Ciaroni, S., Cuppini, R., Cecchini, T., Ferri, P., Ambrogini, P., Cuppini, C., et al. (1999, Aug 30). Neurogenesis in the adult rat dentate gyrus is enhanced by

- vitamin e deficiency. *J Comp Neurol*, 411(3), 495-502. 36
- Claiborne, B. J., Amaral, D. G., and Cowan, W. M. (1986, Apr 22). A light and electron microscopic analysis of the mossy fibers of the rat dentate gyrus. *J Comp Neurol*, 246(4), 435-58. 36
- Cressant, A., Muller, R. U., and Poucet, B. (1997). Failure of centrally placed objects to control firing fields of hippocampal place cells. *J Neurosci*, 17(7), 2531-2542. 41, 42, 83, 84, 85, 113
- Cressant, A., Muller, R. U., and Poucet, B. (1999). Further study of the control of place cell firing by intra-apparatus objects. *Hippocampus*, 9, 423-431. 41, 42, 83, 113
- Csicsvari, J., Jamieson, B., Wise, K., and Buzsáki, G. (2003). Mechanisms of gamma oscillations in the hippocampus of the behaving rat. *Neuron*, 37(2), 311-322. 37
- Cunha, C. D., Silva, M. H., Wietzikoski, S., Wietzikoski, E. C., Ferro, M. M., Kouzmine, I., et al. (2006, Dec). Place learning strategy of substantia nigra pars compacta-lesioned rats. *Behav Neurosci.*, 120(6), 1279-84. 16, 21, 58, 91, 96
- Da Cunha, C., Wietzikoski, S., Wietzikoski, E. C., Miyoshi, E., Ferro, M. M., Anselmo-Franci, J. A., et al. (2003, May). Evidence for the substantia nigra pars compacta as an essential component of a memory system independent of the hippocampal memory system. *Neurobiol Learn Mem*, 79(3), 236-242. 16, 58, 96
- Dean, P. (1990). The cerebral cortex of the rat. In B. Kolb and R. C. Tees (Eds.), (p. 275-307). MIT Press Cambridge, MA. 55
- Deneve, S., Latham, P. E., and Pouget, A. (1999, Aug). Reading population codes: a neural implementation of ideal observers. *Nat Neurosci.*, 2(8), 740-5. 58, 62
- Deneve, S., Latham, P. E., and Pouget, A. (2001, August). Efficient computation and cue integration with noisy population codes. *Nat Neurosci*, 4(8), 826-31. 58
- Devan, B. D., and White, N. M. (1999, Apr 1). Parallel information processing in the dorsal striatum: relation to hippocampal function. *J Neurosci*, 19(7), 2789-98. 21
- Doya, K. (1996). Temporal difference learning in continuous time and space. In D. S. Touretzky, M. C. Mozer, and M. E. Hasselmo (Eds.), *Advances in neural information processing systems* (Vol. 8, pp. 1073-1079). The MIT Press. 6
- Doya, K. (1999, October). What are the computations of the cerebellum, the basal ganglia and the cerebral cortex? *Neural Networks*, 12(7-8), 961-974. 22, 29
- Doya, K. (2000, December). Complementary roles of basal ganglia and cerebellum in learning and motor control. *Curr Opin Neurobiol*, 10(6), 732-9. 6, 20, 29
- Doya, K. (2002). Metalearning and neuromodulation. *Neural Networks*, 15(4-6), 495-506. 20, 29

- Doya, K., and Uchibe, E. (2005). The Cyber Rodent Project: Exploration of Adaptive Mechanisms for Self-Preservation and Self-Reproduction. *Adaptive Behavior*, 13(2), 149-160. 30
- Eichenbaum, H., Stewart, C., and Morris, R. G. (1990, November). Hippocampal representation in place learning. *J Neurosci*, 10(11), 3531-3542. 16, 21, 23, 25, 58, 88, 89, 91, 93, 96, 97
- Etienne, A. S. (1998, December). Mammalian navigation, neural models and biorobotics. *Connection Science*, 10(3-4), 271-289. 21
- Etienne, A. S., and Jeffery, K. J. (2004). Path integration in mammals. *Hippocampus*, 14(2), 180-92. 41
- Etienne, A. S., Maurer, R., and Seguinot, V. (1996, January). Path integration in mammals and its interaction with visual landmarks. *J Exp Biol*, 199(Pt 1), 201-9. 40, 41
- Filliat, D. (2001). *Cartographie et estimation globale de la position pour un robot mobile autonome*. Phd thesis, LIP6/AnimatLab, Université Pierre et Marie Curie, Paris, France. (Spécialité Informatique) 30
- Fodor, J. A. (1983). *The modularity of mind*. Cambridge MA: MIT Press. 22
- Foley, J. D., Dam, A. van, Feiner, S. K., and Hughes, J. F. (1995). *Computer graphics: Principles and practice in c*. Addison-Wesley Professional. 10
- Foster, D. J., Morris, R. G. M., and Dayan, P. (2000). A model of hippocampally dependent navigation, using the temporal difference learning rule. *Hippocampus*, 10(1), 1-16. 26
- Franz, M. O., Schölkopf, B., Mallot, H. A., and Bühlhoff, H. H. (1998, Oct). Where did i take that snapshot? scene-based homing by image matching. *Biol Cybern*, 79(3), 191-202. 67
- Freund, T. F., and Antal, M. (1988, Nov 10). Gaba-containing neurons in the septum control inhibitory interneurons in the hippocampus. *Nature*, 336(6195), 170-3. 34
- Freund, T. F., Powell, J. F., and Smith, A. D. (1984, December). Tyrosine hydroxylase-immunoreactive boutons in synaptic contact with identified striatonigral neurons, with particular reference to dendritic spines. *Neuroscience*, 13(4), 1189-215. 19, 20
- Fuhs, M. C., and Touretzky, D. S. (2006, Apr 19). spin glass model of path integration in rat medial entorhinal cortex. *J Neurosci*, 26(16), 4266-76. 51, 52, 62, 63, 84
- Fyhn, M., Molden, S., Witter, M. P., Moser, E. I., and Moser, M. B. (2004, Aug 27). Spatial representation in the entorhinal cortex. *Science*, 305(5688), 1258-64. 33, 36, 38, 40, 49, 53, 60, 71, 73, 83, 116
- Gallistel, C. R. (1990). *The organization of learning*. Cambridge, MA: MIT Press. 13, 21, 22, 98, 114
- Gaussier, P., Joulain, C., Banquet, J. P., Leprêtre, S., and Revel, A. (2000). The visual

- homing problem: An example of robotics/biology cross fertilization. *Robotics and Autonomous Systems*, 30(1-2), 155–180. 25, 49
- Gaussier, P., Leprêtre, S., Joulain, C., Revel, A., Quoy, M., and Banquet, J. P. (1998). Animal and robot learning: Experiments and models about visual navigation. In *7th european workshop on learning robots*. Edinburgh, UK. 25, 49
- Gaussier, P., Revel, A., Banquet, J. P., and Babeau, V. (2002, January). From view cells and place cells to cognitive map learning: processing stages of the hippocampal system. *Biol Cybern*, 86(1), 15-28. 25, 49
- Gavrilov, V. V., Wiener, S. I., and Berthoz, A. (1996). Whole body rotations enhance hippocampal theta rhythm slow activity in awake rats passively transported on a mobile robot. *Annals of the New York Academy of Sciences*, 781, 385–398. 37
- Gerstner, W., and Abbott, L. F. (1997, January). Learning navigational maps through potentiation and modulation of hippocampal place cells. *J Comput Neurosci*, 4(1), 79-94. 24
- Gillner, S., and Mallot, H. A. (1998, Jul). Navigation and acquisition of spatial knowledge in a virtual maze. *J Cogn Neurosci.*, 10(4), 445-63. 66
- Girard, B. (2003). *Intégration de la navigation et de la sélection de l'action dans une architecture de contrôle inspirée des ganglions de la base*. Phd thesis, LIP6/AnimatLab, Université Pierre et Marie Curie, Paris, France. (Spécialité Informatique) 30
- Girard, B., Filliat, D., Meyer, J.-A., Berthoz, A., and A. Guillot, A. (2005). Integration of navigation and action selection functionalities in a computational model of cortico-basal ganglia-thalamo-cortical loops. *Adaptive Behavior*, 13(2), 115–130. 30
- Girman, S. V., Sauvé, Y., and Lund, R. D. (1999). Receptive field properties of single neurons in rat primary visual cortex. *J. Neurophysiol.*, 82, 301-311. 55
- Glimcher, P. W. (2003). *Decisions, uncertainty, and the brain: The science of neuroeconomics*. Cambridge, MA: MIT Press. 1
- Goodale, M. A., and Carey, D. P. (1990). The cerebral cortex of the rat. In B. Kolb and R. C. Tees (Eds.), (p. 309-340). MIT Press Cambridge, MA. 55
- Gordon, G. J. (1995). Stable function approximation in dynamic programming. In A. Prieditis and S. Russell (Eds.), *Proceedings of the twelfth international conference on machine learning* (pp. 261–268). San Francisco, CA: Morgan Kaufmann. 9
- Gothard, K. M., Skaggs, W. E., and McNaughton, B. L. (1996). Dynamics of mismatch correction in the hippocampal ensemble code for space: Interaction between path integration and environmental cues. *Journal of Neuroscience*, 16(24), 8027–8040. 11, 41, 42, 48, 73, 76, 77, 78, 83, 84
- Graybiel, A. M. (1998, Jul-Sep). The basal ganglia and chunking of action repertoires. *Neurobiol Learn Mem*, 70(1-2), 119-36. 18
- Graybiel, A. M. (2000, Jul 13). The basal ganglia. *Curr Biol.*, 10(14), R509-11. 18

- Guillot, A., and Meyer, J.-A. (2001). The animat contribution to cognitive systems. *Journal of Cognitive Systems Research*, 2(2), 157–165. 10
- Gurden, H., Tassin, J. P., and Jay, T. M. (1999). Integrity of the mesocortical dopaminergic system is necessary for complete expression of in vivo hippocampal-prefrontal cortex long-term potentiation. *Neuroscience*, 94(4), 1019–27. 20
- Gurney, K., Prescott, T. J., and Redgrave, P. (2001a, June). A computational model of action selection in the basal ganglia. i. a new functional anatomy. *Biol Cybern*, 84(6), 401–10. 30
- Gurney, K., Prescott, T. J., and Redgrave, P. (2001b, June). A computational model of action selection in the basal ganglia. ii. analysis and simulation of behaviour. *Biol Cybern*, 84(6), 411–23. 30
- Hafting, T., Fyhn, M., Molden, S., Moser, M. B., and Moser, E. I. (2005, Jun 19). Microstructure of a spatial map in the entorhinal cortex. *Nature*. 33, 38, 43, 49, 53, 61, 63, 73, 75, 83
- Hasselmo, M. E. (2005, July). A model of prefrontal cortical mechanisms for goal-directed behavior. *J Cogn Neurosci*, 17(7), 1115–29. 117
- Hasselmo, M. E., and Bower, J. M. (1993). Acetylcholine and memory. *Trends in Neurosciences*, 16(6), 218–222. 37
- Hastings, N. B., Seth, M. I., Tanapat, P., Rydel, T. A., and Gould, E. (2002, Oct 28). Granule neurons generated during development extend divergent axon collaterals to hippocampal area ca3. *J Comp Neurol*, 452(4), 324–33. 36
- Haykin, S. (1994). *Neural networks: A comprehensive foundation*. Englewood Cliffs NJ: MacMillan. 5
- Heimer, L., Zahn, D. S., and Alheid, G. F. (1995). Basal ganglia. In G. Paxinos (Ed.), *The rat nervous system* (Second ed., pp. 579–628). Academic Press. 18
- Hertz, J., Krogh, A., and Palmer, R. G. (1991). *Introduction to the theory of neural computation*. Santa Fe Institute: Addison-Wesley Publishing Company. 5, 65
- Hill, A. J. (1978). First occurrence of hippocampal spatial firing in a new environment. *Exp Neurol*, 62, 282–297. 75, 83
- Hill, A. J., and Best, P. J. (1981). Effects of deafness and blindness on the spatial correlates of hippocampal unit activity in the rat. *Experimental neurology*, 74, 204–217. 41, 83
- Hollerman, J. R., and Schultz, W. (1998, August). Dopamine neurons report an error in the temporal prediction of reward during learning. *Nat Neurosci*, 1(4), 304–9. 20
- Houk, J. C., Adams, J. L., and Barto, A. G. (1995). A model of how the basal ganglia generate and use neural signals that predict reinforcement. In J. C. Houk, J. L. Davis, and D. G. Beiser (Eds.), *Models of information processing in the basal ganglia* (pp. 249–270). Cambridge, Massachusetts, USA: MIT Press. 20, 22, 29
- Insausti, R., Herrero, M. T., and Witter, M. P. (1997). Entorhinal cortex of the

- rat: Cytoarchitectonic subdivision and the origin and distribution of cortical efferents. *Hippocampus*, 7, 146–83. 34, 35, 36
- Jaakkola, T., Jordan, M. I., and Singh, S. P. (1994). On the convergence of stochastic iterative dynamic programming algorithms. *Neural Computation*, 6(6), 1185–1201. 8
- Jeffery, K. J., and Keefe, J. M. O. (1999). Learned interaction of visual and idiothetic cues in the control of place field orientation. *Exp Brain Res*, 127, 151–161. 76
- Joel, D., Niv, Y., and Ruppin, E. (2002, Jun-Jul). Actor-critic models of the basal ganglia: new anatomical and computational perspectives. *Neural Netw*, 15(4-6), 535–47. 29
- Jung, M. W., and McNaughton, B. L. (1993). Spatial selectivity of unit activity in the hippocampal granular layer. *Hippocampus*, 3(2), 165–182. 36
- Kerr, J. N., and Wickens, J. R. (2001, January). Dopamine d-1/d-5 receptor activation is required for long-term potentiation in the rat neostriatum in vitro. *J Neurophysiol*, 85(1), 117–24. 20
- Khamassi, M., Lachèze, L., Girard, B., Berthoz, A., and Guillot, A. (2005). Actor-critic models of reinforcement learning in the basal ganglia: From natural to artificial rats. *Adaptive Behavior, Special Issue Towards Artificial Rodents*, 13(2), 131–148. 29, 30
- Killcross, S., and Coutureau, E. (2003, April). Coordination of actions and habits in the medial prefrontal cortex of rats. *Cereb Cortex*, 13(4), 400–8. 117
- Knierim, J. J., Kudrimoti, H. S., and McNaughton, B. L. (1995). Place cells, head direction cells, and the learning of landmark stability. *J Neurosci*, 15, 1648–1659. 21, 48
- Kosel, K. C., Hoesen, G. W. V., and West, J. R. (1981). Olfactory bulb projections to the parahippocampal area of the rat. *Journal of Comparative Neurology*, 198, 467–482. 35, 36
- Kubie, J. L., and Ranck, J. B. (1983). Sensory-behavioral correlates in individual hippocampus neurons in three situations: Space and context. In W. Seifert (Ed.), *Neurobiology of the hippocampus* (p. 433–447). New York: Academic Press. 39, 64, 83
- Kuhn, H. G., Dickinson-Anson, H., and Gage, F. H. (1996, Mar 15). Neurogenesis in the dentate gyrus of the adult rat: age-related decrease of neuronal progenitor proliferation. *J Neurosci*, 16(6), 2027–33. 36
- Lavenex, P., and Schenk, F. (1996, jan-feb). Integration of olfactory information in a spatial representation enabling accurate arm choice in the radial arm maze. *Learning & Memory*, 2(6), 299–319. 41
- Learmonth, A. E., Newcombe, N. S., and Huttenlocher, J. (2001, Nov). Toddlers' use of metric information and landmarks to reorient. *J Exp Child Psychol.*, 80(3), 225–44. 107
- Legault, M., Rompré, P.-P., and Wise, R. A. (2000). Chemical stimulation of the ven-

- tral hippocampus elevates nucleus accumbens dopamine by activating dopaminergic neurons of the ventral tegmental area. *Journal of Neuroscience*, 20(4), 1635–1642. 34
- Lewis, J. (1995). Fast template matching. *Vision Interface*, 120-123. 66
- Liu, P., and Bilkey, D. K. (1997). Parallel involvement of perirhinal and lateral entorhinal cortex in the polysynaptic activation of hippocampus by olfactory inputs. *Hippocampus*, 7(3), 296-306. 36
- Maaswinkel, H., and Whishaw, I. Q. (1999, March). Homing with locale, taxon, and dead reckoning strategies by foraging rats: sensory hierarchy in spatial navigation. *Behav Brain Res*, 99(2), 143-52. 21, 40, 106
- Margules, J., and Gallistel, C. R. (1988, November). Heading in the rat: Determination by environmental shape. *Animal Learning & Behavior*, 16(4), 404-410. 22
- Markus, E. J., Barnes, C. A., McNaughton, B. L., Gladden, V. L., and Skaggs, W. E. (1994). Spatial information content and reliability of hippocampal ca1 neurons: Effects of visual input. *Hippocampus*, 4, 410–421. 40, 41, 44
- Markus, E. J., Qin, Y., Leonard, B., Skaggs, W. E., McNaughton, B. L., and Barnes, C. A. (1995). Interactions between location and task affect the spatial and direction firing of hippocampal neurons. *Journal of Neuroscience*, 15, 7079–7094. 40, 42
- McDonald, R. J., Hong, N. S., and Devan, B. D. (2004, November). The challenges of understanding mammalian cognition and memory-based behaviours: an interactive learning and memory systems approach. *Neurosci Biobehav Rev*, 28(7), 719-45. 16
- McDonald, R. J., and White, N. M. (1993, Feb). Triple dissociation of memory systems: hippocampus, amygdala, and dorsal striatum. *Behav Neurosci.*, 107(1), 3-22. 17
- McNaughton, B. L., Barnes, C. A., Gerrard, J. L., Gothard, K., Jung, M. W., Knierim, J. J., et al. (1996, January). Deciphering the hippocampal polyglot: the hippocampus as a path integration system. *J Exp Biol*, 199 (Pt 1), 173-85. 40, 47, 48, 65
- McNaughton, B. L., Barnes, C. A., Meltzer, J., and Sutherland, R. J. (1989). Hippocampal granule cells are necessary for normal spatial learning but not for spatially-selective pyramidal cell discharge. *Exp Brain Res*, 76(3), 485-96. 40
- McNaughton, B. L., Barnes, C. A., and O'Keefe, J. (1983). The contributions of position, direction, and velocity to single unit activity in the hippocampus of freely-moving rats. *Experimental Brain Research*, 52, 41–49. 39, 40, 44
- McNaughton, B. L., Battaglia, F. P., Jensen, O., Moser, E. I., and Moser, M. B. (2006, August). Path integration and the neural basis of the 'cognitive map'. *Nat Rev Neurosci*, 7(8), 663-678. 33, 51, 52, 62, 84
- McNaughton, B. L., Leonard, B., and Chen, L. (1989). Cortical-hippocampal inter-

- actions and cognitive mapping: A hypothesis based on reintegration of the parietal and inferotemporal pathways for visual processing. *Psychobiology*, 17(3), 230–235. 21, 41
- Mehta, M. R., Barnes, C. A., and McNaughton, B. L. (1997). Experience-dependent, asymmetric expansion of hippocampal place fields. In *Proceedings natl. acad. science usa* (Vol. 94, pp. 8918–8921). 40
- Miller, R. (1991). *Cortico-Hippocampal interplay and the representation of contexts in the brain*. Springer-Verlag. 37
- Mink, J. W. (1996, November). The basal ganglia: focused selection and inhibition of competing motor programs. *Prog Neurobiol*, 50(4), 381–425. 18, 29
- Mittelstaedt, H. (1983). The role of multimodal convergence in homing by path integration. *Fortschritte der Zoologie*, 28, 197–212. 41
- Mittelstaedt, M. L., and Mittelstaedt, H. (1980). Homing by path integration in a mammal. *Naturwissenschaften*, 67, 566–567. 41
- Miyoshi, E., Wietzikoski, S., Camplessei, M., Silveira, R., Takahashi, R. N., and Cunha, D. C. (2002, May). Impaired learning in a spatial working memory version and in a cued version of the water maze in rats with-induced mesencephalic dopaminergic lesions. *Brain Res Bull.*, 58(1), 41–7. 16
- Mizumori, S. J., McNaughton, B. L., Barnes, C. A., and Fox, K. B. (1989, November). Preserved spatial coding in hippocampal ca1 pyramidal cells during reversible suppression of ca3c output: evidence for pattern completion in hippocampus. *J Neurosci*, 9(11), 3915–28. 37, 40
- Mizumori, S. J. Y., and Williams, J. D. (1993). Directionally selective mnemonic properties of neurons in the lateral dorsal nucleus of the thalamus of rats. *J Neurosci*, 13, 4015–4028. 67
- Mobini, S., Chiang, T. J., Ho, M. Y., Bradshaw, C. M., and Szabadi, E. (2000, November). Effects of central 5-hydroxytryptamine depletion on sensitivity to delayed and probabilistic reinforcement. *Psychopharmacology (Berl)*, 152(4), 390–7. 20
- Montague, P. R., Dayan, P., and Sejnowski, T. J. (1996). A framework for mesencephalic dopamine systems based on predictive hebbian learning. *Journal of Neuroscience*, 16(5), 1936–1947. 22, 29
- Montes-Gonzalez, F., Prescott, T., Gurney, K., Humphries, M., and Redgrave, P. (2000). An embodied model of action selection mechanisms in the vertebrate brain. In J.-A. Meyer, A. Berthoz, D. Floreano, H. Roitblat, and S. W. Wilson (Eds.), *From animals to animats 6: Proceedings of the sixth international conference on simulation of adaptive behaviour*. Cambridge MA: MIT Press. 29, 30
- Morris, R. G. M. (1981). Spatial localization does not require the presence of local cues. *Learning and Motivation*, 12, 239–260. 1, 16, 87, 88, 89
- Morris, R. G. M., Garrud, P., Rawlins, J. N., and O’Keefe, J. (1982, Jun 24). Place

- navigation impaired in rats with hippocampal lesions. *Nature*, 297(5868), 681-3. 16, 21, 91, 96
- Muller, R. U., Bostock, E., Taube, J. S., and Kubie, J. L. (1994). On the directional firing properties of hippocampal place cells. *Journal of Neuroscience*, 14(12), 7235–7251. 42
- Muller, R. U., and Kubie, J. L. (1987). The effects of changes in the environment on the spatial firing of hippocampal complex-spike cells. *Journal of Neuroscience*, 7, 1951–1968. 40, 41, 42, 83
- Muller, R. U., Kubie, J. L., and Ranck, J. J. B. (1987). Spatial firing patterns of hippocampal complex-spike cells in a fixed environment. *Journal of Neuroscience*, 7, 1935–1950. 39, 64, 83
- Oja, E. (1982). Simplified neuron model as a principal component analyzer. *J Math Biol.*, 15(3), 267-73. 65
- O'Keefe, J., and Burgess, N. (1996). Geometric determinants of the place fields of hippocampal neurons. *Nature*, 381, 425–428. 11, 39, 42, 48, 76, 80, 83, 84
- O'Keefe, J., and Conway, D. H. (1978). Hippocampal place units in the freely moving rat: why they fire where they fire. *Experimental Brain Research*, 31, 573–590. 40, 41, 75, 76, 83
- O'Keefe, J., and Dostrovsky, J. (1971). The hippocampus as a spatial map. preliminary evidence from unit activity in the freely-moving rat. *Brain Research*, 34, 171–175. 33, 36, 71
- O'Keefe, J., and Nadel, L. (1978). *The hippocampus as a cognitive map*. Oxford: Clarendon Press. 13, 16, 33, 35, 37, 43, 58, 70, 71, 87, 114
- O'Keefe, J., and Recce, M. (1993). Phase relationship between hippocampal place units and the EEG theta rhythm. *Hippocampus*, 3, 317–330. 37
- O'Keefe, J., and Speakman, A. (1987). Single unit activity in the rat hippocampus during a spatial memory task. *Experimental Brain Research*, 68, 1–27. 17, 41, 83
- Otmakhova, N. A., and Lisman, J. E. (1996). D1/D5 dopamine receptor activation increases the magnitude of early long-term potentiation at CA1 hippocampal synapses. *Journal of Neuroscience*, 16(23), 7478–7486. 20
- Otmakhova, N. A., and Lisman, J. E. (1998). D1/D5 dopamine receptors inhibit depotentiation at CA1 synapses via cAMP-dependent mechanism. *Journal of Neuroscience*, 18(4), 1270–1279. 20
- Packard, M. G., Hirsh, R., and White, N. M. (1989, May). Differential effects of fornix and caudate nucleus lesions on two radial maze tasks: evidence for multiple memory systems. *J Neurosci*, 9(5), 1465-72. 16, 17
- Packard, M. G., and Knowlton, B. J. (2002). Learning and memory functions of the basal ganglia. *Annu Rev Neurosci*, 25, 563-93. 18, 117
- Packard, M. G., and McGaugh, J. L. (1992a). Double dissociation of fornix and caudate nucleus lesions on acquisition of two water maze tasks: Further evidence

- for multiple memory systems. *Behavioral Neuroscience*, 106(3), 439–446. 16, 21, 23, 25, 113
- Packard, M. G., and McGaugh, J. L. (1992b). Double dissociation of fornix and caudate nucleus lesions on acquisition of two water maze tasks: Further evidence for multiple memory systems. *Behavioral Neuroscience*, 106(3), 439–446. 113
- Packard, M. G., and McGaugh, J. L. (1996a, January). Inactivation of hippocampus or caudate nucleus with lidocaine differentially affects expression of place and response learning. *Neurobiol Learn Mem*, 65(1), 65-72. 53, 96
- Packard, M. G., and McGaugh, J. L. (1996b, January). Inactivation of hippocampus or caudate nucleus with lidocaine differentially affects expression of place and response learning. *Neurobiol Learn Mem*, 65(1), 65-72. 117
- Pavlov, I. P. (1927). *Conditioned reflexes*. Oxford: Oxford University Press. 1
- Pearce, J. M., Good, M. A., Jones, P. M., and McGregor, A. (2004, Apr). Transfer of spatial behavior between different environments: implications for theories of spatial learning and for the role of the hippocampus in spatial learning. *J Exp Psychol Anim Behav Process*, 30(2), 135-47. 22, 88, 107, 108, 111, 114
- Peng, J., and Williams, R. J. (1996). Incremental multi-step q-learning. *Machine Learning*, 22(1-3), 283–290. 9
- Pico, R. M., Gerbrandt, L. K., Pondel, M., and Ivy, G. (1985). During stepwise cue deletion, rat place behaviors correlate with place unit responses. *Brain Research*, 330, 369–373. 41
- Poucet, B. (1993, Apr). Spatial cognitive maps in animals: new hypotheses on their structure and neural mechanisms. *Psychol Rev.*, 100(2), 163-82. 84, 105, 107, 114
- Poucet, B., Lenck-Santini, P.-P., and Save, E. (2003). The neurobiology of spatial behaviour. In K. J. Jeffery (Ed.), (p. 187-198). Oxford, England: Oxford University Press. 42, 84, 105, 107, 113, 114
- Praxinos, G., and Watson, C. (1998). *The rat brain in stereotaxic coordinates* (fourth edition ed.). Academic Press. 34
- Precup, D., Sutton, R. S., and Dasgupta, S. (2001). Off-policy temporal-difference learning with function approximation. In *Proc. 18th international conf. on machine learning* (pp. 417–424). Morgan Kaufmann. 9
- Precup, D., Sutton, R. S., and Singh, S. (2000). Eligibility traces for off-policy policy evaluation. In *Proc. 17th international conf. on machine learning* (pp. 759–766). Morgan Kaufmann, San Francisco, CA. 9
- Quirk, G. J., Muller, R. U., and Kubie, J. L. (1990). The firing of hippocampal place cells in the dark depends on the rat's recent experience. *Journal of Neuroscience*, 10(6), 2008–2017. 41, 44, 75, 76
- Quirk, G. J., Muller, R. U., Kubie, J. L., and Ranck Jr., J. B. (1992). The positional firing properties of medial entorhinal neurons: Description and comparison with hippocampal place cells. *Journal of Neuroscience*, 12(5), 1945–1963. 36, 40,

- 41, 83
- Redgrave, P., Prescott, T. J., and Gurney, K. (1999, April). Is the short-latency dopamine response too short to signal reward error? *Trends Neurosci*, 22(4), 146-51. 20
- Redish, A. D. (1999). *Beyond the Cognitive Map, From Place Cells to Episodic Memory*. London: MIT Press-Bradford Books. 13, 53
- Redish, A. D. (2001, Dec 14). The hippocampal debate: are we asking the right questions? *Behav Brain Res*, 127(1-2), 81-98. 117
- Redish, A. D., Rosenzweig, E. S., Bohanick, J. D., McNaughton, B. L., and Barnes, C. A. (2000, Dec 15). Dynamics of hippocampal ensemble activity realignment: time versus space. *J Neurosci*, 20(24), 9298-309. 41, 42, 76, 83
- Redish, A. D., and Touretzky, D. S. (1997a). Cognitive maps beyond the hippocampus. *Hippocampus*, 7(1), 15-35. 46
- Redish, A. D., and Touretzky, D. S. (1997b). Navigating with landmarks: Computing goal locations from place codes. In K. Ikeuchi and M. Veloso (Eds.), *Symbolic visual learning* (pp. 325-351). Oxford University Press. 46
- Reynolds, J. N., Hyland, B. I., and Wickens, J. R. (2001, Sep 6). A cellular mechanism of reward-related learning. *Nature*, 413(6851), 67-70. 20
- Rolls, E. T., Stringer, S. M., and Elliot, T. (2006, Dec). Entorhinal cortex grid cells can map to hippocampal place cells by competitive learning. *Network.*, 17(4), 447-65. 51, 52, 84
- Rumelhart, D. E., and Zipser, D. (1986). Feature discovery by competitive learning. In D. E. Rumelhart and J. L. McClelland (Eds.), *Parallel distributed processing 1*. Cambridge, Massachusetts: MIT Press. 43, 46
- Samsonovich, A., and McNaughton, B. L. (1997, Aug 1). Path integration and cognitive mapping in a continuous attractor neural network model. *J Neurosci*, 17(15), 5900-20. 39, 48, 78, 83
- Sargolini, F., Fyhn, M., Hafting, T., McNaughton, B. L., Witter, M. P., Moser, M. B., et al. (2006, May 5). Conjunctive representation of position, direction, and velocity in entorhinal cortex. *Science*, 312(5774), 758-62. 52
- Save, E., Cressant, A., Thinus-Blanc, C., and Poucet, B. (1998). Spatial firing of hippocampal place cells in blind rats. *Journal of Neuroscience*, 18(5), 1818-1826. 41
- Save, E., Nerad, L., and Poucet, B. (2000). Contribution of multiple sensory information to place field stability in hippocampal place cells. *Hippocampus*, 10, 64-76. 40, 41, 44
- Schultz, W. (1998). Predictive Reward Signal of Dopamine Neurons. *Journal of Neurophysiology*, 80, 1-27. 20
- Schultz, W. (2002, Oct 10). Getting formal with dopamine and reward. *Neuron*, 36(2), 241-63. 19, 20
- Schultz, W., Apicella, P., Scarnati, E., and Ljungberg, T. (1992, December). Neuronal

- activity in monkey ventral striatum related to the expectation of reward. *J Neurosci*, 12(12), 4595-610. 20
- Schultz, W., Dayan, P., and Montague, P. R. (1997). A neural substrate of prediction and reward. *Science*, 275, 1593–1599. 20, 59, 113
- Sesack, S. R., and Pickel, V. M. (1990, Sep 17). In the rat medial nucleus accumbens, hippocampal and catecholaminergic terminals converge on spiny neurons and are in apposition to each other. *Brain Res*, 527(2), 266-79. 20
- Sharp, P. E. (1991). Computer simulation of hippocampal place cells. *Psychobiology*, 19(2), 103–115. 43, 46, 65
- Sharp, P. E. (1997). Subicular cells generate similar spatial firing patterns in two geometrically and visually distinctive environments: Comparison with hippocampal place cells. *Behavioral and Brain Research*, 85, 71–92. 40
- Sharp, P. E. (1999). Subicular place cells expand/contract their spatial firing pattern to fit the size of the environment in an open field, but not in the presence of barriers: Comparison with hippocampal place cells. *Behavioral Neuroscience*, 113(4), 643–62. 40
- Sharp, P. E., and Green, C. (1994). Spatial correlates of firing patterns of single cells in the subiculum of freely moving rat. *Journal of Neuroscience*, 14(4), 2339–2356. 40, 48
- Sharp, P. E., Kubie, J. L., and Muller, R. U. (1990, September). Firing properties of hippocampal neurons in a visually symmetrical environment: contributions of multiple sensory cues and mnemonic processes. *J Neurosci*, 10(9), 3093-105. 41
- Silva, F. H. L. da, Witter, M. P., Boeijinga, P. H., and Lohman, A. H. M. (1990). Anatomical organization and physiology of the limbic cortex. *Physiological Reviews*, 70, 453–511. 36
- Singh, S. P., Jaakkola, T., Littman, M. L., and Szepesvári, C. (2000). Convergence results for single-step on-policy reinforcement-learning algorithms. *Machine Learning*, 38(3), 287-308. 8
- Skaggs, W. E., Knierim, J. J., Kudrimoti, H. S., and McNaughton, B. L. (1995). A model of the neural basis of the rat's sense of direction. In G. Tesauro, D. S. Touretzky, and T. K. Leen (Eds.), *Advances in neural information processing systems 7* (pp. 173–180). Cambridge, MA: MIT Press. 48, 64
- Skaggs, W. E., McNaughton, B. L., Wilson, M. A., and Barnes, C. A. (1996). Theta phase precession in hippocampal neuronal populations and the compression of temporal sequences. *Hippocampus*, 6(2), 149-72. 37
- Smith, Y., Bennett, B. D., Bolam, J. P., Parent, A., and Sadikot, A. F. (1994, Jun 1). Synaptic relationships between dopaminergic afferents and cortical or thalamic input in the sensorimotor territory of the striatum in monkey. *J Comp Neurol*, 344(1), 1-19. 20
- Solstad, T., Moser, E. I., and Einevoll, G. T. (2006). From grid cells to place cells:

- a mathematical model. *Hippocampus.*, 16(12), 1026-31. 51, 52, 64, 84
- Spiers, H. J., Burgess, N., Hartley, T., Vargha-Khadem, F., and O'Keefe, J. (2001). Bilateral hippocampal pathology impairs topographical and episodic memory but not visual pattern matching. *Hippocampus.*, 11(6), 715-25. 66
- Strösslin, T., Sheynikhovich, D., Chavarriaga, R., and Gerstner, W. (2005). Robust self-localisation and navigation based on hippocampal place cells. *Neural Networks*, 8(19), 1125-1140. 59
- Suri, R. E., and Schultz, W. (1998, August). Learning of sequential movements by neural network model with dopamine-like reinforcement signal. *Exp Brain Res*, 121(3), 350-4. 20
- Suri, R. E., and Schultz, W. (1999). A neural network model with dopamine-like reinforcement signal that learns a spatial delayed response task. *Neuroscience*, 91(3), 871-90. 20
- Suri, R. E., and Schultz, W. (2001, April). Temporal difference model reproduces anticipatory neural activity. *Neural Comput*, 13(4), 841-62. 20
- Sutherland, R. J., Chew, G. L., Baker, J. C., and Linggard, R. C. (1987). Some limitations on the use of distal cues in place navigation by rats. *Psychobiology*, 15(1), 48-57. 97
- Sutherland, R. J., and Rodriguez, A. J. (1990). The role of the fornix/fimbria and some related subcortical structures in place learning and memory. *Behavioral and Brain Research*, 32, 265-277. 18, 23, 25, 91
- Sutherland, R. J., Whishaw, I. Q., and Kolb, B. (1983, Feb). behavioural analysis of spatial localization following electrolytic, kainate- or colchicine-induced damage to the hippocampal formation in the rat. *Behav Brain Res.*, 7(2), 133-53. 16, 96
- Sutton, R., and Barto, A. G. (1998). *Reinforcement learning - an introduction*. Cambridge, MA: MIT Press. 6, 27
- Sutton, R., McAllester, D., Singh, S., and Mansour, Y. (1999). Policy gradient methods for reinforcement learning with function approximation. In *Advances in neural information processing systems 12* (pp. 1057-1063). MIT Press. 9
- Suzuki, S., Augerinos, G., and Black, A. (1980). Stimulus control of spatial behavior on the eight-arm maze in rats. *Learning and motivation*, 11, 1-18. 17, 21, 105
- Suzuki, W. A., and Amaral, D. G. (1994, March). Topographic organization of the reciprocal connections between the monkey entorhinal cortex and the perirhinal and parahippocampal cortices. *J Neurosci*, 14(3 Pt 2), 1856-77. 36
- Thierry, A. M., Gioanni, Y., Dégénétais, E., and Glowinski, J. (2000). Hippocampoprefrontal cortex pathway: anatomical and electrophysiological characteristics. *Hippocampus.*, 10(4), 411-9. 19
- Thompson, L. T., and Best, P. J. (1989). Place cells and silent cells in the hippocampus of freely-behaving rats. *Journal of Neuroscience*, 9(7), 2382-2390. 40

- Tolman, E. C. (1948). Cognitive maps in rats and men. *Psychological Review*, 55, 189–208. 33, 70, 87
- Tolman, E. C., and Honzik, C. H. (1930). Introduction and removal of reward, and maze performance in rats. *Univ. Cal. Pub. Psychol.*, 4(19), 257-275. 70, 71
- Touretzky, D. S., and Redish, A. D. (1996). A theory of rodent navigation based on interacting representations of space. *Hippocampus*, 6(3), 247–270. 46
- Trullier, O., Wiener, S. I., Berthoz, A., and Meyer, J. A. (1997). Biologically-based artificial navigation systems: Review and prospects. *Progress in Neurobiology*, 51, 483–544. 13
- Tsitsiklis, J. N., and Roy, B. V. (1996). Feature-based methods for large scale dynamic programming. *Machine Learning*, 22(1-3), 59-94. 9
- Usher, M., Cohen, J. D., Servan-Schreiber, D., Rajkowski, J., and Aston-Jones, G. (1999). The role of locus coeruleus in the regulation of cognitive performance. *Science*, 283(5401), 549-554. 20
- Wan, H. S., Touretzky, D. S., and Redish, A. D. (1994). Towards a computational theory of rat navigation. In M. Mozer, P. Smolensky, D. S. Touretzky, J. Elman, and A. Weigend (Eds.), *Proceedings of the 1993 connectionist models summer school* (pp. 11–19). Hillsdale, NJ, Erlbaum. 46
- Wang, R. F., and Spelke, E. S. (2003). The neurobiology of spatial behaviour. In K. J. Jeffery (Ed.), (p. 119-143). Oxford, England: Oxford University Press. 22, 76, 98, 99, 105
- Watkins, C. J. C. H. (1989). *Learning from delayed rewards*. Unpublished doctoral dissertation, University of Cambridge, England. 8, 9
- Watkins, C. J. C. H., and Dayan, P. (1992). Q-learning. *Machine Learning*, 8(3/4), 279–292. 8
- White, N. M. (2004, November). The role of stimulus ambiguity and movement in spatial navigation: A multiple memory systems analysis of location discrimination. *Neurobiol Learn Mem*, 82(3), 216-229. 16, 70
- White, N. M., and McDonald, R. J. (2002, March). Multiple parallel memory systems in the brain of the rat. *Neurobiol Learn Mem*, 77(2), 125-184. 17, 53, 113
- Wickens, J. R., Begg, A. J., and Arbuthnott, G. W. (1996, January). Dopamine reverses the depression of rat corticostriatal synapses which normally follows high-frequency stimulation of cortex in vitro. *Neuroscience*, 70(1), 1-5. 20
- Wilson, M. A., and McNaughton, B. L. (1993). Dynamics of the hippocampal ensemble code for space. *Science*, 261, 1055–1058. 21, 39, 83
- Winson, J. (1978). Loss of hippocampal theta rhythm results in spatial memory deficits in the rat. *Science*, 201, 160–163. 37
- Witter, M. P. (1993). Organization of the entorhinal-hippocampal system: A review of current anatomical data. *Hippocampus*, 3, 33–44. 34, 35, 36, 37
- Witter, M. P., Groenewegen, H. J., Silva, F. H. L. da, and Lohman, A. H. M. (1989).

- Functional organization of the extrinsic and intrinsic circuitry of the parahippocampal region. *Progress in Neurobiology*, 33, 161-253. 36
- Witter, M. P., Naber, P. A., Haefliger, T. van, Machielsen, W. C., Rombouts, S. A., Barkhof, F., et al. (2000). Cortico-hippocampal communication by way of parallel parahippocampal-subicular pathways. *Hippocampus*, 10(4), 398-410. 34, 35, 36, 37
- Witter, M. P., Ostendorf, R. H., and Groenewegen, H. J. (1990). Heterogeneity in the dorsal subiculum of the rat. distinct neuronal zones project to different cortical and subcortical targets. *Eur J Neurosci.*, 2(8), 718-725. 18
- Wylie, D. R., Glover, R. G., and Aitchison, J. D. (1999, Jul 1). Optic flow input to the hippocampal formation from the accessory optic system. *J Neurosci.*, 19(13), 5514-27. 114
- Yeckel, M. F., and Berger, T. W. (1990, Aug). Feedforward excitation of the hippocampus by afferents from the entorhinal cortex: redefinition of the role of the trisynaptic pathway. *Proc Natl Acad Sci U S A.*, 87(15), 5832-6. 35

Denis Sheynikhovich

rte des Plaines-du-Loup 16, 1018 Lausanne
Tel: 021.3122703/021.6935591
E-Mail: denis.sheynikhovich@epfl.ch
Web: <http://lcn.epfl.ch/~sheynikh>

Date of birth: 04.11.1973
Married
Nationality: Russian
Permit: B

Curriculum vitae

- 2003-2007 Ph.D. Research Assistant**
Laboratory of Computational Neuroscience, Prof. W. Gerstner.
Ecole Polytechnique Fédérale de Lausanne (EPFL), Switzerland.
- 2002-2003 Graduate Student**
Doctoral School of Computer, Communication and Information Sciences.
Ecole Polytechnique Fédérale de Lausanne (EPFL), Switzerland.
- 1999-2001 Senior Software Engineer**
Artificial Life Inc., Saint-Petersburg branch, Russia.
- 1997-1999 Software Engineer**
Research and Development Telecommunication Institute,
Saint-Petersburg, Russia.
- 1995-1997 MA honors degree in mathematics**
State Institute of Fine Mechanics and Optics (Technical University),
Computer Science Department, Saint-Petersburg, Russia.
- 1991-1995 BA degree in mathematics**
State Institute of Fine Mechanics and Optics (Technical University),
Computer Science Department, Saint-Petersburg, Russia.

Scholarships

- 2002 EPFL Doctoral School Scholarship.
1997 International Soros Science Education Program Grant.

Academic Responsibilities

Teaching

Tutor assistant for ‘Modern Approaches to Machine Learning’ course, EPFL 2003

Supervision

Masters student: Julien Delile,

Title: ‘Redéfinition des représentations d’espace et d’actions dans un modèle de navigation spatiale animale pas apprentissage par renforcement’

Laboratory of Computational Neuroscience, EPFL (2007)

Masters student: Jérémie Knüsel,

Title: ‘Dynamic Parameter Model for Reinforcement Learning in Rodent Navigation Task’

Laboratory of Computational Neuroscience, EPFL (2005)

Masters student: Guillaume Zufferey,

Title: ‘Neural Implementation of a Hidden Markov Model for Spatial Localization Using Continuous 2D Visual Input’,

Laboratory of Computational Neuroscience, EPFL (2004)

Languages

Russian: Mother tongue.

English: Fluent conversational and good writing skills (TOEFL score 257).

German and French: Basic knowledge.

Publications: Journal papers

(9) Effects of Stress and Genotype on Meta-parameter Dynamics in Reinforcement Learning

G. Luksys, J. Knüsel, D. Sheynikhovich, C. Sandi and W. Gerstner (2007)
Advances in Neural Information Processing Systems (NIPS), 19

(8) Adaptive Sensory Processing for Efficient Place Coding

D. Sheynikhovich, R. Chavarriaga, T. Strösslin and W. Gerstner (2006)
Neurocomputing (69:1211-1214)

(7) Robust Self-localization and Navigation Based on Hippocampal Place Cells

T. Strösslin, D. Sheynikhovich, R. Chavarriaga and W. Gerstner (2005)
Neural Networks 18:1125-1140

(6) A Computational Model of Parallel Navigation Systems in Rodents

R. Chavarriaga, T. Strösslin, D. Sheynikhovich and W. Gerstner (2005)
Neuroinformatics 3:223-242

(5) Competition Between Cue Response and Place Response: a Model of Rat Navigation Behaviour

R. Chavarriaga, T. Strösslin, D. Sheynikhovich and W. Gerstner (2005)
Connection Science 17:167-183

(4) Modelling Path Integrator Recalibration Using Hippocampal Place Cells

T. Strösslin, R. Chavarriaga, D. Sheynikhovich and W. Gerstner (2005)
 In: W. Duch et al. (Eds.), *Artificial Neural Networks*, (ICANN 2005),
 Lecture Notes in Computer Science 3696:51-56, Springer-Verlag Berlin Heidelberg.

(3) Interferometric Data Analysis Based on Markov Non-linear Filtering Methodology

Gurov I.P. and Sheynikhovich D.V. (2000)
Journal of the Optical Society of America A 17:21-27

(2) Calculating of Phase Characteristics of Interferometric Pattern by the Method of Markov Non-linear Filtering

Gurov I.P. and Sheynikhovich D.V. (1997)
Optics and Spectroscopy 83:147-152

Publications: Book Chapters

(1) Spatial Representation and Navigation in a Bio-inspired Robot

D. Sheynikhovich, R. Chavarriaga, T. Strösslin and W. Gerstner (2005)
 In: Wermter S., Palm G. and Elshaw M. (Eds.),
Biomimetic neural learning for intelligent robots,
 Lecture Notes in Artificial Intelligence 3575:245-264, Springer-Verlag Berlin Heidelberg.

Publications: Summary

9 publications (no conference abstracts were included).

7 published or accepted in refereed journals (excluding refs. 1, 4).

2 first author papers.